USE OF HYDROGEN/DEUTERIUM EXCHANGE-MASS SPECTROMETRY IN THE STUDY OF CELL WALL DEGRADING ENZYMES AND THEIR INHIBITORS

by

TASNEEM M. BAHRAINWALA

(Under the Direction of RON ORLANDO)

ABSTRACT

Mass Spectrometry has developed in the last decade into a mature tool for the study of biomolecules and proteins. It has proven to be an indispensable tool in determining the primary structure of proteins and more recently has been heavily utilized in the studies on secondary and tertiary protein structures. Mass spectrometry is also used to study protein complexes and their interactions with enzymes, ligands or substrates.

The study of *Aspergillus niger* endopolygalacturonases, EPG-I and EPG-II, in the presence of substrate as well as in the presence of different polygalacturonase inhibiting proteins (PGIPs) are described. The cell wall degrading enzymes produced by the fungus *Aspergillus niger* have many commercial applications and are important in the study of plant pathogenesis. At the same time, PGIPs are part of a plant's first lines of defense against the attack of fungi. PGIPs are extracellular proteins, ionically bound to the cell wall which limit fungal invasion by counter acting EPG activity and permitting for the induction of defense elicitors.

The basis of the research in this dissertation is the utilization of mass spectrometry techniques coupled with hydrogen/deuterium exchange to study the interactions between a protein-carbohydrate binding system as well as protein-protein binding. Hydrogen/deuterium exchange-mass spectrometry offers several advantages, such as a high speed of analysis, sensitivity and reduced sample requirement as compared to other methods such as NMR and X-ray crystallography for studying protein-carbohydrate and protein-protein interactions.

INDEX WORDS: Hydrogen/deuterium exchange-mass spectrometry, Protein-carbohydrate interactions, protein-protein interactions, endopolygalacturonases, polygalacturonase inhibiting proteins, Aspergillus niger, NMR, X-ray crystallography

USE OF HYDROGEN/DEUTERIUM EXCHANGE-MASS SPECTROMETRY IN THE STUDY OF CELL WALL DEGRADING ENZYMES AND THEIR INHIBITORS

by

TASNEEM M. BAHRAINWALA

M.S., Jai Hind College of Arts, Science and Commerce, University of Mumbai, India, 1992

Ph.D., Institute of Science, University of Mumbai, India, 1997

A Dissertation Submitted to the Graduate Faculty of The University of Georgia in Partial Fulfillment of the Requirements for the Degree

DOCTOR OF PHILOSOPHY

ATHENS, GEORGIA

2005

USE OF HYDROGEN/DEUTERIUM EXCHANGE-MASS SPECTROMETRY IN THE STUDY OF CELL WALL DEGRADING ENZYMES AND THEIR INHIBITORS

by

TASNEEM M. BAHRAINWALA

Major Professor: Ron Orlando

Committee: Jonathan Amster
James deHaseth
Rob Woods
Michael Bartlett

Electronic Version Approved:

Maureen Grasso
Dean of the Graduate School
The University of Georgia
August 2005

DEDICATION

This dissertation is dedicated to the most important person in my life:

My Father : Mr. M. H. Bahrainwala, the most loving and caring person I knew. Who inspired me to be a better person yet loved me for who I am. He was my role model whom I can never repay for the love he had given me and the generosity he shared with not only me and my family, but with everyone he came in touch with. “GOD BLESS HIS SOUL” AMEN.

ACKNOWLEDGEMENTS

With profound sincerity and appreciation that I acknowledge and thank the assistance made towards the completion of my research work by:

My research advisor, Dr. Ron Orlando, for introducing me to this vast and interesting field of mass spectrometry. His keen interest, expert guidance and invaluable suggestion through the course of the work. I deeply acknowledge the inspiration and the untiring co-operation which he gave me throughout my research work.

My gratitude and respect is extended to the faculty and staff of the Chemistry Department and all my committee members, Dr. Jonathan Amster, Dr. James deHaseth, Dr. Rob Woods and Dr. Michael Bartlett for their efforts and involvement in the successful completion of my degree.

My appreciation extends to the scientist, faculty, staff and students of the Complex Carbohydrate Research Center for providing many of the resources used in this dissertation, for advice and friendship. I am especially grateful to Dr. Carl Bergmann who provided his assistant at all times, for his suggestions and careful reviews of this dissertation. I would like to thank Dr. Kumar Kolli for all the help rendered to me on a day to day basis. He is the one who taught me the finer details of all the instruments I used and who was always available whenever I called him. I would also I like to thank all my labmates for their support and friendship during the entire time I spent with them.

I will be failing in my duty if I do not acknowledge the support and confidence given to me by my beloved parents Mr. and Mrs. M.H. Bahrainwala. Words are too inadequate to express my deep sense of gratitude and respect to them. All the sacrifices made by them throughout my

studies and who were only a phone call away whenever I needed them. This dissertation also owes a great deal to my brother and his wife and to my sisters and their husbands, who have always been their for me, encouraging me at each and every step to pursue whatever goal I set for my life. For all this and much more, I would like to thank all of my family members from the bottom of my heart and to whom I am forever in debt.

TABLE OF CONTENTS

Page

LIST OF TABLES

Page

LIST OF FIGURES

Page

CHAPTER 1

INTRODUCTION

Since its beginnings almost 100 years ago, mass spectrometry (MS) has become a virtually ubiquitous research tool. The definition of a mass spectrometer may seem simple: it is an instrument that can ionize a sample and measure the mass-to-charge ratio of the resulting ions. However, the versatility of this function has made it a vital tool in a wide range of fields such as biotechnology, with pharmaceutical, clinical, environmental and geological applications as well. This versatility arises from the fact that mass spectrometers can give qualitative and quantitative information on the elemental, isotopic, and molecular composition of organic and inorganic samples.[1] Furthermore, samples can be analyzed from the gas, liquid, or solid state, and masses that can be studied range from single atoms (several Da) to proteins (over 300,000 Da).[2] The application of mass spectrometry began in the 1940s[3] and since that time advances in technology have increased the range of masses that could be measured, which further diversified the applications of mass spectrometry. During the decade of the 1990s, changes in MS instrumentation and techniques revolutionized protein chemistry and fundamentally changed the analysis of proteins. These changes were catalyzed by two technical breakthroughs in the late 1980s, the development of the ionization methods known as electrospray ionization (ESI) and matrix-assisted laser desorption/ionization (MALDI).[4-6] These methods solved the difficult problem of generating ions from large, nonvolatile analytes such as proteins and peptides without significant analyte fragmentation. MS continues to evolve, and the importance of this can be seen as new types of mass spectrometers come into design to take advantage of the inherent sensitivities of these high efficiency ion sources. As a result, the measurement of biomolecular masses with high resolution and accuracy can now be performed routinely. This is especially evident in the field of proteomics, where both qualitative and quantitative analyses of proteins rely on MS.

The ease with which proteins and peptides could be ionized by these methods rapidly made MS a complimentary technique to nuclear magnetic resonance[7-9], X-ray crystallography[10-12], circular dichroism, and the classical methods of protein chemistry for the study of diverse aspects of protein structure and function.[13,14] Numerous reports document the success MS has enjoyed in studies in the four structural classifications of proteins, namely, the primary structure or linear sequence of amino acids, the secondary structure or the folding of stretches of amino acids into defined structural motifs, the tertiary structure or the overall three-dimensional fold, and the quaternary structure or the spatial arrangement of folded polypeptides in multiprotein complexes.

Proteins are abundant in all organisms and are indeed fundamental to life. The study of protein structure is therefore not only of fundamental scientific interest in terms of understanding biochemical processes, but also produces very valuable practical benefits. The coupling of chromatographic and electrophoretic techniques with mass spectrometry has produced powerful tools for the simultaneous separation and detection of complex mixtures down to the femtomole range. As a result, the applications of MS in biochemistry have grown significantly.

One of the applications where MS is used is hydrogen/deuterium exchange to examine higher order structural features of proteins.[15] Protein folding studies are performed by comparing the location and degree of deuterium incorporation in various folded, unfolded or denatured states. The effect of various parameters such as pH and temperature on protein folding can also be measured.[14] These experiments are based on the assumption that not all of the potentially exchangeable hydrogens in a protein exchange at the same rate and that the rate of exchange reflects the structural properties of the protein. Examples of structural features that can be analyzed in this way include solvent accessibility, based on the observation that solvent exposed

hydrogens exchange more rapidly than those shielded from the solvent access, and hydrogen bonding, based on the observation that hydrogens involved in hydrogen bonds exchange at a slower rate than those not involved in hydrogen bonds.

The research presented in this dissertation focuses on the application of mass spectrometry to the study of proteins and carbohydrates using hydrogen/deuterium exchange. Chapter 3 focuses on the application of hydrogen/deuterium exchange to the study of the enzymes secreted by the pathogenic fungi, *Aspergillus niger*, that digest pectic polysaccharides present in the plant cell wall. These enzymes, known as endopolygalacturonases (EPGs), were studied in combinations with oligomers of polygalacturonic acid (PGA) as a system of study. Chapter 4 focuses on the study of interaction of the EPGs with plant derived polygalacturonase inhibiting proteins (PGIPs) and PGA.

Reference List

1. Willard, H.H.; Merritt, Jr. L.L.; Dean, J.A.; Settle, Jr. F.A. *Instrumental Methods of Analysis* **1988,** Wadsworth Publishing Co., Belmont, CA, pp. 465-507.
2. Guo, B. *Anal. Chem.* **1999,** 71, 333-337.
3. de Laeter, J.R. *Applications of Inorganic Mass Spectrometry,* **2001,** John Wiley and Sons, Inc., New York.
4. Fenn, J.B.; Mann, M.; Meng, C.K.; Wong, S.F.; Whitehouse, C.M. *Science* **1989,** 246, 64-71.
5. Cole, R.B. *Electrospray Ionization Mass Spectrometry, Fundamentals, Instrumentation and Applications* **1997,** Wiley, New York.
6. Karas, M.; Hillenkamp, F. *Anal. Chem.* **1988,** 60, 2299-2301.
7. Bai, Y.; Sosnick, T.R.; Mayne, L.; Englander, S.W. *Science* **1990,** 249, 755.
8. Green, E.D., Adelt, G.; Aenziger, J.U.; Wilson, S.; Van Halbeek, H. *J. Biol. Chem.* **1988,** 263, 18253-18268.
9. Koerner, T.A.; Prestegard, J.H.; Yu, R.K. *Method Enzymol.* **1987,** 138, 38-59.
10. Creighton, T.E. *Protein Structures and Molecular Properties,* **1984,** Freeman, New York.
11. Creighton, T.E. *Biochemistry J.* **1990,** 270, 1-16.
12. Woods, R.J. *Current Opinion in Structural Biology* **1995,** 5, 591-598.
13. Katta, V; Chait, B.T. *Rapid Commun. Mass Spectrom.* **1991,** 5, 214-217.
14. Katta, V.; Chait, B.T. *J. Am. Chem. Soc.* **1993,** 115, 6317-6321.
15. Wood, T.D.; Chorush, R.A., Wampler, F.M.; Little, D.P.; O'Connor, P.B.; McLafferty, F.W. *Proc. Natl. Acad. Sci. U.S.A.* **1995**, 92, 2451.

CHAPTER 2

LITERATURE REVIEW

Mass Spectrometry

The foundation of mass spectrometry (MS) had its beginnings in J.J. Thomson's vacuum tube where in the early part of the century the existence of electrons and "positive rays" was demonstrated.[1] J.J. Thomson observed that the new technique could be used profitably by chemists to analyze chemicals. Despite this far-sighted observation, the primary application of mass spectrometry remained in the realm of physics for nearly thirty years. It was used to discover a number of isotopes, to determine the relative abundance of the isotopes, and to measure their "exact masses". These important fundamental measurements laid the foundation for later developments of mass spectrometry in diverse fields, resulting in it becoming an "interdisciplinary research methodology" impacting virtually every area of science, from physics through chemistry and biology.[2,3] Because all molecules contain mass, mass spectrometry has the inherent characteristic of being universally applicable to all materials.[3]

Mass spectrometry is an analytic technique that measures the masses of individual molecules and atoms. As conceptualized in Figure 2.1, the first essential step in mass spectrometric analysis is to convert the analyte molecules into gas-phase species. Early mass spectrometers required a sample to be volatile, but recent advances in ionization methods, such as matrix-assisted laser desorption/ionization (MALDI) and electrospray ionization (ESI) have made it possible for non volatile analytes to be directly analyzed in liquid solution or embedded in a solid matrix. The excess energy transferred to the molecule during the ionization event may lead to fragmentation. Next, a mass analyzer separates these molecular ions and their charged fragments according to their m/z (mass/charge) ratio. The ion current due to these mass-separated ions is detected by a suitable detector and displayed in the form of a mass spectrum. To

enable the ions to move freely in space without colliding or interacting with other species, each of these steps is carried out under high vacuum (10^{-4} – 10^{-8} torr).

Most biological samples are polar, nonvolatile and thermally unstable and cannot be vaporized easily without decomposition. These samples therefore, are not ionizable by traditional ionization methods such as chemical ionization (CI) or electron ionization (EI). Both these techniques are limited by their inability to handle nonvolatile compounds. With the advent of modern ionization methods, mass spectrometry has enjoyed vast success in the analysis of such species as synthetic polymers,[4] large and small bio-polymers,[5] whole proteomes,[6] whole cells[7] and others which encompass the realm of large non-volatile molecules. This relatively broad applicability, coupled with ultrahigh sensitivity and resolution as well as large mass ranges easily accounts for the widespread use of mass spectrometry in industrial, clinical and academic settings. Among the most notable of these innovations are the development of MALDI-MS and ESI-MS.

Matrix Assisted Laser Desorption/Ionization – Mass Spectrometry (MALDI-MS)

In the early 1960s, it was demonstrated that the irradiation of low-mass organic molecules with a high-intensity laser pulse lead to the formation of ions that could be successfully mass analyzed. This was the origin of laser desorption (LD) ionization. In the next few decades, the technique underwent substantial development, culminating in the extension of the technique to the analysis of nonvolatile biopolymers and organic macromolecules. These experiments, however, revealed an upper mass limit of 5-10 kDa. Another restriction was the short duration of the ion burst following the laser pulse. Thus, LD was only really successful once it was coupled to TOF mass analyzers.

In 1987, Michael Karas and Franz Hillenkamp successfully demonstrated the use of a matrix (a small organic molecule) in LD to circumvent the mass limitation.[8] The principle behind this is that the analyte is mixed with a suitable matrix that absorbs radiation from a UV laser and because of the low mass sublimes, thus creating a burst of ions with each laser pulse.[9-11] This was the foundation of matrix-assisted laser desorption/ionization (MALDI). Later developments by Koichi Tanaka demonstrated the application of MALDI to a whole range of biological macromolecules.[12]

In practice, the sample is mixed with an excess of host matrix material, which is then dried to form a sample-matrix crystal. The crystal thus formed is irradiated with a laser beam using short pulses of 1-20 ns duration. Various laser systems have been used to rapidly deposit energy into the sample-matrix combination. Most applications have used UV lasers such as the nitrogen laser (337 nm) or Nd: YAG laser having frequencies of 266 nm or 355 nm respectively.[13-15] IR lasers such as Er: YAG (λ = 2.94 μm) or CO_2 (λ = 10.6 μm) have also been used to obtain MALDI spectra.[16-18] UV and IR lasers both yield similar spectra for proteins.

A saturated solution (or nmol/ml concentration) of the matrix is first prepared in a ratio of 1:1 acetonitrile or methanol : water containing 0.1% TFA. The sample – matrix molar ratio is 1:1000 or 1:10,000. The matrix performs two important functions. First, it absorbs photon energy from the laser beam and transfers it into excitation energy of the solid system. Additionally, a large excess of matrix serves as a solvent for the analyte, so that the intermolecular forces are reduced and aggregation of the analyte molecule or sample is held to a minimum. The matrix must absorb energy at the wavelength of the laser radiation. This combination allows a large amount of energy to be absorbed efficiently by the matrix and subsequently transferred to the sample in a controlled manner. Absorption of energy from the laser beam causes evaporation of

the matrix. The sample and analyte molecules are entrained in the resultant gas-phase plume and become ionized via gas-phase proton-transfer reactions (Figure2.2). MALDI typically produces singly charged molecular ions, although in some cases can produce multiply charged ions as well. In addition, the Na^+ and K^+ adducts are also a common feature of MALDI spectra.

As with other desorption ionization methods, the preparation of the sample for the MALDI analysis also requires utmost care. The homogeneity of the sample-matrix is a critical factor to obtain good sample ion yields. Fortunately, MALDI-MS is relatively more tolerant of impurities, buffers, salts and mixtures.[19] Literature reviews suggest several techniques for sample preparation.[20]

Once in the gas phase, the charged molecules are directed electrostatically from the MALDI ionization source into the mass analyzer. Time-of-flight (TOF) mass analyzers are often used to separate the ions. The pulsed nature of MALDI is directly applicable to TOF analyzers since the ions initial time of flight can be started with each pulse of the laser and completed when the ions reach the detector.

The linear time-of-flight mass analyzer (figure 2.3) is the simplest mass analyzer. It has enjoyed a renaissance with the invention of MALDI. The linear TOF instrument consists of a source, a field free region and the detector. Ions are separated on the basis of different masses. Though they have the same amount of initial energy, the lighter ions reach the detector first because of their greater velocity, while the heavier ions take longer to reach the detector. Ions are expelled from the sources in bundles or by a transient application of potentials on the lenses. They are accelerated by a potential V_s and fly a distance d before reaching the detector. Mass-to-charge ratios are determined by measuring the time that ions take to move through a field free region between the source and detector. Theoretically, all the ions with the same charge have the

same final kinetic energy upon entering the field free region. An ion with mass m and charge of q = ze, has a kinetic energy of

$$E_k = ZeV_s = qV_s = 1/2mv^2$$

The time needed to fly the distance d is given by

$$t = d/v$$

Thus,

$$t^2 = m/z\ (d^2/2V_se)$$

This equation shows that m/z can be calculated from a measurement of t^2. All other factors being equal, the lower the mass of the ion, the faster it will reach the detector. In principle, the TOF instrument has no upper mass range, making it suitable for soft ionization techniques.[21,22] Another advantage of TOF instruments is their high transmission efficiency which leads to high sensitivity. Thus, the detection of 100-200 amol of various proteins have been obtained with TOF analyzers.[23,24] All ions are produced in a short time scan and temporal separation of these ions allows all of them to be directed towards the detector together. Therefore, all the ions formed are analyzed.

Factors such as the length of the ion formation pulse, the size of the volume where the ions are formed and the variation of the initial kinetic energy of the ions will all affect mass resolution. Thus, poor mass resolution is one of the drawbacks of the linear TOF analyzer. However, this can be improved by increasing the length of the flight tube and lowering the acceleration voltage. Also kinetic energy of ions can be reduced by introducing a time delay between ion formation and extraction.[25,26] In this the ions are first allowed to expand into a field free region in the source and after a certain delay (hundreds of nanoseconds to several microseconds) a voltage pulse is applied to extract the ions outside the source. In this mode, the

ions initially are allowed to separate according to their kinetic energy in the field free region. For ions of the same m/z ratio, those with more energy move further towards the detector than the initially less energetic ions. The extraction pulse applied after a certain delay transmits more energy to the ions that remained for a long time in the source. Thus, initially less energetic ions receive more kinetic energy and join the initially more energetic ions at the detector. This feature helps to reduce peak broadening. This mode of operation is referred to as delayed extraction and was first developed by Wiley and McLaren in 1950s.[27]

Another way of improving mass resolution is to use an electrostatic reflector, also called a reflectron[22,28] (figure 2.4). The back of the reflector is at a voltage slightly higher than the source accelerating voltage. The reflector works by slowing an ion until it stops, is turned around, and is re-accelerated back to a second detector. Ions with an initial kinetic energy lower than the accelerating voltage will not penetrate the reflector as deeply and therefore will turn around sooner allowing them to "catch up" to ions with a higher kinetic energy. Ions with energies greater than the accelerating voltage will penetrate more deeply into the reflector and be turned around later. Their flight time is retarded, allowing the other ions to "catch up". All this gives a distribution of ions with the same m/z ratio similar flight times, thus improving resolution. An additional contribution to improving the resolution comes from the longer ion path-length in the reflectron TOF instrument. The gain in resolution, however, is at the expense of sensitivity. This is because transmission losses occur when ions pass through the reflector. The improvement in resolution by a reflector is most noticeable at masses of ~3000 or below, making it very useful for the analysis of trypsin generated peptides that are generated during proteomics analysis[29,30]

The MALDI process can lead to fragmentations that occur as a result of the excess energy that is imparted to the analyte during the desorption/ionization process. Three different types of fragmentation are:

i) Prompt fragmentation: occurs on a time scale equal to or less than the desorption event

ii) Fast fragmentation: occurring in the source after the desorption event but before the acceleration event

iii) Post source decay (PSD) fragmentation: occurs after the acceleration region

The first two lead to product ions that are always observed in the MALDI spectra, whereas product ions from PSD fragmentation need certain instrumental conditions to be observed.

MALDI-MS has been used primarily for the molecular mass determination of proteins. Two approaches – delayed extraction of in-source fragmentation[31] and the post source decay (PSD) process[32,33] have been developed to sequence peptides. Several other important classes of compounds such as oligonucleotides,[34] lipids,[35] and oligosaccharides[36] are also accessible to MALDI-MS. It is also an effective technique for the characterization of synthetic polymers.[37,38]

Electrospray Ionization – Mass Spectrometry (ESI-MS)

The significance of the development of the electrospray technique and the reason for its enormous contribution to modern MS methodology is its unique coupling of a method of solution introduction with the facility for ionization of highly polar and nonvolatile compounds. Much of the current importance of the electrospray mass spectrometry comes from the pioneering work of Fenn,[39] but Dole et al.[40] first recognized the possibility of generating gas-phase ions of macromolecules by spraying a solution from the tip of an electrically charged capillary. This early work, however, was hampered by the use of an ion-drift spectrometer, rather

than a mass spectrometer, for analysis. Building on Dole et.al's ideas, Fenn and co-workers[41] developed electrospray as a true interface for mass spectrometry. Thus, ESI is a method to produce gaseous ionized molecules from a liquid solution by creating a fine spray of droplets in the presence of a strong magnetic field.

A solution of the analyte is passed through a capillary which is held at high potential. The effect of the high electric field as the solution emerges is to generate a mist of highly charged droplets which pass down a potential and pressure gradient towards the analyzer portion of the mass spectrometer (figure 2.5). During that transition, the droplets reduce in size by evaporation of the solvent or by 'Coulombic explosion' i.e. further division of droplets resulting from the high charge density. Finally, fully desolvated ions result from complete evaporation of the solvent or by field desorption from the charged droplets. Nebulization of the solution emerging from the capillary may be facilitated by a sheath flow of nebulizer gas. Nebulizer gas is commonly incorporated on instruments, but its need for use is determined by the flow rate used, the composition of the solvent and the sign of the potential applied to the capillary tip. A high negative potential, in particular, may lead to a corona discharge unless suppressed by the use of the gas. A flow gas or controlled heating is usually applied to the interface[41,42] to promote droplet evaporation. Sampling of the desolvated ions is made using a capillary or a skimmer device.

Mechanism of the several stages of the electrospray process

The process is divided into three stages:[43]

1). Droplet formation

2). Droplet shrinkage

3). Gaseous ion formation

The solution delivered to the tip of the electrospray capillary experiences the electric field associated with the maintaining the tip at high potential. Assuming positive potential, positive ions will drift downfield in the solution, that is, towards the meniscus of the liquid, and negative ions will drift away from the surface. The mutual repulsion between the positive ions at the surface will overcome the surface tension of the liquid and the surface will begin to expand, allowing the positive charges and liquid to move downfield. A cone forms, called a 'Taylor cone'[44] (figure 2.6) and if the applied field is sufficiently high, a fine jet emerges from the cone tip which breaks up into small charged droplets. The diameter of the droplets formed is influenced by a number of parameters, including the applied potential, the flow rate and solvent properties.[45] Evaporation of solvent from the initially formed droplets, as they traverse a pressure gradient towards the analyzer of the mass spectrometer, leads to a reduction in diameter, with collisional warming.

The exact mechanism of the formation of gas phase ions from the charged droplets is a widely debated topic.[43,46-51] Two widely accepted mechanisms are: i) the charge residue model and ii) the ion desorption model.[46-48] According to the charge residue model as the droplets shrink in size due to the solvent evaporation, the charge density on their surface increases until it reaches the Rayleigh instability limit. At this point, the repulsive Coulombic forces exceed the droplet surface tension, causing the droplets to break into smaller and highly charged offspring droplets. The sequence of the solvent evaporation and fission of the droplets is repeated several times until the droplet size becomes so small that each contains only one solute molecule. As the last of the solvent is evaporated, this molecule is dispersed into the ambient gas, retaining some of the charge of the droplets. The ion desorption model was proposed by Iribarne and Thomson.[52] In this model also, the sequence of solvent evaporation and droplet fission is

repeated. However, instead of droplets becoming so small that they contain only one solute molecule, at some intermediate droplet size the electric field due to the surface charge density is sufficiently high to overcome the droplet cohesive forces leading to direct ion desorption.

To achieve the full benefits of the ESI and LC/ESIMS combination, a mass spectrometer should have high scan speed, adequate mass range, reasonable mass resolution, and high sensitivity. Although several types of mass analyzers are available, a quadrupole mass filter offers most of these desirable features.[53,54]

Electrospray has also been implemented with other types of mass analyzers, including ion-trap,[52] magnetic-sectors,[55] FT-ICR,[56] and TOF-based mass spectrometers.[57,58] The coupling of ESI with TOFMS has been accomplished by using an orthogonal ion extraction approach, in which ESI produced ions are stored between each duty cycle, and are pushed into the flight tube in the pulse mode.[57]

Quadrupoles are dynamic mass analyzers, in which the ion trajectories are controlled by a set of time-dependent forces that are generated by applied direct current (dc) and radiofrequency (rf) potentials to a set of electrodes. A quadrupole mass analyzer is a two-dimensional quadrupole field device. A shown in figure 2.7, it consists of four accurately aligned parallel rods that are arranged symmetrically in a square array. The field within the square array is created by electrically connecting opposite pairs together. Ions are ejected at one end of the quadrupole structure in the direction of the quadrupole rod. The separation of different m/z ions is accomplished through the criterion of path stability with the quadrupole field. In other words, at a given set of operating parameters, ions of very narrow m/z range have stable trajectories, whereas the remainder of the ions will have unstable trajectories.[58] To obtain a mass spectrum, the quadrupole field is varied to force other ions to follow a stable path.

The mass range and resolution of a quadrupole mass spectrometer are both dependent on the length, and diameter of the quadrupole rods, the applied voltage, the rf frequency and the initial kinetic energy of ions. In principle, the upper mass limit can be increased by increasing the amplitude of the rf signal, decreasing its frequency, and using small-diameter rods. As a consequence, an upper mass limit of only 4000 Da is accessible.[59] Typically quadrupole mass spectrometers operate at unit mass resolution, which is sufficient to separate two peaks one mass unit apart. Resolution can be improved by decreasing the velocity of ions, increasing the frequency of the rf signal and using longer rods.

Several useful attributes of a quadrupole mass filter are; low cost, mechanical simplicity, high scan speeds, high transmission, increased sensitivity, independence from energy distribution ions, and linear mass range. Quadrupoles can tolerate relatively high pressures in the ion source and mass analyzer regions and it is this feature that has led to their widespread use as detectors for liquid chromatography, gas chromatography and capillary electrophoresis techniques.

Application of Mass Spectrometry in Hydrogen/Deuterium Exchange Studies

Biochemists traditionally have employed a variety of biophysical techniques for the study of structural changes in proteins. These methods include infrared[61-63] and ultraviolet absorption spectroscopy,[61,62,64,65] tryptophan fluorescence,[66] circular dichroism (CD),[61,62,67] X-ray crystallography,[61,62] nuclear magnetic resonance spectroscopy,[61,62,68] viscometry,[61,62] and neutron diffraction.[69] IR[63] and UV[64,65] spectroscopy techniques, in conjunction with hydrogen/deuterium (H/D) exchange, have been used to characterize fluctuations between different protein conformations. Although these techniques can quantify the incorporated deuterium levels of a whole protein, they are unable to access the deuterium incorporation in specific regions of a protein. One- and two-dimensional NMR, combined with H/D exchange, has been applied with a

great success in the detection of changes in protein structures. One-dimensional NMR, however, is restricted to small, highly soluble proteins.[70] Since two-dimensional NMR is a high resolution technique, it is applicable to proteins with increased number of peptide linkages. The technique has been successfully used in a number of situations that include studies of protein-ligand binding,[71,72] folding-unfolding dynamics,[68,73,74] mutants,[75,76] and functional variants.[77] However, the large-sized proteins (>50,000 Da) are still outside the realm of NMR analysis. The response in CD is sensitive to the secondary structure of a protein, therefore, the relative proportions of α-helical, β-sheet, and random-coil structures are easily assessed with this technique.[78] CD has gained popularity as a convenient technique for studying variations in conformational states in proteins that are induced as a result of changes in temperature, pH, salt, ligand binding, and quaternary structure. Although CD and fluorescence methods are both simple, they provide only an overview of the protein structure.

Mass spectrometry has also been incorporated in the protocols for the determination of the conformational changes in proteins.[79,80] This development was made possible with the advent of electrospray ionization (ESI) as a means of transforming dissolved proteins and peptide molecules into gas-phase ions.[81,82] A rationale for the use of ESIMS for probing conformational structures of proteins is that during the ESI process the solution-phase structure of the protein is largely preserved. Therefore, the ESI mass spectra of a protein can be considered a reflection of its aqueous solution chemistry.[83-86] The multiple-charging feature of ESI is also a valuable asset because it allows the study of much larger proteins. Although differences in the charge profile of molecular ions are related to the conformational changes in a protein's tertiary structure, they cannot be a reliable measure of the protein's conformation because of the fact that the ESI ion profile may change with changes in certain experimental variables in the ESI ion source, such as

gas flows, voltage settings, and unavoidable altered solution conditions (slight variation in pH, the presence of counterions, surface tension, rate of desolvation and declustering, protein concentration, etc.). A more precise method for gauging the conformational state is isotopic hydrogen exchange. This term refers to the replacement of the labile amide hydrogens in proteins with the hydrogens of different isotopic composition (deuterium) in solvent water. In conjunction with H/D exchange, ESIMS has gained prominence as a technique for studies concerned with the conformational structures of proteins. Katta and Chait were the first to combine H/D exchange with mass spectrometry to probe the conformational changes in proteins.[87,88] Wagner and Anderegg suggested that such measurements must be performed with care to ensure that the exchange rates are not affected due to changes in chemical environment.[89]

Determination of the amide hydrogen exchange rate in proteins has become a prominent technique for study of their conformational structures. This approach is based on the premise that the exchange rate of amide hydrogens is sensitive to the conformational states of proteins: faster exchange is indicative of a more open structure, and slower exchange is related to a tightly folded, compact state.[90,91] In the native state, only the surface hydrogens exchange at a relatively fast rate, whereas the inner-core hydrogens exchange much more slowly, and often have no detectable exchange even after several days. Solvent inaccessibility and hydrogen bonding in the compact structure of proteins are the principal factors that have been implicated for slow exchange rates (figure 2.8).

In addition to a protein's structure, the isotopic exchange rate is also affected by the experimental variables such as pH and temperature (figure 2.9 and 2.10). An additional factor that has a bearing on the exchange rate is the neighboring effect of adjacent amino acid residues.

Thus, considerable structural information can be gleaned by determining the hydrogen exchange rates of different amide linkages in proteins.[90,91]

Hydrogen exchange in proteins is catalyzed by H^+ and OH^- ions.[92] The rate constant for hydrogen exchange (k_{ex}) is the sum of the rate constants for acid-(k_H) and base-catalyzed (k_{OH}) reactions as shown in the equation:

$$k_{ex} = k_H[H^+] + k_{OH}[OH^-]$$

The shape of the curve that illustrates the effect of pH on the exchange rate is given in figure 2.9, which indicates that the slowest rate occurs close to pH 2.8. At more basic pH values, the exchange rate is affected by OH^- ion activity, and at more acid pH, by H^+ ion activity. It can be seen from figures 2.9 and 2.10 that the exchange rate changes by a factor of 10 for each unit change of pH. It can also be seen from the figure 2.10 that temperature also plays an important role in the study. By dropping the pH down to around pH 2.7, the exchange rates have decreased dramatically but the time required to carry out the analysis is still relatively short. This can be overcome by decreasing the temperature to 0^oC which then gives another 10 fold decrease in exchange rate, allowing sufficient time to carry out the measurements. The opening of the secondary and tertiary structures of a protein may increase the amide hydrogen exchange rate for a particular residue by as much as 10^8. This large change in the exchange rate forms the basis of the use of amide hydrogen exchange as a sensitive probe to study the conformational changes in protein.

Several different mass spectrometric approaches are used to determine the amide hydrogen exchange rates. Continuous labeling and pulsed labeling are two common approaches, and both can be used to study global as well as localized structural changes.

Hydrogen Exchange for Detection of Global Changes in Proteins

In order to detect global changes, hydrogen/deuterium exchange is performed by ESIMS on an intact protein. This experiment provides the exchange rate averages over all amide hydrogens in a protein. In a typical ESIMS procedure for the measurement of the rate constant for the folding process, the protein is dissolved in D_2O buffered to the desired pH.[93] The solution is heated to a high enough temperature to ensure that the protein is completely unfolded. If a protein cannot withstand heating, an alternative approach such as lowering the temperature or addition of a denaturant is used. Because of the unfolding of the protein, all amide hydrogens can be accessed. The fully deuterated protein is lyophilized and redissolved in D_2O. The exchange is initiated by diluting the concentrated D_2O solution of the protein with H_2O that has been adjusted to the desired pH. The samples are withdrawn at several time points, and are analyzed by ESIMS.

In order to study the kinetics of the unfolding process, the lyophilized folded protein is dissolved in D_2O at a pH where folded and unfolded states both coexist. The samples are withdrawn at different time intervals, and are analyzed by ESIMS. A particular charge state of the folded protein is selected, and deuterium incorporation is estimated from these measurements by the increase in mass of the peak. The intensity of the deuterated peak is a measure of the amount of the unfolded state. The change in abundance of the native and deuterated peaks is monitored at different time periods.

Hydrogen exchange in the *pulsed-labeling* technique is studied using a quench-flow apparatus.[93,94] The approach is well suited to determination of the isotopic exchange rates of rapidly exchanging amide hydrogens. In *pulsed-labeling* experiments, the exposure of the protein to D_2O is short relative to the time scale of the folding/unfolding dynamics. Since little unfolding

or folding occurs during the labeling step, the deuterium levels resulting from *pulsed-labeling* indicate the instantaneous populations of folded and unfolded molecules. Although pulsed labeling has been used in several NMR studies,[95-97] it has been used in only few MS studies.[98-102] A schematic diagram of a quench-flow apparatus that can be used in the pulsed-labeling technique is shown in figure 2.11. As with the *continuous-labeling* procedure, the protein is exposed to D_2O while the populations of folded and unfolded states are changing. Molecules that are or become unfolded during the labeling time are completely deuterated and molecules that did not unfold during this time have less deuterium incorporation. Deuterium levels in proteins labeled continuously effectively integrate the number of molecules that unfold during the labeling time, which may be as short as milliseconds or as long as days.

Determination of Hydrogen Exchange in Short Segments of Proteins

Although hydrogen exchange measurements by ESIMS on an intact protein allow the global changes to be readily assessed, the resolution of the method is limited and so it is not applicable to identification of the localized structural changes during hydrogen exchange. In order to overcome this limitation, *fragmentation-mass spectrometry* method has been developed, in which hydrogen exchange is combined with proteolytic fragmentation of the protein. In this approach, first developed by Smith and his associates, the deuterated protein is cleaved into small segments by pepsin digestion, followed by mass spectrometric analysis of the protein digest.[101,102]

A typical continuous-labeling procedure used for protein fragmentation-mass spectrometry is illustrated in figure 2.12. In this protocol, the exchange is performed for a defined time interval by incubating the folded protein in a D_2O solution at an appropriate pH. At the end of the defined time interval, the exchange process is quenched by adjusting the pH to 2.5

and temperature to 0°C. Next, the protein is digested with pepsin, which is chosen because it has maximum proteolytic activity at an acidic pH. The deuterium levels of all peptide fragments of the digest are determined using HPLC coupled on-line with ESIMS under conditions that minimize any hydrogen back-exchange at the peptide amide linkages.[98,103-105] The extent of deuterium incorporation is determined by comparing the ESI mass spectra with reference spectra of the same peptide that contains no deuterium. In the past, an on-line combination of HPLC and continuous-flow FAB was also implemented for this purpose.[102,106-108]

The pulsed-labeling approach can also be used to study the isotope exchange in short segments of a protein.[98-100,103] A quench-flow apparatus is used for these experiments. The apparatus shown in figure 2.11 can be modified to suit these experiments. First, a pepsin column is added to perform an on-line peptide digestion. Second, the proteolytic fragments are separated and analyzed by the HPLC-ESIMS combination. A schematic diagram of this modified apparatus is shown in figure 2.13.

Matrix-Assisted Laser Desorption/Ionization for Study of Conformational Changes

In contrast to ESIMS, only a handful of studies have been reported that use MALDIMS to probe the conformational changes in proteins and peptides.[109-111] Mandell et al. have used the combined fragmentation-mass spectrometry-hydrogen/deuterium exchange approach with MALDIMS to determine the kinetics of hydrogen/deuterium exchange in proteins.[109] As usual, the isotopic exchange of the amide hydrogens is performed by incubating the protein for variable times in D_2O at a pH of 7.2. The exchange is quenched at pH 2.5 and 0°C. Next, the labeled protein is digested with an enzyme, and the protein digest and the matrix are loaded onto the chilled MALDI target for mass analysis. The advantages of using MALDIMS over ESIMS are the elimination of an HPLC separation step, the ability to analyze smaller sample amounts, and

faster analysis times. Russell and colleagues have used MALDIMS and hydrogen/deuterium exchange to probe the conformational changes in a few medium-sized peptides such as Bradykinin, α-melanocyte-stimulating hormone, and melittin.[110,111] It was found that these peptides acquire a more compact structure in organic solvents.

In an interesting application, MALDI-TOFMS, in combination with hydrogen/deuterium exchange, has been successfully used to determine the conformational states of proteins,[112] that come into contact with solid surfaces during isolation or experimental studies. The conformation of proteins can be altered when they are adsorbed on solid surfaces. As a consequence, the biological functioning of proteins may be affected. Therefore, it is important to know the stability of proteins that are physically adsorbed onto solid substrates.

Hydrogen/Deuterium Exchange for Study of Noncovalent Complexes

The technique of hydrogen/deuterium exchange has achieved a high level of success in the detection of protein denaturation, conformational states, and folding-unfolding dynamics.[79,88,102] The protocol can also be used to detect noncovalent complexes of proteins.[113-115] The basic premise is that the regions of the proteins that participate in molecular interactions should have a different rate of exchange relative to the regions that are more accessible to the solvent. In a typical procedure for the study of antigen-antibody complexes[116], the protein is first deuterated at a pH between 6 and 7, then passed through an antibody column, and deuteriums of the antigen-antibody complex are exchanged back to hydrogens (deuteriums of the bound epitope are unaccessible to hydrogen/deuterium exchange). After quenching the hydrogen/deuterium exchange, the antigen-antibody complex is digested with pepsin, and the peptide fragments are analyzed by LC-ESIMS. Epitopic peptides show an increase in mass as a result of retention of the deuterium labels. Examples of the use of this technique are the detection

of the complex between the molecular chaperone GroEL and bovine α-lactalbumin[113] and the interaction of the enzyme *E.coli* dihyrodipicolinate reductase with its substrate nicotinamide adenine dinucleotide and an inhibitor 2,6-pyridinedicarboxylate.[115]

Smith el. al. have discussed the merits of mass spectrometry over NMR in protein conformation studies.[79,80] Mass spectrometry offers several distinct advantages in terms of sensitivity and extended mass range, as well as providing information complementary to NMR. The ESIMS approach is at least three orders of magnitude more sensitive than NMR. NMR is limited to proteins with a molecular mass of <30,000 Da[79,80], whereas mass spectrometry can be used to study much higher molecular mass and complex multimeric, mutlidomain proteins. Another advantage of mass spectrometry over NMR is the timescale. With the combined ESIMS H/D exchange procedure, the exchange rates of the most rapidly exchanging amide hydrogens can be determined.

The Cell Wall

To be successful in attacking a host cell, a pathogen must pass the outer barrier of a cell. In plants, the outer barrier is the cell wall which consist of three layers; the middle lamella, primary cell wall and secondary cell wall. The middle lamella, derived from the cell plate, can be found at the most exterior part of the cell wall – the layer that lies in the middle of two adjoining cells. The next layer is the primary cell wall, formed after the middle lamella, which consists of a skeleton of cellulose microfibrils cross-linked by hemicellulosic polymers and embedded in a gel-like pectin matrix. The third layer, the secondary cell wall, is produced in certain cell types inside the primary wall after enlargement is complete.[117,118] With each layer the strength of the cell wall increases as the cell continues to take on more of its role in the life of the plant (figure 2.14).

The cell wall can be divided into the polysaccharide networks[119] known as the

i) Cellulose/hemicellulose network and

ii) the pectin network

Cellulose represents the major constituent of cell wall polysaccharide and consists of a linear polymer of β-1,4-linked D-glucose residues. The cellulose polymers are present as ordered structures (fibers) and their main function is to ensure the strength of the plant cell wall. Hemicelluloses are heterogeneous polysaccharides and are the second most abundant organic structure in the plant cell wall.

Pectin forms another group of heteropolysaccharides and consists of a backbone of α-1,4-linked D galacturonic acid residues. In primary cell walls, the pectin network consists of smooth regions composed of homogalacturonans (HG) which are linear chains of 1,4-linked α-D-galactopyranosyluronic acid residues in which some of the carboxyl groups are methyl esterified. In some cases they can also be acetylated at C-2 or C-3 chains.[120] The hairy region in the pectin network is composed of the highly branched rhamnogalacturonans I and II (RG-I and RG-II).[121,122] RG-I contains a backbone of a repeating disaccharide [-4)-α-D-Gal*p*A (1-2)-α-L-Rha*p*-(1-]. The backbone Gal*p*A is typically not substituted with oligosaccharides but 20-80% of the Rha*p* residues are substituted at C-4 with neutral and acidic oligosaccharides side chains.[123] In RG-II, the backbone is composed of 1,4-linked α-D-Gal*p*A residues and resembles more closely to HG structure.

While the pectic polysaccharides are more or less structurally independent of the cellulose-hemicellulose network, however functionally the cellulose-hemicellulose network are co-dependent.[124,125] The primary roles of the pectin network are thought to be control of the wall's mechanical properties and cementing of adjacent cells together. Some studies suggest

pectins are held in place in the wall by their interactions with divalent cations, especially calcium. In some cases where the pectins are heavily methylated or when low calcium levels are present in the cell wall, they are held together by hydrogen bonds.[126] Other studies suggest that pectins are covalently cross-linked.[127,128] For example, RGII molecules are cross linked as part of a borate complex diester.[129]

The complexity of the cell wall and the ability of the plant to defend itself against pathogens severely limit the number of successful pathogenic attacks. However, upon attack the plant elicits a series of active responses that further enable the plant to defend itself. The wall's active lines of defense include the hypertensive response, callose deposition, synthesis of phytoalexins and accumulation of pathogenesis-related proteins.[130] This last class of defense actively works to counteract the presence of the attacking pathogen. Pathogenesis-related proteins are proteins coded for by the host plant, but are not induced until the presence of a pathogen is detected.[131] These proteins are therefore defined in this way because of their increased presence during pathogenic attack.[132] Polygalacturonase inhibiting protein is an example of this type of protein. Its goal is to limit the destruction of the cell wall caused by certain pectin degrading enzymes.

Polygalacturonases and Polygalacturonase Inhibiting Proteins

Given that the cell wall is the plant's first line of defense against pathogens, a pathogen must be able to break through the cell wall in order to successfully invade the plant. Primarily this is achieved through the use of cell wall degrading enzymes. The most extensively studied cell wall degrading enzymes are polygalacturonases produced by fungi, which cleave the linkages between D-galacturonic acid residues in non-methylated homogalacturonan, a major component of pectin.[133,134] This is consistent with observations that fungi initially attack the

middle lamella. The middle lamella contains the highest concentrations of pectic polymers, therefore the fungi uses these enzymes as a pretreatment so that other cell wall degrading enzymes can successfully attack their substrate. Oligosaccharides derived from fungal and plant cell wall polysaccharides are one class of well characterized elicitors, that, in some cases, can induce defense response.[135] Cell wall oligosaccharides elicit numerous defense mechanisms that have evolved in plants to prevent invasion by pathogenic fungi.[136-139].

The elicitor activity of oligogalacturonic acid (OGA) has been reported in many dicotyledonous plants, but there has been no report in monocot plants. This might be due to the substantially lower content of pectic polysaccharides in monocot cell walls. Therefore, a pathogen that feeds off of dicots must produce more pectin degrading enzymes then pathogens that use monocots as a host.[140-142] The pathogen must also overcome obstacles within its host. The action of pectin degrading enzymes needs to be altered due to complex structure of pectin polysaccharides.[143,144]

The ability of pathogens to penetrate the cell wall may be significantly affected by the diversity and complexity of pectin polysaccharides found in the cell walls. PGs from a single species of fungus can exist in several isoforms to combat this diversity of cell wall polysaccharides. The differences in primary structure between isoforms affect their degrees of stability, substrate preference, specific activity, and pattern of hydrolysis.[145-148]. For example most PGs hydrolyze pectin polymers in either an endo- or exo- fashion. Endo-PGs randomly cleave internal regions of homogalacturonan polysaccharide releasing oligogalacturonic acid. Exo-PGs only cleave at the non-reducing terminal end of a homogalacturonan polysaccharide releasing galacturonic acids.[143,149] Another class of PGs hydrolyze pectin polymers in both an endo-and exo- fashion. Thus, due to the complexity of the pectin network, a successful attack is

often not accomplished by the action of a single polygalacturonase isoform. The success is determined by the combination of the various isoforms that it contains. Targeted gene disruption of pectinase genes has been performed to evaluate the role of some of these enzymes in pathogenicity and a reduced virulence was observed in several fungi that caused tissue maceration. An example that demonstrates this observation is Botrytis Cinerea, a fungus that causes gray mold rot.[150]

Plants have evolved successful defense mechanisms against the attack of a wide range of pathogenic microorganisms. As they lack a circulatory system of antibodies, their defense relies on the capability of each cell to recognize the presence of pathogens and subsequently activate defense responses.

Polygalacturonase-inhibiting proteins (PGIPs) are extracellular proteins, ionically bound to the plant cell wall which limits the fungal invasion by counteracting PG activity.[145] Their inhibitory activity favors the accumulation of fragments of homogalacturonan, which acts as elicitors of plant responses.[151] Plants have evolved PGIPs with different recognition capabilities against many PGs secreted by pathogenic fungi. Moreover the expression of various PGIPs is regulated and is induced by different stress related molecules through separate transduction pathways.[152]

The typical structure of PGIPs is comprised of a signal peptide for translocation into the ER and a mature polypeptide of amino acids displaying several potential glycosylation sites. The mature PGIPs are characterized by the presence of 9-10 repeats, each derived from modifications of a 24 amino acid leucine-rich peptide. The LRR element contains the consensus sequence L**xxLxLxx**NxLT/SGxIPxxLxxLxx, where residues indicated in bold form a β-strand/β-turn structure, the region responsible for binding PGs.[153] Through the use of site-directed

mutagenesis, Leckie et al. were able to demonstrate the importance of the amino acids that lie within the solvent exposed β-strand/β-turn structure to the specificity of interactions.[154] The role of PGIPs as important players in the defense response is highlighted by the factor that they are induced during infection, retard PG function, prevent cell wall degradation and limit fungal growth and colonization.

Although effective in their ability to regulate a wide range of PGs, PGIPs are only effective against fungal PGs and not against other PGs of either microbial or plant origin.[155] The versatility of the LRR protein scaffold should allow researchers to obtain more potent inhibitors of pathogen enzyme or inhibitors with novel recognition abilities by *in vitro* 'directed' evolution. The interactions of PGIPs with PGs play an important role in the understanding of how plants are able to resist certain pathogens. Understanding these interactions is of great importance to agricultural industries because it can lead to engineering of pathogen resistant plants.

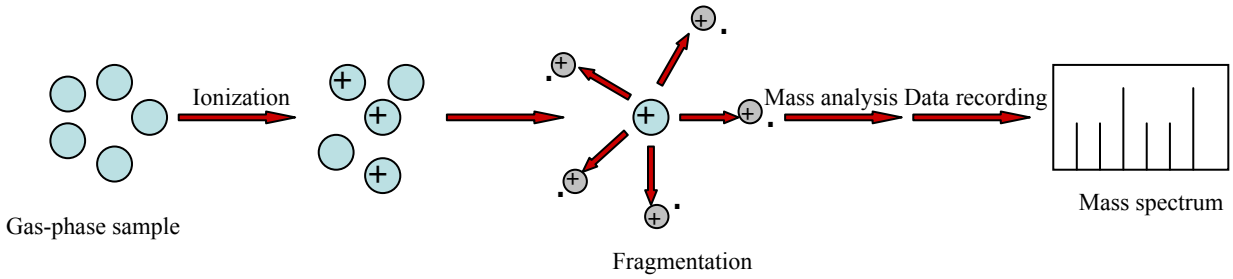

Figure 2.1: Basic concept of mass spectrometry analysis

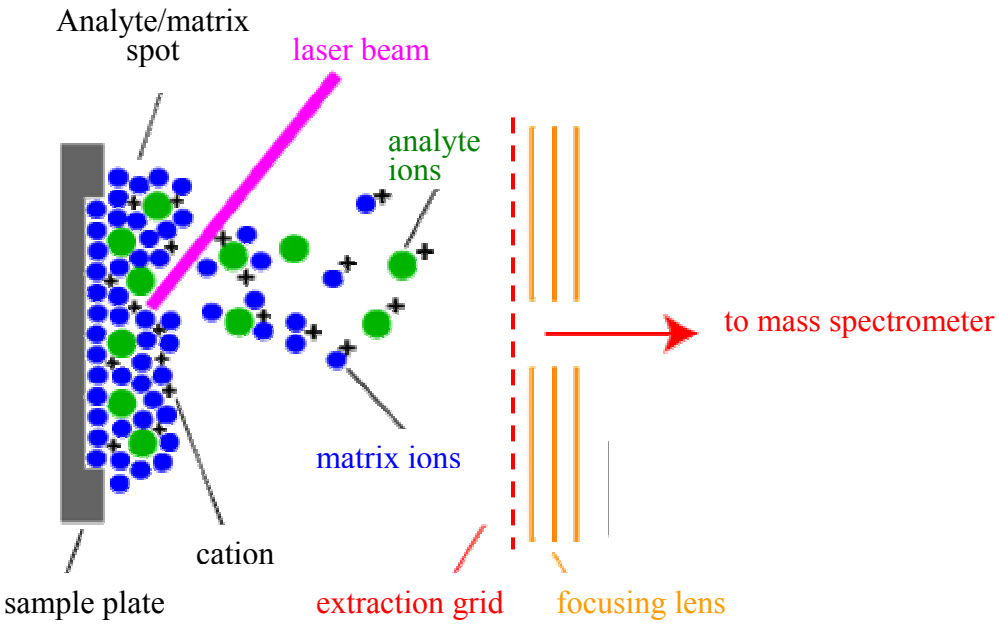

Figure 2.2: A schematic diagram of the mechanism of MALDI

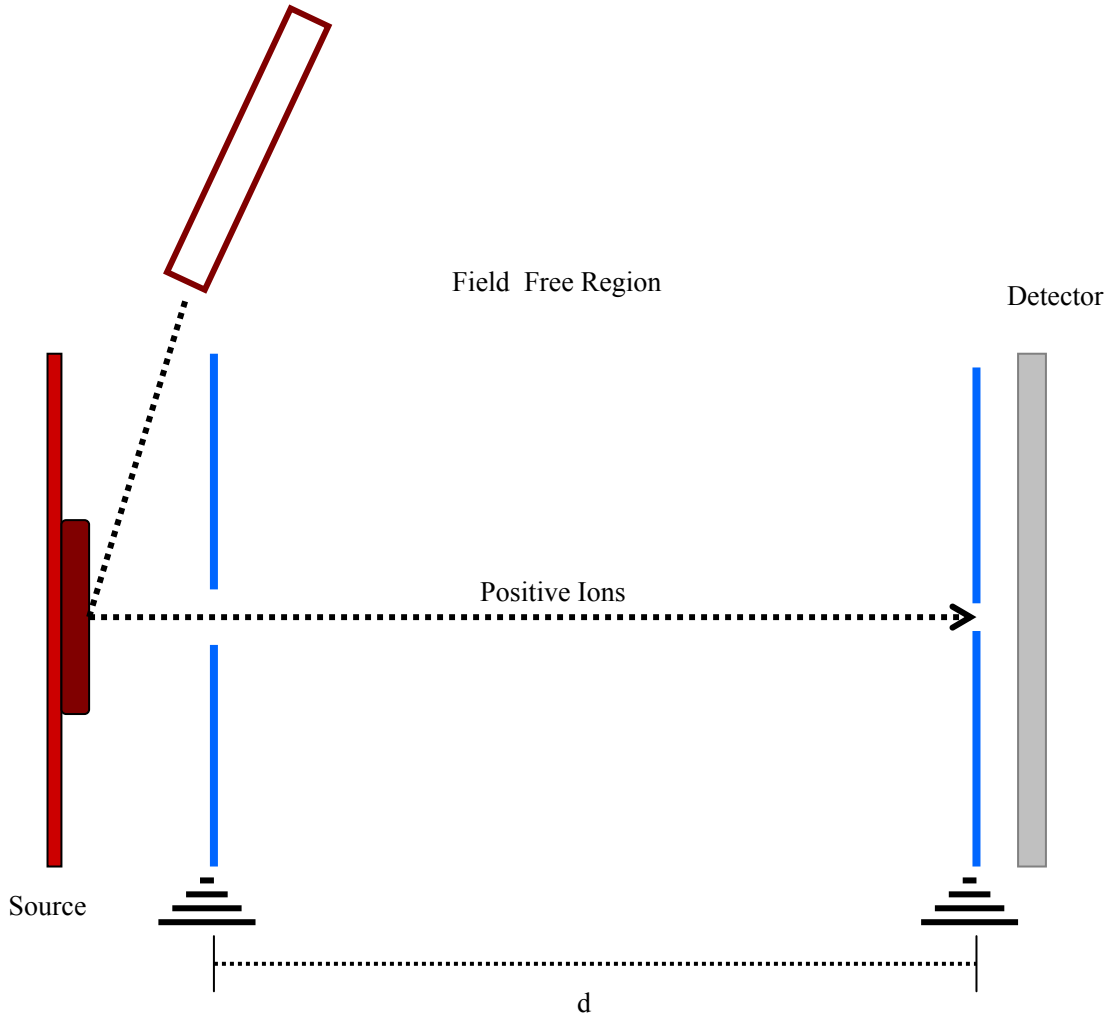

Figure 2.3: Schematic of a linear time-of-flight mass analyzer

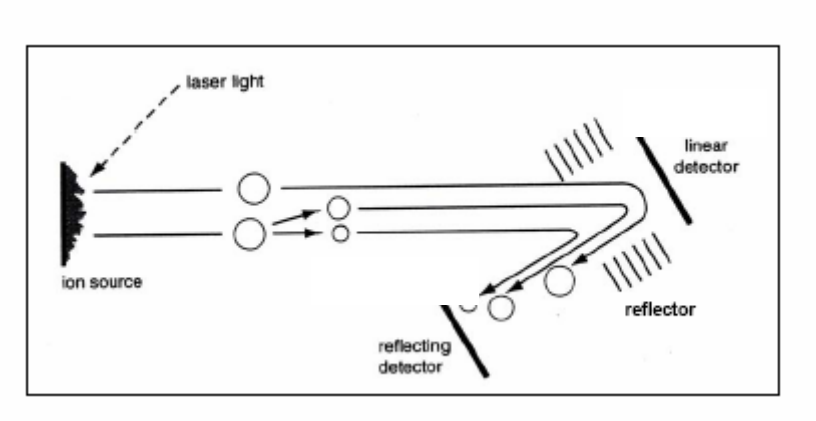

Figure 2.4: A schematic of time-of-flight mass spectrometer operating in reflectron mode

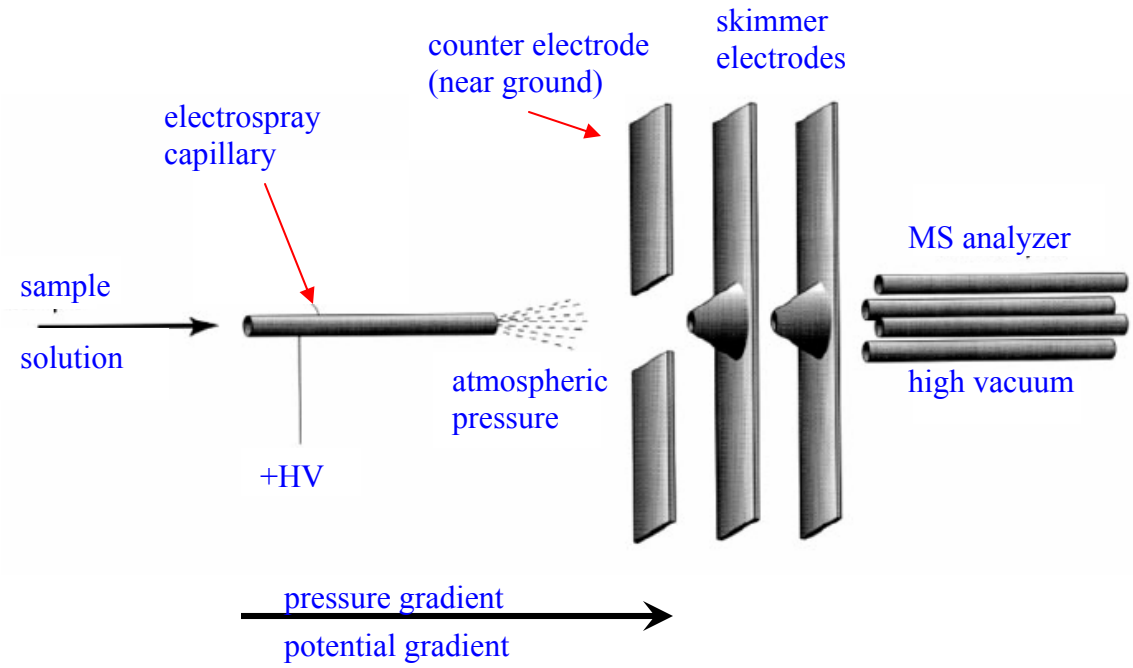

Figure 2.5: Essential features of the electrospray interface

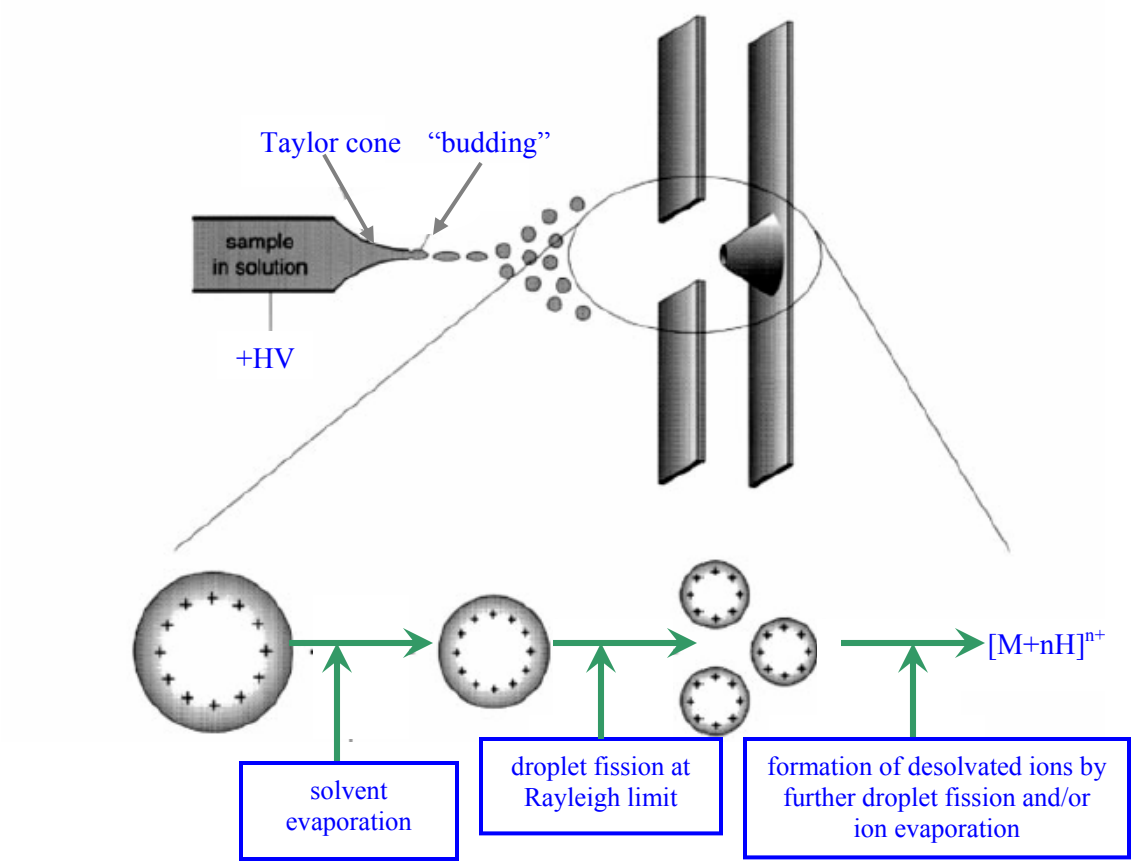

Figure 2.6: Droplet formation in an electrospray interface

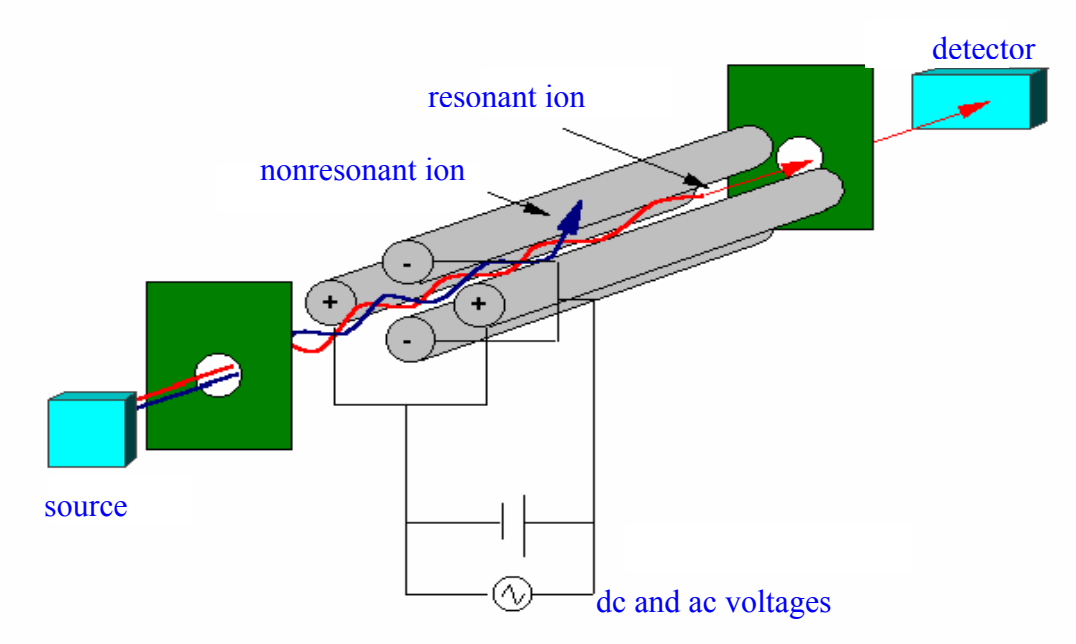

Figure 2.7: A schematic of quadrupole mass analyzer

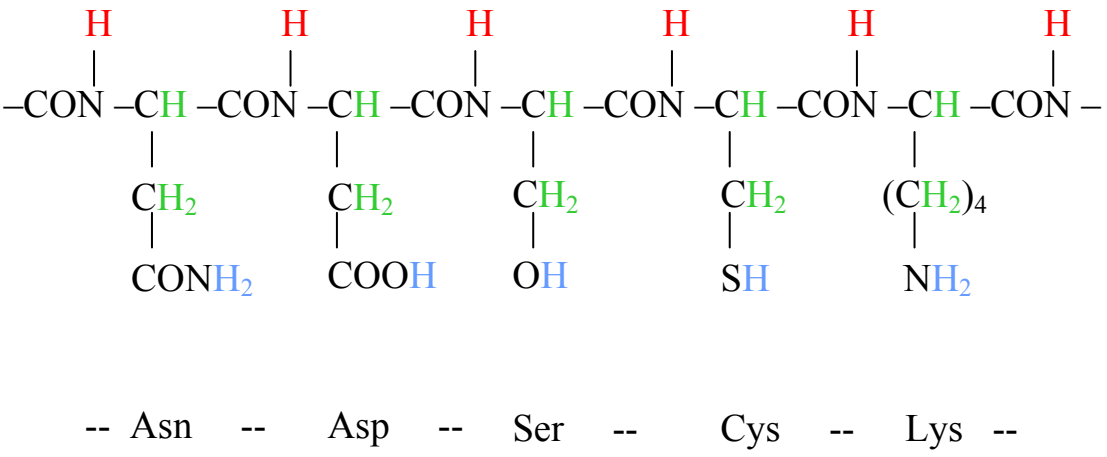

Figure 2.8: Hydrogens in proteins[156]

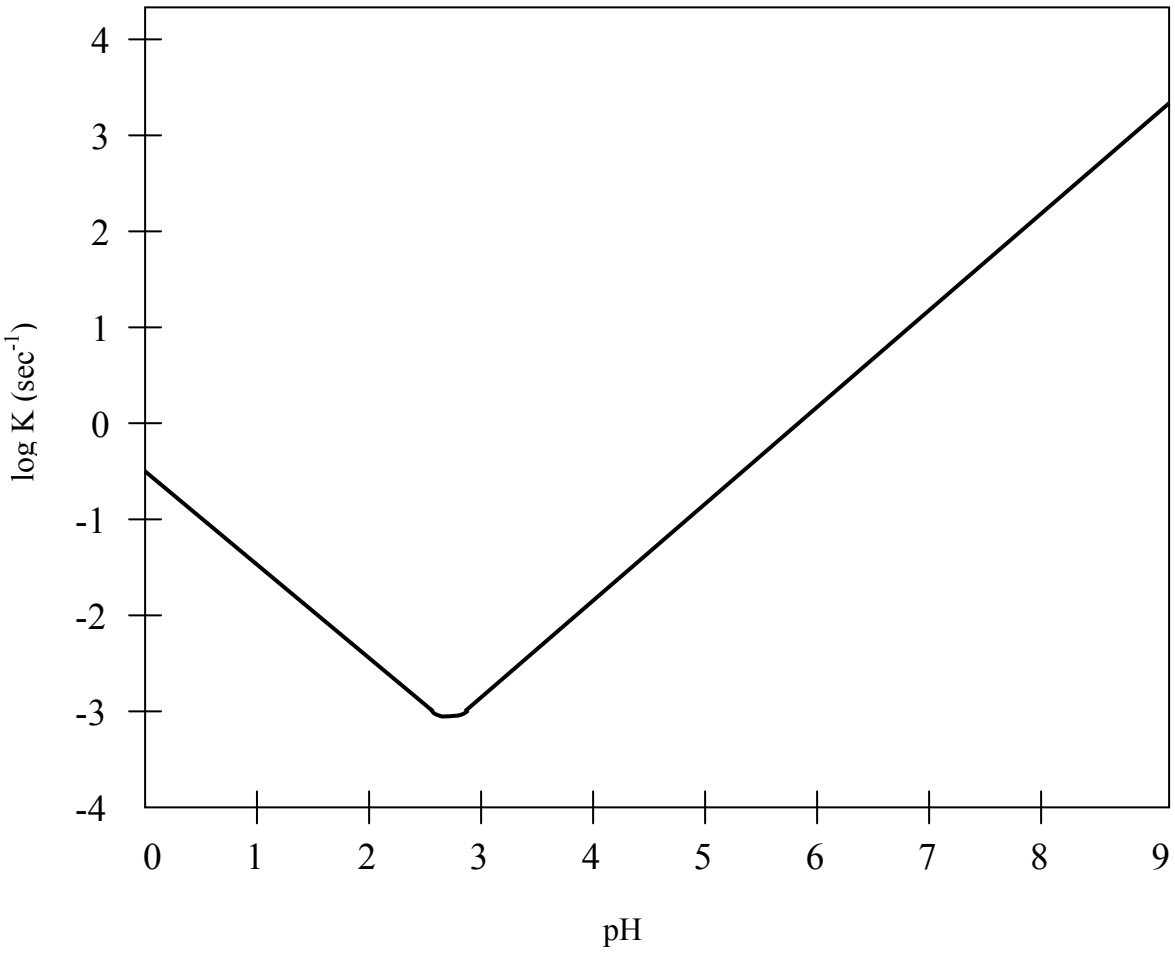

Figure 2.9: Peptide amide hydrogen exchange rate constant vs. pH[79]
[Reproduced from Ref.79 by permission of John Wiley and Sons, Ltd (Copyright 1997).]

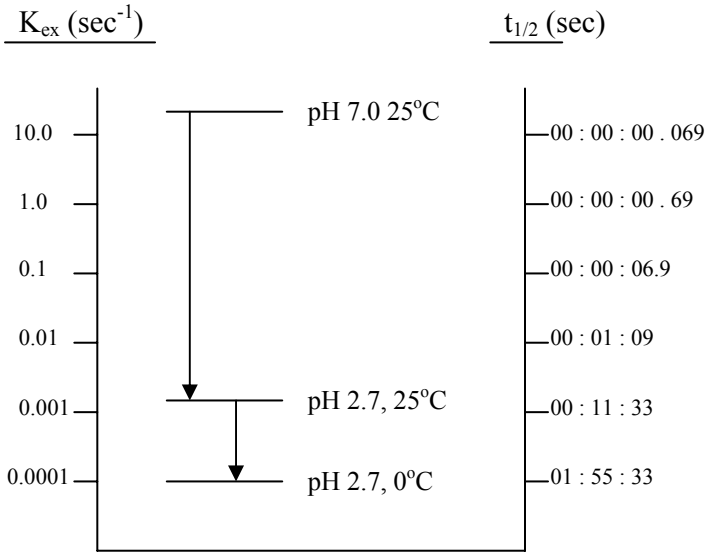

Figure 2.10: pH control and temperature[156]

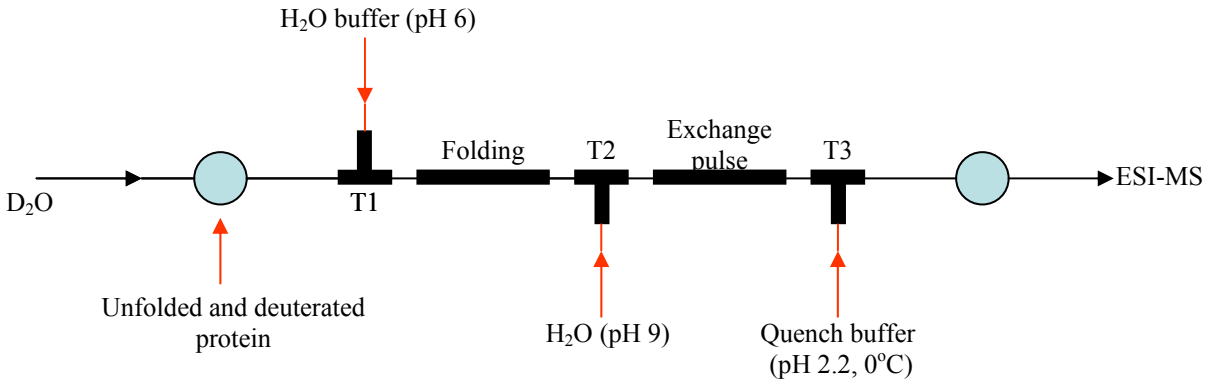

Figure 2.11: A schematic diagram of a quench-flow apparatus that can be used in the pulsed-labeling technique

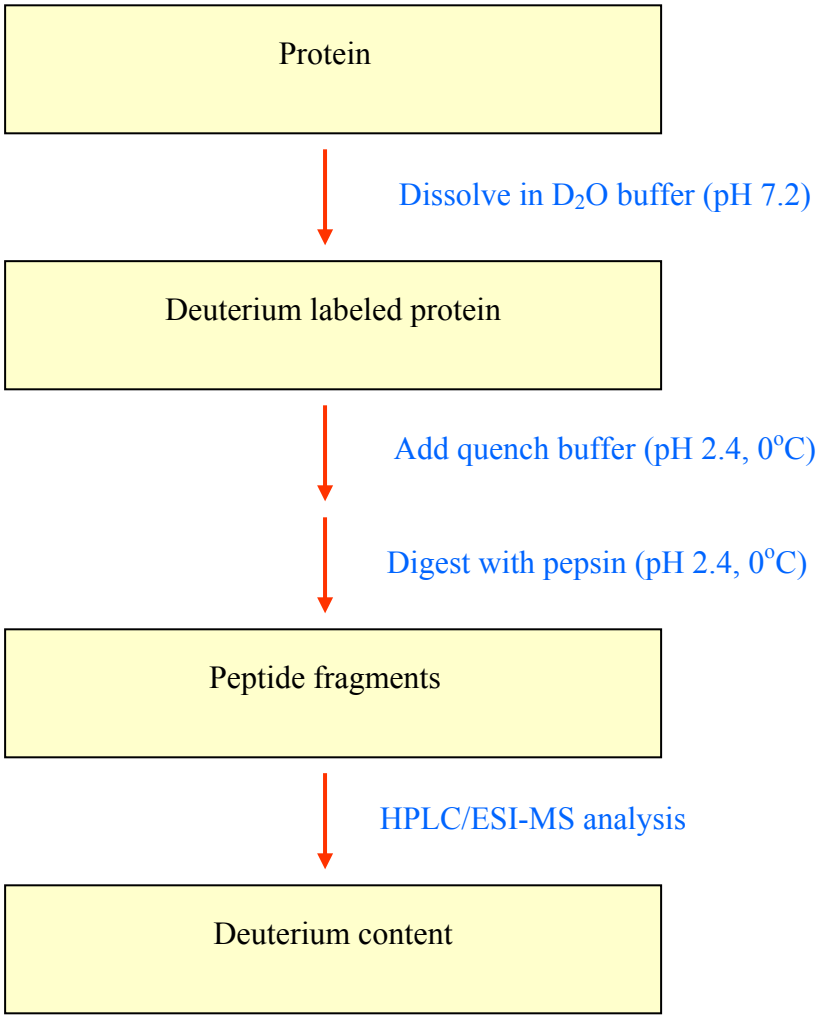

Figure 2.12: A flow diagram of a typical procedure used to determine deuterium levels at peptide amide linkages in short segments of intact proteins following hydrogen/deuterium exchange

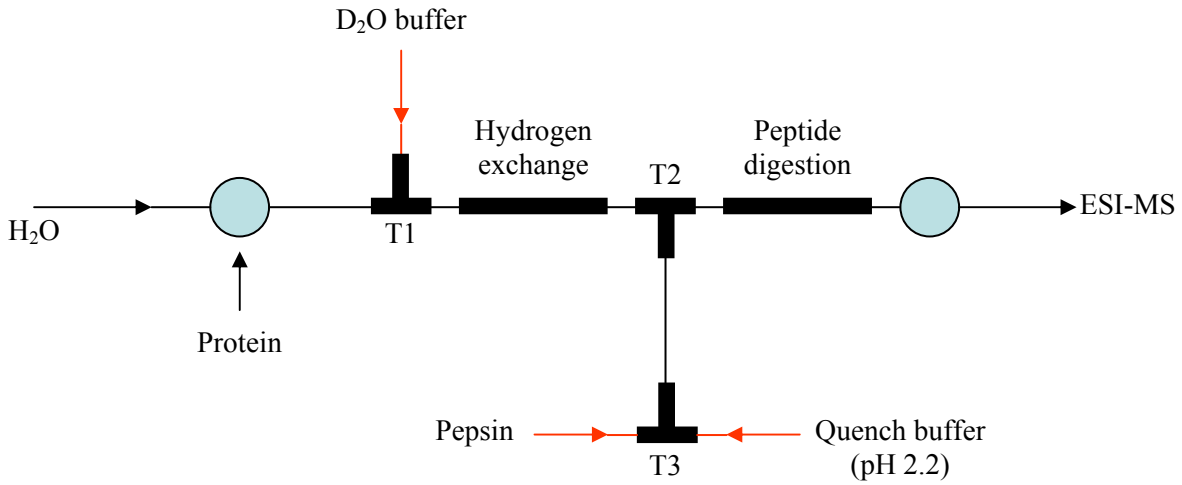

Figure 2.13: A schematic diagram of a quench-flow apparatus used in pulse-labeling technique for the determination of hydrogen/deuterium exchange in short segments of intact proteins

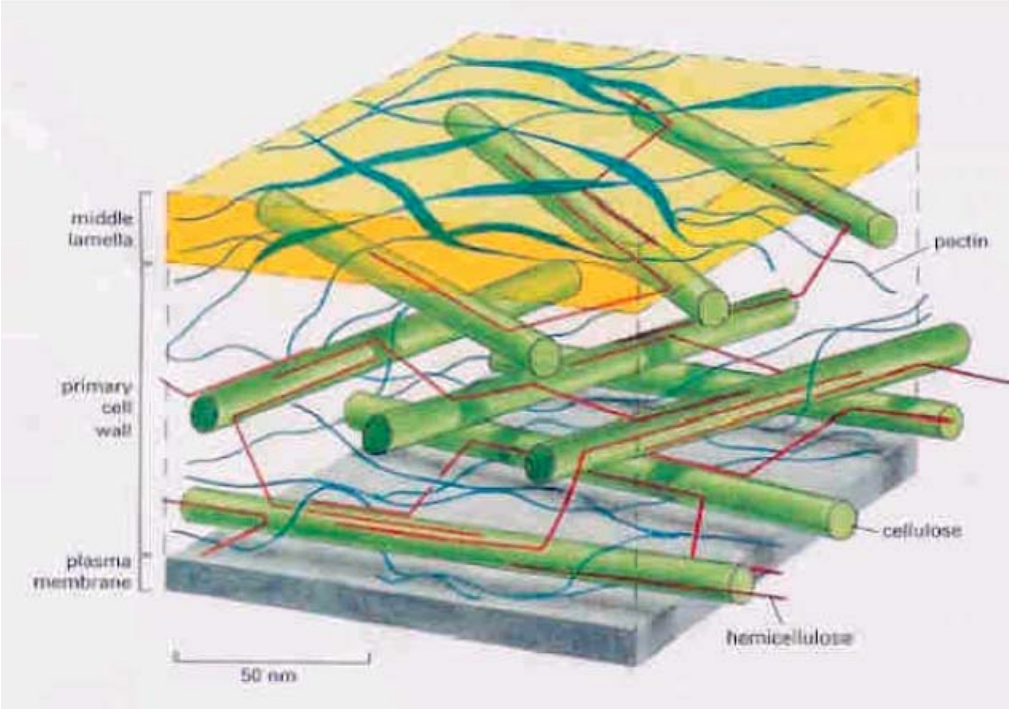

Figure 2.14: Structure of primary plant cell wall[118]

Reference List

1. Thomson, J.J. *Philos. Mag.* **1897,** 44, 293.
2. McLuckey, S.A.; Wells, M.J. *Chem. Rev.* **2001,** 101, 571-606.
3. Bierbaum, V.M. *Chem. Rev.* **2001,** 101, 209-210.
4. Prebyl, B.; Johnson, J.D.; Tuinman, A.A.; Zhou, S.; Cook, K.D. *J. Am. Soc. Mass Spectrom.* **2002,** 13, 921-927.
5. Jonsson, A.P. *Cellular and Molecular Life Sciences* **2001,** 58, 868-884.
6. Mann, M.; Hendrickson, R.C.; Pandey, A. *Annu. Rev. Biochem.* **2001,** 70, 437-473.
7. Fenselau, C.; Demirev, P.A. *Mass Spectrom. Rev.* **2001,** 20, 157-171.
8. Karas, M.; Hillenkamp, F. *Int. J. of Mass Spectrom. And Ion Processes* **1987,** 78, 53.
9. Beavis, R.C.; Chait, B.T. *Rapid Commun. Mass Spectrom.* **1989,** 3, 432.
10. Beavis, R.C.; Chait, B.T. *Organic Mass Spectrometry* **1992,** 27, 156.
11. Karas, M.; Hillenkamp, F. *Organic Mass Spectrometry* **1993,** 28, 1476.
12. Tanaka, K.; et al. *Rapid Commun. Mass Spectrom.* **1988,** 2, 151.
13. Karas, M.; Hillenkamp, F. *Anal. Chem.* **1988,** 60, 2299-2301.
14. Hillenkamp, F.; Karas, M. *Methods in Enzymology* **1990,** Academic Press, New York, 193, 280-295.
15. Beavis, R.C..; Chait, B.T. *Rapid Commun. Mass Spectrom.* **1989,** 3, 233-237.
16. Niu, S.; Zhang, W.; Chait, B.T. *J. Am. Soc. Mass Spectrom.* **1998,** 9, 1-7.
17. Overberg, A.; Karas, M.; Hillenkamp, F. *Rapid Commun. Mass Spectrom.* **1990,** 4, 128.
18. Sutton, C.W.; Wheeler, C.H.; Sally, U.; Corbett, J.M.; Cotrell, J.S.; Dunn, M.J. *Electrophoresis* **1996,** 18, 424.
19. Beavis, R.C.; Chait, B.T. *Anal. Chem.* **1990,** 62, 1836-1840.

20. Dass, C. *Principles and Practice of Biological Mass Spectrometry* **2001,** Wiley-Interscience Series on Mass Spectrometry, New York, 30-32.

21. Imrie, D.C.; Pentney, J.M.; Cottrell, J.S. *Rapid Commun. Mass Spectrom.* **1995,** 9, 1293.

22. Moniatte, M.; VanderGoot, F.G.; Buckley, J.T.; et al. *FEBS Lett.* **1996,** 384(3), 269.

23. Lange, W.; Greifendorf, D.; VanLeyen, D.; et al. *Springer Proc. Phys.* **1986,** 9, 67.

24. Mamyrin, B.A.; Karataev, V.I.; Schorikk, D.V.; et al. *Sov. Phys. JEPT* **1973**, 37, 45-48.

25. Qin, J.; Chait, B. *J. Am. Chem. Soc.* **1995,** 117, 5411-5412.

26. *Anal. Chem*. **1995,** 67, 2498-2509.

27. Wiley, W.C.; McLaren, J.B. *Rev. Sci. Instrum.* **1955,** 16, 1150.

28. Onnerfjord, P.; Nilsson, J.; Wallman, L. *Anal. Chem.* **1998,** 70, 4755.

29. Colby, S.M.; King, T.B.; Reilly, J.P. *Rapid Commun. Mass Spectrom.* **1994,** 8, 865-868.

30. Brown, S.M.; Lennon, J.J. *Anal. Chem.* **1995,** 67, 1950-1954.

31. Brown, R.S.; Carr, B.L.; Lennon, J.J. *J. Am. Soc. Mass Spectrom.* **1996,** 7, 225-232.

32. Rouse, J.C.; Yu, W.; Martin, S.A. *J. Am. Soc. Mass Spectrom.* **1995,** 7, 822-835.

33. Griffin, P.R.; MacCoss, M.J.; Eng, J.K.; Blevines, R.A.; Aaronson, J.S.; Yates, III.J.R. *Rapid Commun. Mass Spectrom.* **1995,** 67, 3202-3210.

34. Wu, H.; Morgan, R.L.; Aboleneen, H. *J. Am. Soc. Mass Spectrom.* **1998,** 9, 660-667.

35. Harvey, D.J. *J. Mass Spectrom.* **1995,** 30, 1333-1346.

36. Orlando, R.; Yang, Y. in B.S. Larsen and C.N. McEwen, eds., *Mass Spectrometry of Biological Materials* **1998,** Marcel Dekker, New York, 215-245.

37. Okamoto, M.; Takahashi, K.I.; Doe, T.; Takimoto, Y. *Anal. Chem.* **1997,** 69, 2919-2926.

38. Jacson, A.; Yates, H.T.; Scrivens, J.H.; Green, M.R.; Bateman, R.H. *J. Am. Soc. Mass Spectrom.* **1998,** 9, 269-274.

39. Fenn, J.B. *J. Am. Soc. Mass Spectrom.* **1993**, 4, 524.

40. Dole, M.; Hines, R.C.; Mack, R.C.; Mobley, R.C.; Ferguson, L.D.; Alice, M.B. *J. Chem. Phys.* **1968,** 49, 2240.

41. Whitehouse, C.M.; Dreyer, R.N.; Yamashita, M.; Fenn, J.B. *Anal. Chem*. **1985**, 57, 675.

42. Allen, M.H.; Vestal, M.L. J. *Am. Soc. Mass Spectrom*. **1992,** 3, 18.

43. Kebarle, P.; Tang, L. *Anal. Chem.* **1993**, 65, 972A-986A.

44. Taylor, G.I. *Proc. R. Soc. London A* **1964,** A280, 383.

45. Wilm, M.S.; Mann, M. *Int. J. Mass Spectrom. Ion Processes* **1994,** 136, 167.

46. Fenn, J.B.; Mann, M. in D.M. Desiderio, ed., *Mass Spectrometry, Clinical and Biomedical Applications,* Plenum Press, New York, **1992,** Vol.1, pp 1-35.

47. Fenn, J.B.; Rosell, J.; Nohmi, J.; Shen, S.; Banks, I.J.Jr. in A.P. Snyder, ed., *Biochemical and Biotechnological Application of Electrospray Ionization Mass Spectrometry,* ACS, Washington, DC, **1995,** pp 60-80.

48. Smith, D.L.; Light-Wahl, K.J. *Biol. Mass Spectrom*. **1993**, 22, 493-501.

49. Schmelzeisen-Redeker, G.; Butfering, L.; Rollgen, F.W. *Int. J. Mass Spectrom. Ion Processes* **1989,** 90, 139.

50. Guevremont, R.; LeBlanc, J.C.Y.; Siu, K.M.W. *Org. Mass Spectrom.* **1993,** 28, 1345-1352.

51. Juraschek, R.; Dulcks, T.; Karas, M. J. *Am. Soc. Mass Spectrom*. **1999,** 10, 300-308.

52. Irbine, J.V.; Thompson, B. *J. Chem. Phys.* **1976,** 64, 2287-2294.

53. Winger, B.E.; Hofstadler, S.A.; Bruce, J.E.; Udseth, H.R.; Smith, R.D. *Nature,* **1993,** 379, 466-469.

54. Smith, R.D.; Bruce, J.E.; Wi, Q.; Cheng, X.; Hofstadler, S.A. *Mass Spectrometry in the Biological Sciences,* A.L. Burlingame; S.A. Carret, et. al. Eds., Humana Press, Totowa, NJ. **1996.**

55. Thompson, B.A.; Iribrane, J.V. *J. Chem. Phys*. **1979,** 71, 4451.

56. Guvremont, R. *Org. Mass Spectrom.* **1993,** 28, 579.

57. de la Mora, J.F.; Van Berkel, G.J.; Enke, C.G.; Cole, R.B.; Martinez-Sanchez, M; Fenn, J.B. *J. Mass Spectrom*. **2000,** 35, 935-952.

58. Korner, R.; Wilm, M.; Morand, K.; Schubert, M.; Mann, M. *J. Am. Soc. Mass Spectrom*. **1996,** 7, 150-156.

59. Verentchikov, A.N.; Ens, W.; Standing, K.G. *Anal. Chem*. **1994,** 66, 126-133.

60. Mirgorodskaya, O.A.; Shevchenko, A.A.; Miroshnikov, A.I. *Anal. Chem.* **1994**, 66, 99-107.

61. Creighton, T.E. *Protein Structures and Molecular Properties,* Freeman, New York **1984**.

62. Creighton, T.E. *Biochemistry J.* **1990,** 270, 1-16.

63. Osborne, H.B.; Nabedryk-Viala, E. *Methods in Enzymol.* **1982,** 88, 676-680.

64. Englander, J.J.; Calhoun, D.B.; Englander, S.W. *Anal. Biochem.* **1979,** 92, 517-524.

65. Thomson, J.A.; Shirley, B.A.; Grimsley, G.R.; Pace, C.N. *J. Biol. Chem.* **1988,** 264, 11614-11620.

66. Eftink, M. *Biophys. J.* **1994,** 66, 481-501.

67. Swint, L.; Robertson, A.D. *Prot. Sci.* **1993,** 2, 2037-2049.

68. Bai, Y.; Sosnick, T.R.; Mayne, L.; Englander, S.W. *Science* **1995,** 269, 192-197.

69. Kossiakoff, A.A. *Nature (Lond.)* **1982,** 296, 713-721.

70. Jeng, M.F.; Englander, S.W.; Elove, G.A.; Wand, A.J.; Roder, H. *Biochemistry* **1990,** 29, 10433-10437.

71. Paterson, Y.; Englander, S.W.; Roder, H. *Science* **1990,** 249, 755.

72. Benjamin, D.C.; Williams, D.C.; Poljak, R.J.; Rule, J.S. *J. Mol. Biol.* **1996,** 257, 866.

73. Hooke, S.D.; Radford, S.E.; Dobson, C.M. *Biochemistry* **1994,** 33, 5867.

74. Jones, B.E.; Matthews, C.R. *Prot. Sci.* **1995,** 4, 167.

75. Clarke, J.; Hounslow, A.M.; Fersht, A.R. *J. Mol. Biol.* **1995,** 253, 505.

76. Rothemund, S.; Beyermann, M.; Krause, E.; Krause, G.; Bienert, M.; Hodges, R.S.; Sykes, B.D.; Sonnichsen, F.D. *Biochemistry* **1995,** 34, 12954.

77. Jeng, M.F.; Dyson, H.J. *Biochemistry* **1995,** 34, 611.

78. Johnson, W.C. *Annu. Rev. Biophys. Chem.* **1988,** 17, 145.

79. Smith, D.L.; Deng, Y.; Zhang, Z. *J. Mass Spectrom*. **1997,** 32, 135-146.

80. Smith, D.L.; Zhang, Z. *Mass Spectrom. Rev.* **1994,** 13, 411-429.

81. Fenn, J.B.; Mann, M.; Meng, C.K.; Wang, S.F.; Whitehouse, C.M. *Science* **1989,** 246, 64-67.

82. Smith, R.D.; Loo, J.A.; Ogorzalek, R.R.; Busman, M.; Udseth, H.R. *Mass Spectrom. Rev.* **1991,** 10, 359-451.

83. Guevremont, R.; Siu, K.W.M.; LeBlanc, J.C.Y.; Berman, S.S. *J. Am. Soc. Mass Spectrom.* **1992,** 3, 216-224.

84. Loo, J.A.; Edmonds, C.G.; Barinaga, C.J. Udseth, H.R.; Smith, R.D. *Anal. Chem.* **1990,** 62, 693-698.

85. Smith, R.D.; Loo, J.A.; Edmonds, C.G.; Barinaga, C.J.; Udseth, H.R. *Anal. Chem.* **1990,** 62, 882-899.

86. Loo, J.A.; Udseth, H.R.; Smith, R.D. *Biol. Environ. Mass Spectrom.* **1988,** 17, 411-414.

87. Katta, V.; Chait, B.T. *Rapid Commun. Mass Spectrom.* **1991,** 5, 214-217.

88. Katta, V.; Chait, B.T. *J. Am. Chem. Soc.* **1993,** 115, 6317-6321.

89. Wagner, D.S.; Anderegg, R.J. *Anal. Chem.* **1994,** 66, 706-711.

90. Englander, S.W.; Sosnick, T.R.; Englander, J.J.; Mayne, L. *Curr. Opin. Struct. Biol.* **1996,** 6, 18-23.

91. Englander, S.W.; Kallenbach, N.R. *Quart. Rev. Biophys.* **1984,** 16, 521, 655.

92. Bai, Y.; Mitne, J.S.; Mayne, L.; Englander, S.W. *Prot. Struct. Funct. Genet.* **1993,** 17, 75-86.

93. Robinson, C.V. in Chapman, J.R.ed. *Protein and Peptide Analysis by Mass Spectrometry,* Humana Press, Totowa, NJ., **1996,** pp.129-139.

94. Miranker, A.; Robinson, C.V.; Radford, S.E.; Aplin, R.T.; Debson, C.M. Science **1993,** 262, 896-900.

95. Heidary, D.K.; Gross, L.A.; Ray, M.; Jennings, P.A. *Nature Struct. Biol.* **1997,** 4, 725-731.

96. Udgaonkar, J.B.; Baldwin, R.L. *Nature (Lond.)* **1988,** 335, 694-699.

97. Englander, S.W.; Mayne, L. *Ann. Rev. Biophys. Biomol. Struct.* **1992,** 21, 243-265.

98. Deng, Y.; Smith, D.L. *Biochemistry* **1998,** 37, 6256-6262.

99. Yang, H.H.; Smith, D.L. *Biochemistry* **1997,** 36, 14992-14999.

100. Zhang, Z.; Li, W.; Li, M.; Logan, T.M.; Guan, S.; Marshall, A.G. *Tech. Protein Chem. VIII* **1997,** 703-713.

101. Raza, A.S.; Dharmasiri, K.; Smith, D.L. *J. Mass Spectrom*. **2000,** 35, 612-617.

102. Zhang, Z.; Smith, D.L. *Prot. Sci.* **1993**, 2, 522-531.

103. Deng, Y.; Zhang, Z.; Smith, D.L. *J. Am. Soc. Mass Spectrom*. **1999,** 10, 675-684.

104. Johnson, R.S.; Walsh, K.A. *Prot. Sci.* **1994,** 3, 2411-2418.

105. Dharmasiri, K.; Smith, D.L. *Anal. Chem.* **1996,** 68, 2340-2344.

106. Liu, Y.; Smith, D.L. *J. Am. Soc. Mass Spectrom.* **1994,** 5, 19-28.

107. Zhang, Z.; Post, C.B.; Smith, D.L. *Biochemistry* **1996**, 35, 779-791.

108. Zhang, Z.; Smith, D.L. *Prot. Sci.* **1996,** 5, 1282-1289.

109. Mandell, J.G.; Falick, A.M.; Komives, E.A. *Anal. Chem.* **1998,** 70, 3897-3995.

110. Figueroa, I.D.; Torres, O.; Russel, D.H. *Anal. Chem.* **1998,** 70, 4527-4533.

111. Figueroa, I.D.; Russel, D.H. *J. Am. Soc. Mass Spectrom.* **1999,** 10, 719-731.

112. Buijs, J.; Vera, C.C.; Ayala, V.E.; Steensma, E.; Hakansson, P. *Anal. Chem.* **1999,** 71, 3219.

113. Robinson, C.V.; Gross, M.; Eyles, S.J.; Ewbank, J.J.; Mayhew, M.; Hartl, F.U.; Dobson, C.M.; Radford, S.E. *Nature (Lond.)* **1996,** 372, 645-651.

114. Anderegg, R.J.; Wagner, D.S. *J. Am. Chem. Soc*. **1995,** 117, 308-312.

115. Wang, F.; Blanchard, J.S.; Tang, X.J. *Biochemistry* **1997,** 36, 3755-3759.

116. Baerga-Ortiz, A.; Hughes, C.A.; Mandell, J.G.; Komives, E.A. *Protein Sci.* **2002,** 11, 1300-1308.

117. Sengbusch, P.V. *"Botany Online: Cell Wall"* 26 October 2001, http://www.biologie.uni-hamburg.de/b-online/e26/26.htm

118. Carpita, N.C.; Gibeaut, D.M. *Plant J.* **1993,** 3, 1-30.

119. McNeill, M.; Darvill, A.G.; Fry, S.C.; Albersheim, P. Annu. Rev. Biochem. **1984,** 53, 625-663.

120. Cillece-Castro, B.L.; Burlingame, A.L. *Methods in Enzymol*. **1990,** 193, 689-712.

121. Harvey, D.J.; Bateman, R.H.; Green, M.R. *J. Mass Spectrom*. **1997**, 32, 167-187.

122. Stephen, S.E.; Maslen, S.L.; Green, L.G.; Williams, D.H. *Anal. Chem.* **2004,** 76, 2343-2354.

123. Willats, W.G. *Plant Mol. Biol.* **2001**, 47, 9-27.

124. Varner, J.E.; Lin, S.L. *Cell* **1989,** 56, 231-239.

125. Talbott, L.F.; Ray, P.M. *Plant Physiol.* **1973,** 51, 174-187.

126. Wilkinshaw, M.D.; Arnott, S. *J. Mol. Biol.* **1981,** 153, 1075.

127. Kobayashi, M.; Maton, T.; Azuma, *J. Plant Physiol.* **1996,** 110, 1017-1020.

128. O'Neill, M.A.; Wareenfeltz, D.; Kates, K.; Pallerin, P.; Doco, T.; Darvill, A.G.; Albersheim, P. *J. Biol. Chem.* 1**996**, 271, 22923-22930.

129. O'Neill et al. J. Biol. Chem. 1996, 272, 22923.

130. Vidyasekaran, P. *Fungal Pathogenesis in Plants and Crops* : Molecular Biology and Host Defense Mechanism, Mercel Dekker, Inc. New York **1997.**

131. Antoniw, J.F.; Peirpoint, W.S. *Biochem. Society Transactions* **1978,** 6, 248-250.

132. VanLoon, L.C.; Pierpoint, W.S.; Boller, T.; Conjero, V. *Plant Molecular Biology Reporter* **1994**, 12, 245-264.

133. Cooper, M. *Biochem. Plant Pathol.* **1983**, 101-135.

134. Van Den Heuvel, J.; Naterreus, L.P. *J. of Plant Pathol.* **1985**, 91, 253-264.

135. Robertson, B. *Physiol. Mol. Plant Pathol*. **1986**, 28, 137-148.

136. Bruce, R.J.; West, C.A. *Plant Physiol.* **1982**, 69, 1181-1188.

137. Roby, D.; Toppan, A.; Esurre-Tugaye, M.T. *Plant Physiol.* **1985,** 77, 700-704.

138. Roco, A.; Castaneda, P.; Perez, L.M. *Phytochemistry* **1993,** 33, 1301-1306.

139. Branca, C.; DeLorenzo, G.; Cervone, F. *Physiol. Plant* **1988,** 72, 499-504.

140. Darvill, A.; McNeil, M.; Albersheim, P.; Delmer, D.P. The *Primary Cell Wall of Flowering Plants, The Biochemistry of Plants,* Vol. 1 (N.E. Tolbert, Ed.), Academic Press, **1980,** pp 92-157.

141. Cooper, R.M. *The Mechanisms and Significance of Enzymatic Degradation of Host Cell Walls by Parasites,* Biochemical Plant Pathology (J.A. Callow, Ed.), John Wiley, Chickester, UK, **1983,** pp 101-135.

142. Selvendran, R.R. *J. Cell Sci. Suppl.* **1985,** 2, 51-88.

143. Cooper, R.M.; Wardman, P.A.; Skelton, J.E.M. *Physiol. Plant Pathol.* **1981,** 18, 239-255.

144. LeCam, B.; Massiot, P.; Rouxed, F. *Physiol. Mol. Plant Pathol.* **1994,** 45, 139-151.

145. De Lorenzo, G.; D'Ovidio, R.; Cervone, F. *Annu. Rev. Phytopathol.* **2001,** 39, 313-335.

146. De Lorenzo, G.; Castoria, R.; Bellincampi, D.; Cervone, F. *Fungal Invasion Enzyme and Their Inhibition.* The Mycota V. Plant Relationships, Part B, (Carrol, G.C.; Tudzynski, P. Eds.) Springer-Verlag, Berlin, **1997,** 61-83.

147. Herron, S.R.; Benen, J.A.; Scaretla, R.D.; Visser, J.; Jurnak, F. *Proc. Natl. Acad. Sci. USA,* **2000,** 97, 8762-8769.

148. Walton, J.D. *Plant Physiol.* **1994,** 104, 1113-1118.

149. Cook, B.J.; Clay, R.P.; Bergmann, C.W.; Albersheim, P.; Darvill, A.G. *Mol. Plant Microbe In.* **1999**, 12, 703-711.

150. Ten Hare, A.; Mulder, W.; Visser, J.; Van Kan, J.A.L. *Mol. Plant-Microbe Interact.* **1998**, 11, 1009-1016.

151. Ridley, B.L.; O'Neill, M.A.; Mohnen, D. *Phytochem.* **2001,** 57, 929.

152. Ferrari, S.; Vairo, D.; Ausubel, F.M., Cervone, F.; De Lorenzo, G. *Plant Cell,* **2003,** 15, 93.

153. De Lorenzo, G.; Cervone, F.; Bellincampi, D.; Caprari, C.; Clark, A.J.; Desiderio, A,; Devoto, A.; Forrest, R.; Leckie, F.; Nuss, L.; Salvi, G. *Biochemical Society Transactions* **1994,** 22, 396-399.

154. Leckie, F.; Matlei, B.; Capodicasea, C.; Hemmings, A.; Nuss, L.; Aracri, B.; De Lorenzo, G.; Cervone, F. *EMBO Journal,* **1999,** 9, 2352-2363.

155. Cervone, F.; De Lorenzo, G.; Pressey, R.; Darvill, A.G.; Ablersheim, P. *Phytochem.* **1990,** 29, 447-449.

156. Engen, J. *"HXMS.COM"* 4 July 2002, http://www.hxms.com

CHAPTER 3

APPLICATION OF HYDROGEN/DEUTERIUM EXCHANGE TO STUDY PROTEIN-CARBOHYDRATE INTERACTIONS BY MASS SPECTROMETRY[1]

[1]Bahrainwala T.M., Kumar K.V.S., Bergmann, C., Orlando, R. To be submitted to *Rapid Communications in Mass Spectrometry.*

Abstract

Many recognition events involve interactions between an extracellular carbohydrate epitope and a receptor protein. These processes have been observed in such diverse biological processes as fertilization, cell adhesion, viral and bacterial infection, inflammatory responses, and the maintenance of lung integrity. As a result of the importance of these interactions, a variety of approaches have been used to better understand those factors affecting protein-carbohydrate interactions. We present here a study using hydrogen/deuterium exchange mass spectrometry to investigate protein-carbohydrate interactions using a Micromass nanospray assembly. The pectin degrading enzymes, endo-polygalacturonase-I (EPG-I wildtype) and endo-polygalacturonase-II (EPG-II wildtype and mutant D201E) from *Aspergillus niger*, in combination with oligomers of polygalacturonic acid, were chosen as the system of study. The degree of deuterium incorporation into wildtype EPG-I and both wildtype and mutant EPG-II was monitored with and without the oligomeric substrate to verify the degree to which a carbohydrate can provide protection of the amide hydrogens in a protein's binding cleft from exchange with deuterated solvent. It was observed that substrate protected a number of amide-hydrogens from exchange in the active site cleft for the enzymes studied. Fluorescence experiments were also carried out to provide additional information for any conformational changes observed in EPGs as a result of substrate binding. These results demonstrated the potential of hydrogen/deuterium exchange-mass spectrometry as a complimentary technique to the more common methods for characterizing protein-carbohydrate complexes.

Introduction

Protein-carbohydrate interactions underlie many aspects of cellular recognition including cell adhesion, trafficking, apoptosis, and the immune response.[1-4] These specific interactions occur through glycoprotein, glycolipid, and polysaccharide displays with proteins carrying carbohydrate-binding domains.[5] Tools for studying protein-carbohydrate interactions are necessary to gain an understanding of biological function and the roles these interactions play in disease states. While many biophysical methods such as ultraviolet circular dichroism, differential calorimetry, ultracentrifugation and infrared spectroscopy have been used, most of the techniques provide global information.[6,7] Only X-ray crystallography and nuclear magnetic resonance (NMR) can give localized, high resolution structural information on these interactions. The utility of both crystallography and NMR is well recognized and substantial efforts are continuously made to further develop and utilize these technologies. Both techniques, however, have limitations in applicability and throughput. For crystallography, crystallization remains the major obstacle and certain proteins, including many membrane proteins and intrinsically disordered proteins, are inherently noncrystallizable.[8,9] Even with state-of-the-art high field magnets, selective labeling methods, and new pulse sequences, many or most proteins are too large for analysis by NMR.[10] In addition, for both techniques, samples can be studied only under a limited set of conditions, such as in the solid state for crystallography and at high concentrations (1mM) for NMR. Therefore, the ability of mass spectrometry (MS)-based hydrogen/deuterium exchange (H/D-Ex) methodology to examine structure and dynamics in a nearly unlimited set of solution conditions and concentrations fills an existing gap in the study of protein-carbohydrate interactions.[11]

Hydrogen/Deuterium Exchange Mass Spectrometry (H/D-Ex MS)

A general procedure for hydrogen/deuterium exchange analysis is shown in Figure 3.1. The experiment can be divided into four parts: (1) deuterium exchange (2) quenching, denaturation and fragmentation (3) peptide separation and mass spectrometry and (4) peptide identification and mapping. Exchange of deuterium is performed under native conditions in D_2O buffer. The exchange reaction is stopped by simultaneous lowering of the temperature (~0^oC) and by addition of a "quench" solution of acid that denatures the protein and reduces the pH (or pD) to 2-3. This minimizes back exchange of deuterium with hydrogen, as amide hydrogen exchange for the polypeptide is slowest between pH 2.0 and 3.0.[12] The denatured protein is proteolyzed with pepsin under conditions of low pH and temperature. Fragments typically ranging from 6-10 amino acids[13] are separated by reverse phase chromatography to minimize mass overlap and suppression of peptides and the effluent is interfaced to a tandem MS with an electrospray ionization mass spectrometer (ESI-MS). Digests are analyzed and peptides are identified by de novo sequencing in combination with accurate peptide mass measurement. Absolute levels of deuterium incorporation are determined for each peptide fragment by mass spectrometry. Solvent exposed, rapidly exchanging sites have increased deuterium incorporation and thus show the greatest shift in mass. Parallel experiments in the absence of deuterium provide a control for comparisons of the level of deuteration. With a reliable identification of peptides and an assessment of deuterium exchange for all fragments, a high-resolution map can be pieced together depicting regional levels of deuterium incorporation.

Hydrogen/deuterium exchange mass spectrometry has been used to track structural changes in proteins involved in processes such as viral infection,[14,15] blood coagulation,[16-18] and kinase-mediated signal transduction.[19-24] Analogous methods have been developed to study

protein structure,[11,25] protein dynamics,[26-28] protein-ligand interactions,[29,30] and protein-protein interactions.[24,31,32]

What follows is an overview of the application of H/D-exchange MS in studying protein-carbohydrate interactions. The study is an investigation of the interaction of endopolygalacturonase-I (EPG-I) and endopolygalacturonase-II (EPG-II), from the fungus *Aspergillus niger,* with the substrate polygalacturonic acid (PGA).

Experimental Methods

Materials:

Pepsin and D_2O were purchased from Sigma Aldrich (St. Louis, MO). Hydrochloric acid was purchased from J.T. Baker (Phillipsburgh, NJ). The hydrolytically inactive D201E mutant form of EPG-II, and the wild type EPG-I and EPG-II were generous gifts of the laboratory of Jaap Visser of Wageningen Agricultural University, The Netherlands, and were prepared as published.[33,34] The mixture of GalA oligomers of dp 6-15 was a kind gift of Stefan Eberhard of the CCRC. The liquid chromatography (LC) buffers were made with formic acid from J.T. Baker (Phillipsburg, NJ) and acetonitrile from Sigma Aldrich (St. Louis MO). The mobile phases for gradient elution were 0.1% formic acid (v/v) in milliQ-H_2O (buffer A) and 0.1% formic acid (v/v) in acetonitrile (buffer B).

Procedures

EPG-I (Wild Type Enzyme):

Three conditions were studied using wildtype EPG-I enzyme; EPG-I in H_2O (1), EPG-I in 50% D_2O (2) and EPG-I in the presence of the oligosaccharide substrate in 50% D_2O (3). The wild type EPG-I stock solution was 1.2 mg/ml and 10µl aliquots were placed into each of three Q-TOF vials. The substrate was at a 20 mg/ml concentration, and a 1000 fold molar excess of

substrate over enzyme was added to vial 3 and allowed to incubate at room temperature overnight. Subsequently, 30µl of H_2O was added to vial 1 and 30µl of D_2O was added to vials 2 and 3. The samples were allowed to exchange for overnight before digestion and were analyzed by LC/MS. At the end of the incubation period, the vials were placed in an icebath and 10.0 µl of cold 10mM HCl was added to quench the exchange. 10.0 µl of cold 1mg/ml pepsin was then added and the digestion was allowed to progress for 10 minutes.

EPG-II (Wild Type Enzyme):

Three experiments were performed with wildtype EPG-II using experimental conditions similar to those used for wildtype EPG-I. The stock solution of wildtype EPG-II was 1.0mg/ml.

EPG-II (Mutant D201E):

Three experiments were performed for the mutant EPG-II (mEPG-II). A 100 fold molar excess of substrate over enzyme was added to vial 3 and allowed to incubate at room temperature overnight. Subsequently, 10µl of H_2O was added to vial 1 and 10µl of D_2O was added to vials 2 and 3. The samples were allowed to exchange for overnight before digestion and were analyzed by LC/MS. At the end of the incubation period, the vials were placed in an icebath and 5.0 µl of cold 10mM HCl was added to quench the exchange. 10.0 µl of cold 1mg/ml pepsin was then added and the digestion was allowed to progress for 10 minutes. The mutant EPG-II sample was approximately 1.0mg/ml in concentration.

To minimize any back-exchange of deuterium, the LC apparatus was modified in-house to incorporate an ice-bath. A Styrofoam box was used to cool the 100 µl loops carrying the solvents (Figure 3.2). The original Waters CapLC solvent delivery configuration was also modified to minimize the dead volume between the mixer and the reverse-phase nanocapillary column (150 µm I.D. x 5 cm, Vydac C18, 5 µm, 300 Å, Grace Vydac, USA). The pepsin

digested samples were introduced into the Q-TOF-II (Micromass) mass spectrometer using the modified Waters CapLC. The mobile phases used for the gradient elution consisted of water (A) with 0.1% formic acid and acetonitrile (B) with 0.1% formic acid. A linear gradient from 15.0% to 70.0% B over 15 min and a flow rate of 4.0 μl/min was used to elute the peptides. The Q-TOF-II was operated in MS only mode and spectra were acquired from 400 – 1800 m/z at a rate of 1scan/second in the positive ion mode.

Angiotensin-II was used as a standard reference to test the modified LC-system and to determine how much back exchange occurred. Angiotensin-II was allowed to incubate with 50% deuterium overnight, and the deuterated sample was then analyzed using the LC-MS apparatus. Minimum back exchange was observed when the deuterated sample was run, indicating a high efficiency for the system (data not shown).

UV Fluorescence

Fluorescence studies were carried out for all of the above three enzymes, EPG-I (wildtype), EPG-II (wildtype) and EPG-II (mutant D201E) respectively. Two experiments were performed in each case: 1) free EPG, and 2) EPG in presence of substrate. A Shimadzu RF-5301 PC spectrofluorophotometer was used to carry out the experiments. In each of the three experiments, two vials of 10 nM sample of EPG were prepared. A 100 fold molar excess of PGA was added in the case of EPG-II (mutant) and a 1000 fold molar excess of PGA was added in the case of the EPG-I (wildtype) and EPG-II (wildtype) enzymes to one of the vials in each of the experiments. All samples were then incubated at room temperature overnight. The samples were excited at 292 nm, and their emission scanned from 250-350 nm.

Results and Discussion

A study of protein-carbohydrate interactions between the D201E mutant of EPG-II and polygalacturonic acid (PGA) using hydrogen deuterium exchange has been previously carried out in our laboratory, [35] using a Micromass conventional electrospray probe assembly.

In this work we demonstrate the ability of hydrogen/deuterium exchange mass spectrometry to study the interactions of PGA with the wildtype enzymes using a Micromass nanoflow assembly. Polygalacturonases such as EPGs specifically hydrolyze polygalacturonic acid, the major constituent of plant cell wall pectin.[33] EPG-I is a processive enzyme while EPG-II which is 60% sequence identical to EPG-I shows a random mode of action. While processive enzymes do not release the substrate following the hydrolytic event, the random enzymes do.[36] The pH optima for both EPG-I and EPG-II enzymes is 4.2.[37] The 1.70 Å resolution structure of EPG-I[36] reveals a narrower substrate binding cleft than the 1.68 Å resolution structure of EPG-II[33], as shown in Figure 3.3. The loops bordering the active site cleft are shown in ball-and-stick representation for EPG-I [residues 124-128 (left) and 299-301 (right)] (figure 3.3A) and EPG-II [residues 121-123 (left) and 293-295 (right)] (figure 3.3B). The substrate used in this study was a mixture of oligosaccharides of PGA with a dp range of 6-15. The X-ray structure of *Aspergillus niger* EPG-II reveal that the enzyme folds into a right-handed parallel β-helix with 10 complete turns.[33] The loop regions form a cleft on the exterior of the β-helix and site directed mutagenesis studies demonstrate that it is this region that is involved in substrate binding. Similarly, X-ray structure and site directed mutagenesis studies have shown the cleft in EPG-I as the location of substrate binding.[36] A number of EPG-II mutants have been prepared by our collaborators and the hydrolytically inactive D201E mutant was selected in this study because it has a binding constant for the substrate that is similar to the wildtype EPG-II enzyme.[34]

It can be seen from the crystal structures that a majority of the protein consists of β-pleated sheets, including the active site cleft. The amide hydrogens involved in hydrogen bonding within these sheets have exchange rates that are very slow, and it is therefore not likely that much deuterium incorporation can occur in these regions.[38,35]

The peptide peaks obtained from the trials with H_2O in all three experiments, EPG-I (wildtype), EPG-II (wildtype) and EPG-II (mutant D201E), were identified by matching their masses to those of a computer generated peptic *in silico* digest (using Masslynx version 3.5, Micromass) of EPG-I and EPG-II. MS digest (http://prospector.ucsf.edu/ucsfhtml4.0/msdigest.htm), an online program that generates a theoretical pepsin digest of the protein was also used to identify the peptide masses that were obtained from H_2O trials. Only those peptides that matched peptides found in these digests were used for analysis. Following assignment of the peaks, the amount of deuterium incorporation into each peptide was determined by comparing the spectra obtained in the presence and absence of deuterium.

Calculation of the Deuterium Labeled Peptides

Methods used for calculating the number of deuterium atoms incorporated into the peptide in H/D-exchange studies generally involve finding the centroid masses of the peptide fragments.[10,39] The shift of the centroid mass as a result of deuterium exchange corresponds to the mean deuterium incorporation. Literature studies have shown that the determination of exact values of deuterium incorporation is not essential for binding studies, as any reduction in the level of deuterium incorporation is sufficient to indicate ligand binding and protection from the solvent.[10] In this study, the total amount of deuterium incorporated into each peptide was determined following deuterium exchange by multiplying the change in m/z of the average isotopic envelope by the charge of the peptide. This approach was found to be of sufficient

sensitivity for this type of study and was a simple way of following deuterium incorporation and has been used by Smith, D.L. et al[40-42].

For example in figure 3.4, 3.4A shows a doubly charged peptide with m/z of 676.44. When the deuterium exchange experiment was carried out for the EPG-II (mutant), it was found that the average isotopic peak in the absence and presence of the substrate had a mass increase of 0.88 Da and 0.97 Da as shown in figures 3.4B and 3.4C respectively, indicating that approximately 1.76 and 1.94 deuterons were incorporated into the peptide. The peptide in this example was not protected in the presence of substrate.

In the same sample, there were several peptides that were deuterated in the free EPG, which showed a reduced level of deuterium incorporation in the presence of substrate, thus indicating that these peptides are protected. These peptides were found to be present in the cleft region of the EPG-II. Figure 3.5 shows the spectra of one such peptide with an m/z of 734.42, that incorporated 1.62 deuterons in the free EPG, but which was subsequently protected in the presence of substrate.

Table 3.1 and 3.2 show various peptides (residue #) in EPG-II (mutant) that were protected and exposed to deuterium incorporation in the presence of the substrate. Calculations for deuterium incorporation and protection for each of the peptide with respect to the substrate was done as explained above and are shown in their respective tables.

When EPG-I (wildtype) and EPG-II (wildtype) experiments in the absence and presence of the substrate were carried out, a decrease in the level of deuterium incorporation was observed in the cleft regions of both enzymes. These peptides initially had incorporated deuterium in the free EPG experiments. This similarity observed between these enzymes can probably be attributed to the fact that EPG-I and EPG-II have very similar structures. Both have a rather open

binding region from which substrates can easily diffuse away, although as previously mentioned, the cleft in EPG-I is narrower than that of EPG-II (Figure 3.3). This narrowing is caused by the insertion of an asparagine residue after Thr125 in the N terminal loop above the binding site. Table 3.3 and 3.4 represent calculations for EPG-I (wildtype) and Tables 3.5 and 3.6 represent calculations for EPG-II (wildtype) in the presence of the substrate respectively.

Table 3.7, 3.8 and 3.9 show the peptides from EPG-I (wildtype), EPG-II (wildtype) and EPG-II (mutant) that showed the same percentage of deuterium incorporation in all the free EPG experiments as well as in the presence of the substrate. The amino acids not observed in the EPGs studied are shown below the respective table.

Table 3.10, 3.11 and 3.12 gives the summary of peptides showing either protection against or exposure to deuterium incorporation in EPG-I (wildtype), EPG-II (wildtype) and EPG-II (mutant) in absence and presence of the substrate respectively.

Figure 3.6, 3.7 and 3.8 show the cartoon representations of the *Aspergillus niger* EPG-I (wildtype), EPG-II (wildtype) and EPG-II (mutant) crystal structures. The percentage of deuterium incorporation and protection are shown as colored percentages in the respective figures. The color cyan in all the figures indicates the same percentage of deuterium incorporation in the free EPG experiments as well as in the presence of the substrate. The color grey represents the amino acids that were not observed in each of the EPG enzymes studied.

Fluorescence experiments demonstrated that upon binding of substrate to the EPGs, fluorescence increases dramatically. This change in fluorescence intensity has been demonstrated to correspond to a change in the environment of the tryptophan residues indicating a conformational change in the EPGs upon substrate binding. Figures 3.9, 3.10 and 3.11 show the fluorescence spectra's of the EPG-II (mutant), EPG-II (wildtype) and EPG-I (wildtype) along

with each respective EPG-substrate complex. This is consistent with what we have observed in hydrogen/deuterium exchange-MS experiments, in which conformational changes occur within EPGs when it binds to the substrate, resulting in a disruption of β-pleated sheets in the backbone.[35] The experiment is covered in a greater detail elsewhere[43].

Conclusion

The union of classic hydrogen/deuterium exchange method with modern mass spectrometry has resulted in a powerful platform for studying protein-carbohydrate interactions. This has provided the means to assess carbohydrate binding sites on proteins. The presence of carbohydrate (substrate) in the binding cleft of the protein protected the amide hydrogens from exchange with the deuterated solvent. The regions that were protected by the substrate were found to be similar for both the EPG-I and EPG-II samples and this is because of the structural similarities present between the two enzymes. One of the regions in the case of the EPG-II was found to be near the residue numbers 256-258 as shown by ball and stick representation in figure 3.6. Site directed mutagenesis experiments have revealed these residues could be crucial for substrate binding. For the EPG-I site directed mutagenesis experiment revealed that the residue Arg96 plays an important role in binding the substrate. Our experiments for EPG-I in presence of substrate showed protection in that region. Arg96 is shown by ball and stick representation in figure 3.7. Relatively little binding site data was obtained for any of the enzymes studied and this is attributed to the fact that a large percent of the protein consists of a high degree of β-pleated sheets within the binding cleft where the substrate binds. The data is in agreement with X-ray crystallography and site-specific mutagenesis, which indicated the cleft as the location of carbohydrate binding.

Acknowledgement

The authors would like to thank the National Science Foundation (MCB-0115132) and the National Institutes of Health (1 P41 RR018502) for grants that supported this project. We would also like to express our gratitude to the laboratory of Jaap Visser at Wageningen Agricultural University, The Netherlands, for supplying us with the EPG samples required for carrying out the project work and also Stefan Eberhard of the CCRC for the polymeric substrate.

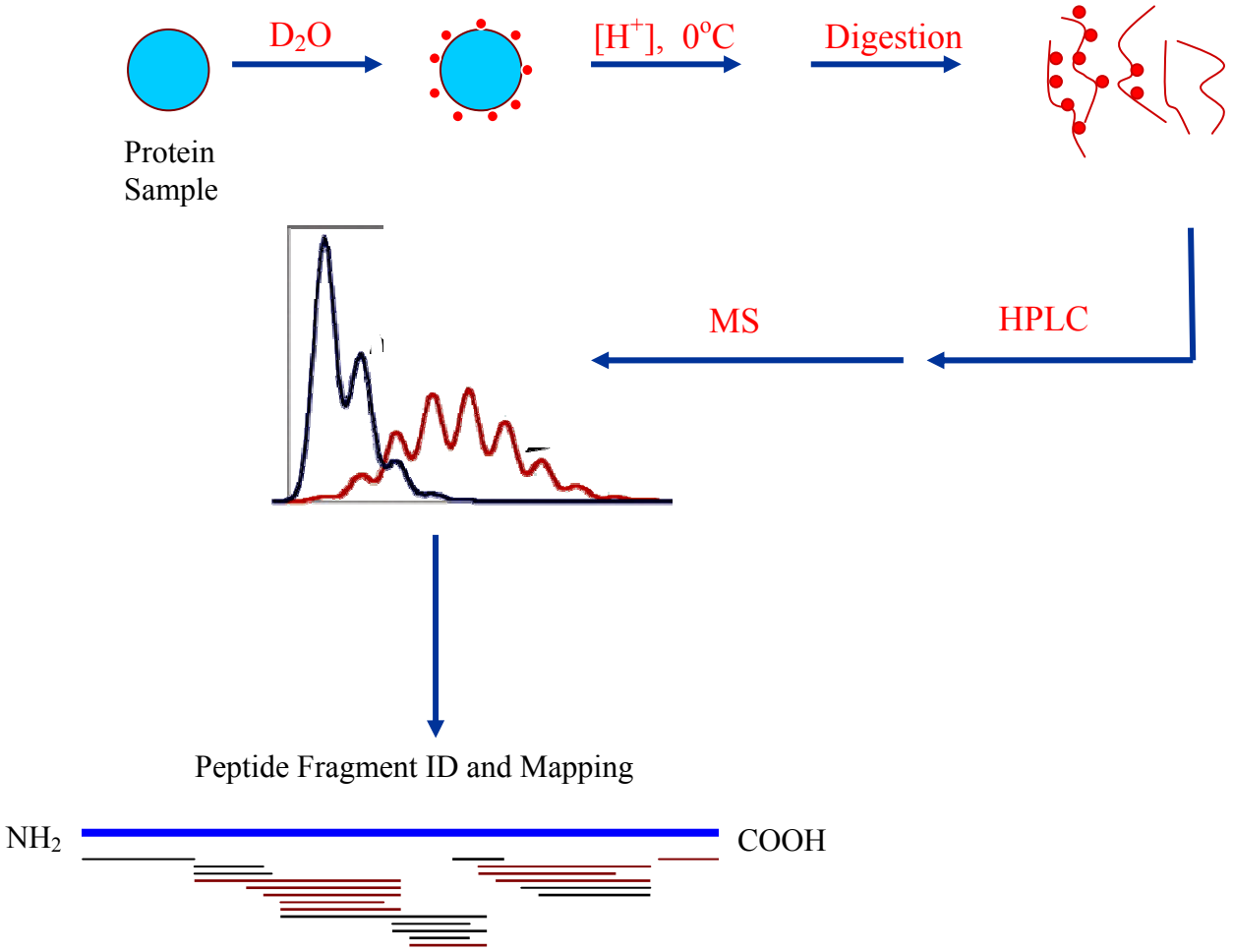

Figure 3.1: Schematic representation of H/D-Ex MS procedure

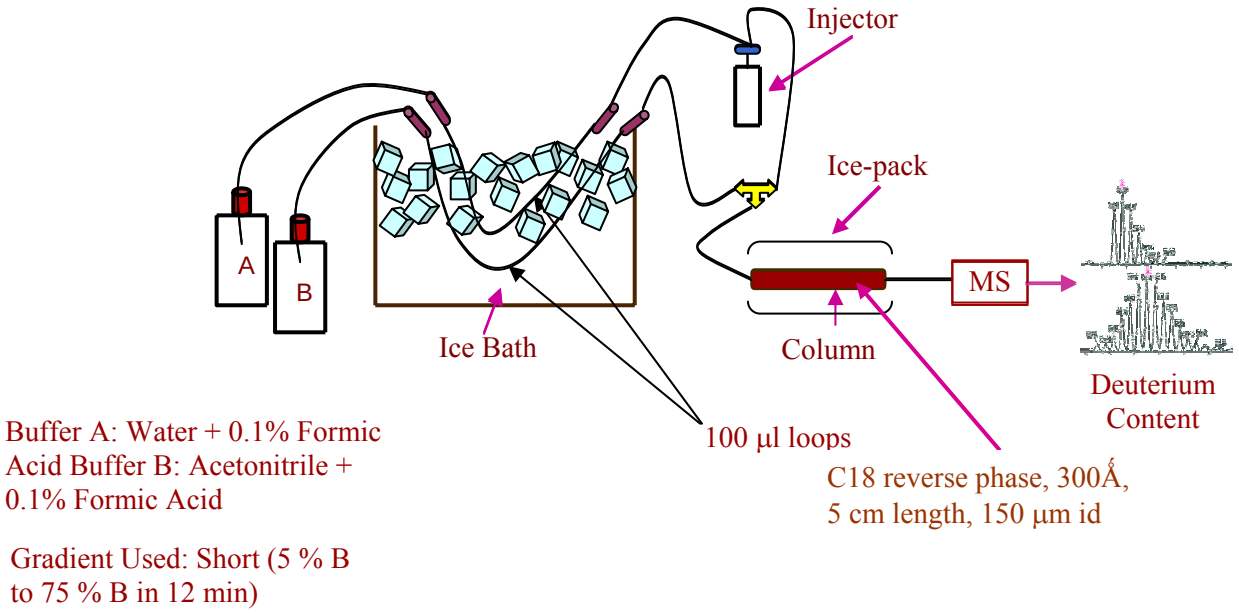

Figure 3.2: Schematic diagram of the apparatus used in the study

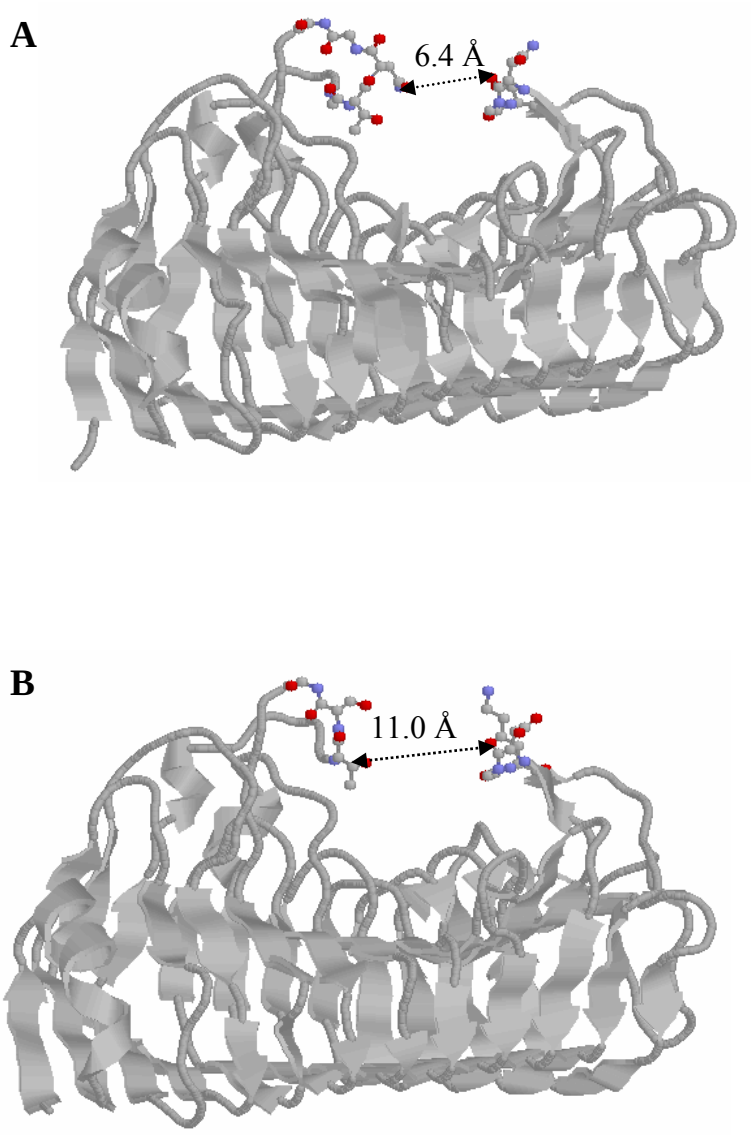

Figure 3.3: The cartoon structure of (A) Endopolygalacturonase-I and (B) Endopolygalacturonase-II. The distance at the entry of the active site is shown with a dashed line and the value is shown[36].

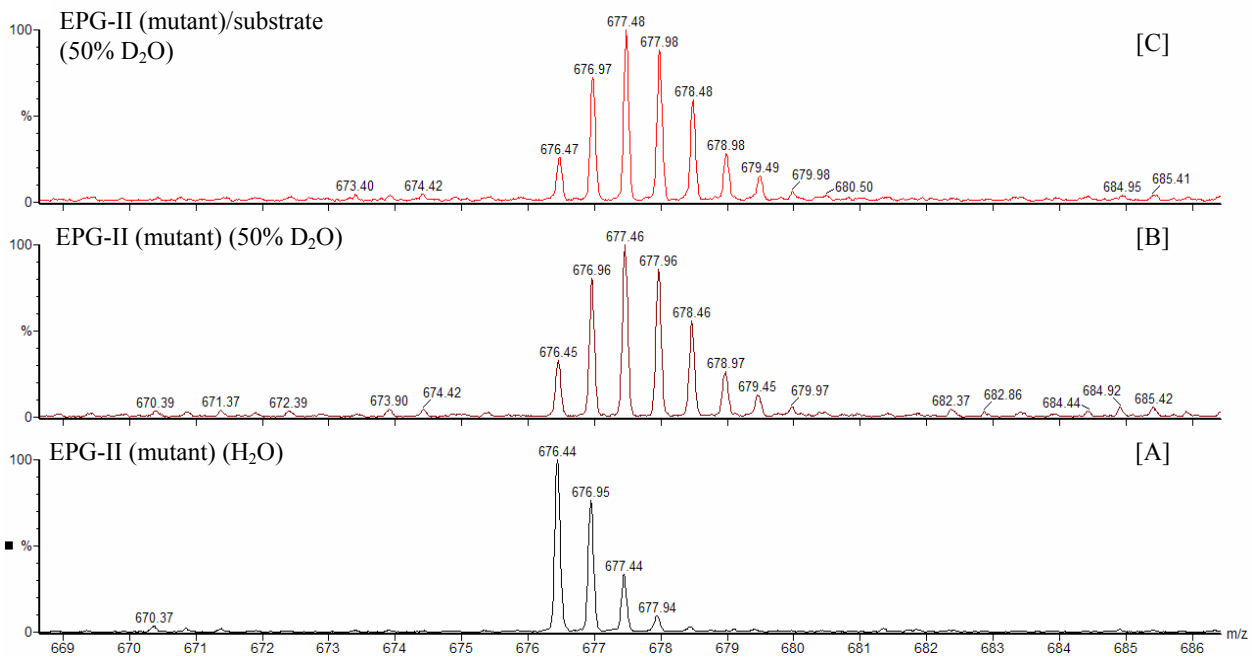

Figure 3.4: Spectra of 676.44 m/z Peptide

Figure 3.4A shows a doubly charged peptide of EPG-II (mutant) with m/z of 676.44. Figure 3.4B and 3.4C are EPG-II (mutant) spectra in 50% D_2O in the absence and presence of substrate which show a shift of the average isotopic peak as shown in the figure. The average isotopic peak shows an increase by a mass of 0.88 Da and 0.97 Da in figure 3.4B and 3.4C respectively, indicating that the mean level of deuterium incorporation was approximately 1.76 and 1.94 deuterons respectively.

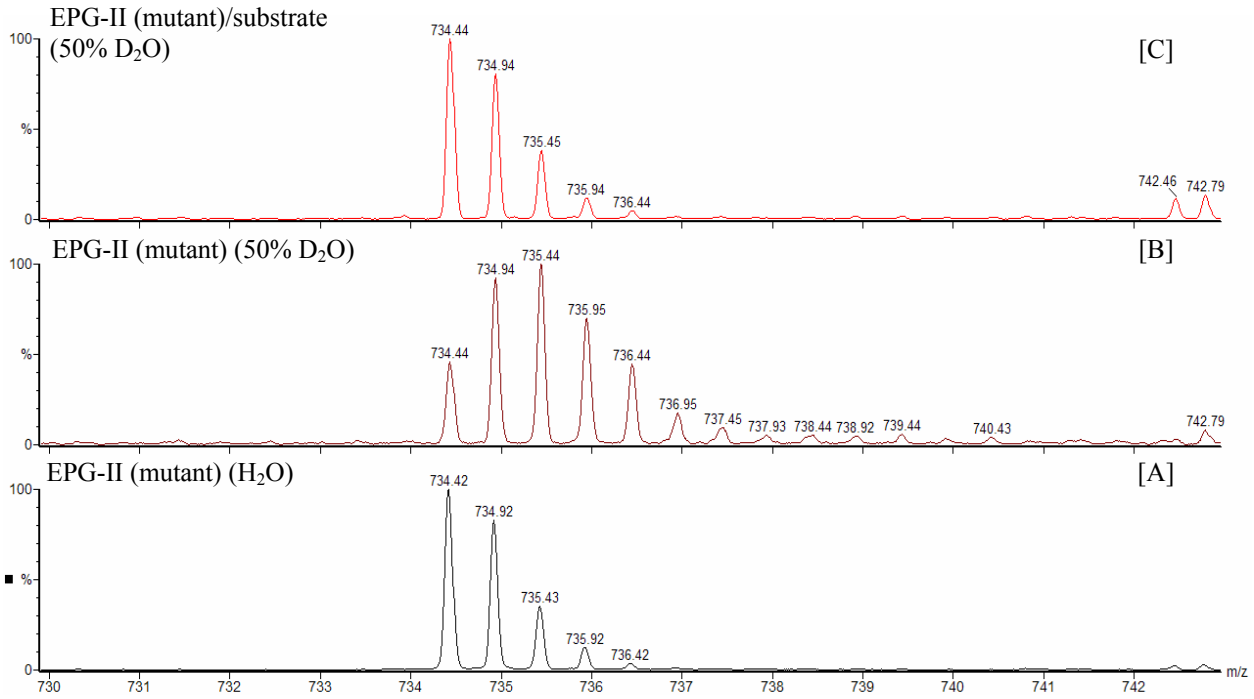

Figure 3.5: Spectra of 734.42 m/z Peptide

Figure 3.5A shows a doubly charged peptide of EPG-II (mutant) with m/z of 734.42. Figure 3.5B and 3.5C are EPG-II (mutant) spectra in 50% D_2O in absence and presence of substrate. Figure 3.5B shows a shift of the average isotopic peak by 0.81 Da indicating that the mean level of deuterium incorporation was 1.62. Figure 3.5C has the same isotopic pattern as 3.5A indicating that no deuterium was incorporated for the peptide and that it was protected in presence of substrate.

Residue #	Amino Acid Sequence	Average incorporation of deuterium in free EPG-II (mutant) (50% D_2O)			Average incorporation of deuterium in EPG-II (mutant) presence of substrate (50% D_2O)		
		Average Shift in isotopic envelope[1]	Total # of deuterons[2]	% Incorporation[3]	Average shift in isotopic envelope[4]	Total # of deuterons	% Incorporation
28-34	DSCTFTT	0.02±0.01	0.02±0.01	0.2±0.2	3.03±0.02	3.03±0.02	43.3±0.3
51-58	NNIEVPAG	0.05±0.01	0.11±0.01	1.5±0.2	2.10±0.03	4.21±0.06	60.1±0.9
65-73	GLTSGTKVI	0.02±0.01	0.05±0.01	0.5±0.1	3.91±0.02	7.81±0.03	86.8±0.3
140-145	TGLNIK	0.06±0.01	0.06±0.01	0.9±0.1	5.14±0.02	5.14±0.02	85.7±0.3
189-195	GVNIIKP	0.03±0.01	0.03±0.01	0.4±0.1	2.09±0.02	2.09±0.02	34.9±0.3
237-243	VVKNVTI	0.03±0.01	0.06±0.02	0.9±0.3	1.57±0.02	3.15±0.03	45.0±0.4
274-281	NIVMSGIS	0.03±0.02	0.05±0.03	0.7±0.4	1.03±0.01	2.05±0.02	25.7±0.3

[1]Average shift in isotopic envelope = Average m/z of peptide in free EPG-II (mutant) (50% D_2O) – Average m/z of peptide in water

[2]Total # of deuterons = Average shift in isotopic envelope * Charge on peptide

[3]% of deuterium incorporation = Total # of deuterons/Total # of Amino Acids in the peptide * 100 (Proline does not have an amide hydrogen and was not used in the calculations)

[4]Average shift in isotopic envelope = Average m/z of peptide in free EPG-II (mutant)/substrate (50% D_2O) – Average m/z of peptide in water

Table 3.1: Regions on EPG-II (mutant) showing average deuterium incorporation in presence of the substrate

Residue #	Amino Acid Sequence	Average incorporation of deuterium in freeEPG-II (mutant) (50% D_2O)			Average protection against deuterium in EPG-II (mutant) presence of substrate (50% D_2O)		
		Average Shift in isotopic envelope[1]	Total # of deuterons[2]	% Incorporation[3]	Average shift in isotopic envelope[4]	Total # of deuterons	% Incorporation
59-64	TTIDLT	1.44±0.02	1.44±0.02	23.9±0.3	0.04±0.02	0.04±0.02	0.6±0.3
109-116	CDGARWWD	2.06±0.02	4.13±0.04	51.6±0.5	0.02±0.01	0.04±0.02	0.5±0.3
129-135	TYAHGLD	5.76±0.02	5.76±0.02	82.6±0.3	0.02±0.01	0.02±0.01	0.2±0.1
151-155	AFSVQ	1.52±0.01	1.52±0.01	30.2±0.2	0.03±0.01	0.03±0.01	0.6±0.2
196-203	WYHNQDDC	2.32±0.02	4.63±0.03	57.9±0.4	0.04±0.02	0.07±0.03	0.9±0.4
204-209	LAVNSQ	2.17±0.02	2.17±0.02	36.2±0.3	0.01±0.01	0.01±0.01	0.2±0.1
254-260	AVRIKTI	2.09±0.03	4.18±0.02	59.7±0.8	0.03±0.01	0.05±0.02	0.8±0.3
282-288	DYGVVIQ	3.15±0.02	6.30±0.03	90.0±0.5	0.03±0.01	0.06±0.02	0.9±0.3
291-297	YEDGKPL	4.62±0.02	4.62±0.02	77.1±0.3	0.04±0.02	0.04±0.02	0.7±0.3
325-332	IYLLEGSG	2.61±0.02	5.22±0.03	65.3±0.4	0.04±0.01	0.08±0.02	1.0±0.3

[1]Average shift in isotopic envelope = Average m/z of peptide in free EPG-II (mutant) (50% D_2O) – Average m/z of peptide in water

[2]Total # of deuterons = Average shift in isotopic envelope * Charge on peptide

[3]% of deuterium incorporation = Total # of deuterons/Total # of Amino Acids in the peptide * 100 (Proline does not have an amide hydrogen and was not used in the calculations)

[4]Average shift in isotopic envelope = Average m/z of peptide in free EPG-II (mutant)/substrate (50% D_2O) – Average m/z of peptide in water

Table 3.2: Regions on EPG-II (mutant) showing average protection against deuterium incorporation in presence of the substrate

Residue #	Amino Acid Sequence	Average incorporation of deuterium in free EPG-I (WT) (50% D_2O)			Average incorporation of deuterium in EPG-I (WT) in presence of substrate (50% D_2O)		
		Average Shift in isotopic envelope[1]	Total # of deuterons[2]	% Incorporation[3]	Average shift in isotopic envelope[4]	Total # of deuterons	% Incorporation
33-39	STCTFTS	0.02±0.01	0.02±0.01	0.3±0.1	2.18±0.04	2.18±0.04	31.2±0.6
50-57	CSDVVLSS	0.05±0.01	0.10±0.02	1.3±0.3	1.80±0.04	3.60±0.07	45.0±0.9
102-108	LTVTMAD	0.02±0.01	0.02±0.01	0.3±0.1	1.88±0.02	1.88±0.02	26.9±0.3
144-152	TFKGINIKN	0.06±0.01	0.06±0.01	0.7±0.1	1.38±0.04	1.38±0.04	15.4±0.4
164-174	NVHLNDFTIDW	0.04±0.01	0.04±0.01	0.4±0.1	2.70±0.04	2.70±0.04	24.5±0.3
320-329	VTGTLEDDAT	0.04±0.01	0.04±0.01	0.4±0.1	1.48±0.02	1.48±0.02	14.8±0.2

[1]Average shift in isotopic envelope = Average m/z of peptide in free EPG-I (wildtype) (50% D_2O) – Average m/z of peptide in water

[2]Total # of deuterons = Average shift in isotopic envelope * Charge on peptide

[3]% of deuterium incorporation = Total # of deuterons/Total # of Amino Acids in the peptide * 100 (Proline does not have an amide hydrogen and was not used in the calculations)

[4]Average shift in isotopic envelope = Average m/z of peptide in free EPG-I (wildtype)/substrate (50% D_2O) – Average m/z of peptide in water

Table 3.3: Regions on EPG-I (wildtype) showing average deuterium incorporation in presence of the substrate

Residue #	Amino Acid Sequence	Average incorporation of deuterium in free EPG-I (WT) (50% D_2O)			Average protection against deuterium in EPG-I (WT) in presence of substrate (50% D_2O)		
		Average Shift in isotopic envelope[1]	Total # of deuterons[2]	% Incorporation[3]	Average shift in isotopic envelope[4]	Total # of deuterons	% Incorporation
92-98	GPLIRFG	1.48±0.02	1.48±0.02	24.7±0.3	0.06±0.01	0.06±0.01	1.0±0.2
131-137	KPKFMYI	2.04±0.02	2.04±0.02	34.1±0.3	0.01±0.01	0.01±0.01	0.2±0.1
157-162	AISVQA	1.08±0.02	1.08±0.02	18.0±0.3	0.02±0.01	0.02±0.01	0.3±0.1
178-184	DDNGGHN	2.34±0.03	2.34±0.03	33.4±0.5	0.05±0.01	0.05±0.01	0.7±0.2
207-214	DDCIAINS	2.21±0.02	4.43±0.04	55.3±0.5	0.02±0.01	0.04±0.02	0.5±0.3
260-267	GVRIKTIY	2.08±0.02	4.17±0.04	52.1±0.5	0.03±0.01	0.05±0.02	0.7±0.3
287-294	TDYGIVIE	3.17±0.03	3.17±0.03	39.6±0.3	0.02±0.01	0.02±0.01	0.3±0.1
297-308	YENGSPTGTPST	4.64±0.04	4.64±0.04	46.4±0.4	0.05±0.01	0.05±0.01	0.5±0.1

[1]Average shift in isotopic envelope = Average m/z of peptide in free EPG-I (wildtype) (50% D_2O) – Average m/z of peptide in water

[2]Total # of deuterons = Average shift in isotopic envelope * Charge on peptide

[3]% of deuterium incorporation = Total # of deuterons/Total # of Amino Acids in the peptide * 100 (Proline does not have an amide hydrogen and was not used in the calculations)

[4]Average shift in isotopic envelope = Average m/z of peptide in free EPG-I (wildtype)/substrate (50% D_2O) – Average m/z of peptide in water

Table 3.4: Regions on EPG-I (wildtype) showing average protection against deuterium incorporation in presence of the substrate

Residue #	Amino Acid Sequence	Average incorporation of deuterium in free EPG-II (WT) (50% D_2O)			Average incorporation of deuterium in EPG-II (WT) in presence of substrate (50% D_2O)		
		Average Shift in isotopic envelope[1]	Total # of deuterons[2]	% Incorporation[3]	Average shift in isotopic envelope[4]	Total # of deuterons	% Incorporation
28-34	DSCTFTT	0.02±0.01	0.02±0.01	0.2±0.2	3.03±0.02	3.03±0.02	43.3±0.3
44-49	KCSTIT	0.05±0.01	0.05±0.01	0.8±0.2	2.10±0.03	2.10±0.03	35.1±0.5
69-79	GTKVIFEFTTT	0.04±0.02	0.11±0.05	1.0±0.4	2.99±0.02	8.97±0.06	81.5±0.5
96-102	HITVTGA	0.06±0.01	0.06±0.01	0.8±0.2	1.03±0.02	1.03±0.02	14.7±0.2
138-143	SITGLN	0.03±0.02	0.03±0.02	0.6±0.3	3.76±0.02	3.76±0.02	62.6±0.3
210-216	NIWFTGG	0.03±0.01	0.06±0.02	0.9±0.3	1.57±0.02	3.15±0.03	45.0±0.4
274-281	NIVMSGIS	0.03±0.02	0.05±0.03	0.7±0.4	1.13±0.02	2.27±0.04	28.3±0.5
313-319	SVTGSVD	0.04±0.02	0.04±0.02	0.3±0.2	2.30±0.02	2.30±0.02	32.9±0.2

[1]Average shift in isotopic envelope = Average m/z of peptide in free EPG-II (wildtype) (50% D_2O) – Average m/z of peptide in water

[2]Total # of deuterons = Average shift in isotopic envelope * Charge on peptide

[3]% of deuterium incorporation = Total # of deuterons/Total # of Amino Acids in the peptide * 100 (Proline does not have an amide hydrogen and was not used in the calculations)

[4]Average shift in isotopic envelope = Average m/z of peptide in free EPG-II (wildtype)/substrate (50% D_2O) – Average m/z of peptide in water

Table 3.5: Regions on EPG-II (wildtype) showing average deuterium incorporation in presence of the substrate

Residue #	Amino Acid Sequence	Average incorporation of deuterium in free EPG-II (WT) (50% D_2O)			Average protection against deuterium in EPG-II (WT) in presence of substrate (50% D_2O)		
		Average Shift in isotopic envelope[1]	Total # of deuterons[2]	% Incorporation[3]	Average shift in isotopic envelope[4]	Total # of deuterons	% Incorporation
58-63	GTTLDL	3.10±0.03	3.10±0.03	51.7±0.4	0.04±0.01	0.04±0.01	0.7±0.2
85-93	WAGPLISMS	1.42±0.03	2.84±0.06	35.5±0.8	0.05±0.01	0.10±0.02	1.3±0.2
109-116	CDGARWWD	2.21±0.02	4.42±0.03	55.3±0.4	0.04±0.02	0.07±0.03	0.9±0.4
152-157	FSVQAN	1.21±0.02	1.21±0.02	20.2±0.3	0.06±0.01	0.06±0.01	0.9±0.2
196-203	WVHNQEDC	3.76±0.02	7.51±0.03	93.9±0.4	0.03±0.02	0.07±0.03	0.8±0.4
204-209	LAVNSE	3.10±0.03	3.10±0.03	51.7±0.4	0.04±0.01	0.04±0.01	0.7±0.2
251-258	SENAVRI	1.57±0.02	3.51±0.03	45.0±0.4	0.03±0.01	0.06±0.02	0.9±0.3
291-297	YEDGKPT	1.07±0.02	1.07±0.02	17.9±0.3	0.03±0.02	0.03±0.02	0.4±0.3
325-332	IYLLCGSG	2.25±0.03	4.50±0.06	56.3±0.7	0.04±0.02	0.07±0.03	0.9±0.4

[1]Average shift in isotopic envelope = Average m/z of peptide in free EPG-II (wildtype) (50% D_2O) – Average m/z of peptide in water

[2]Total # of deuterons = Average shift in isotopic envelope * Charge on peptide

[3]% of deuterium incorporation = Total # of deuterons/Total # of Amino Acids in the peptide * 100 (Proline does not have an amide hydrogen and was not used in the calculations)

[4]Average shift in isotopic envelope = Average m/z of peptide in free EPG-II (wildtype)/substrate (50% D_2O) – Average m/z of peptide in water

Table 3.6: Regions on EPG-II (wildtype) showing average protection against deuterium incorporation in presence of the substrate

Residue #	Amino Acid Squence	Average amount of deuterium incorporation in free EPG-I (WT) (50% D_2O)			Average amount of deuterium incoporation in EPG-I (WT) in presence of substrate (50% D_2O)		
		Average shift in isotopic envelope[1]	Total # of deuterons[2]	% incorporation[3]	Average shift in isotopic envelope[4]	Total # of deuterons	% incorporation
58-67	IEVPAGETLD	1.03±0.01	2.05±0.02	22.8±0.3	1.03±0.01	2.07±0.01	23.0±0.1
76-83	TITFEGTT	1.45±0.02	2.90±0.03	36.3±0.4	1.46±0.01	2.92±0.02	36.5±0.3
120-126	WDSKGTN	1.03±0.02	1.03±0.02	14.8±0.3	1.01±0.01	1.01±0.01	14.4±0.1
138-143	HDVEDS	1.33±0.01	1.33±0.01	22.1±0.1	1.32±0.01	1.32±0.01	22.0±0.2
194-201	TGVYISGA	1.81±0.02	1.81±0.02	22.6±0.2	1.81±0.02	1.81±0.02	22.6±0.2
215-223	GESISFTGG	2.15±0.01	4.31±0.01	47.9±0.1	2.15±0.01	4.29±0.01	47.7±0.1
242-249	NTVKNVTI	2.27±0.02	4.54±0.04	56.8±0.5	2.24±0.02	4.48±0.04	56.0±0.5
278-284	YSNIQLS	1.14±0.01	1.14±0.01	16.3±0.1	1.14±0.01	1.14±0.01	16.3±0.1
338-345	GSCSDWTW	1.97±0.02	3.94±0.03	49.3±0.4	1.97±0.02	3.95±0.01	49.3±0.1
359-368	CENVPSGASC	2.91±0.02	5.83±0.04	64.7±0.5	2.91±0.02	5.83±0.04	64.7±0.5

Residue #	Amino Acid Sequence	Residue #	Amino Acid Sequence
40-49	ASEASESISS	224-241	TCSGGHGLSIGSVGGRDD
68-75	LSDAADGS	250-259	SDSTVSNSAN
84-91	SFGYKEWK	268-277	KETGDVSEIT
99-101	GKD	285-286	GI
109-119	GAVIDGDGSRW	295-296	QD
127-130	GGKT	309-319	GIPITDVTVDG
153-156	TPVQ	330-337	QVYILCGD
185-193	TDGFDISES	346-358	SGVDLSGGKTSDK
202-206	TVKNQ		

[1]Average shift in isotopic envelope = Average m/z of peptide in free EPG-I (wildtype) (50% D_2O) – Average m/z of peptide in water

[2]Total # of deuterons = Average shift in isotopic envelope * Charge on peptide

[3]% of deuterium incorporation = Total # of deuterons/Total # of Amino Acids in the peptide * 100 (Proline does not have an amide hydrogen and was not used in the calculations)

[4]Average shift in isotopic envelope = Average m/z of peptide in free EPG-I (wildtype)/substrate (50% D_2O) – Average m/z of peptide in water

Table 3.7: Regions on EPG-I (wildtype) showing average deuterium incorporation in free EPG-I (50% D_2O) as well as in presence of the substrate. Amino acids not observed in the experiment are shown below the table

Residue #	Amino Acid Squence	Average amount of deuterium incorporation in free EPG-II (WT) (50% D_2O)			Average amount of deuterium incoporation in EPG-II (WT) in presence of substrate (50% D_2O)		
		Average shift in isotopic envelope[1]	Total # of deuterons[2]	% incorporation[3]	Average shift in isotopic envelope[4]	Total # of deuterons	% incorporation
50-57	LNNIEVPA	1.06±0.01	1.06±0.01	15.1±0.1	1.05±0.01	1.05±0.01	15.1±0.1
103-108	SGHLIN	1.43±0.01	1.43±0.01	20.4±0.1	1.45±0.03	1.45±0.03	20.7±0.5
117-123	GKGTSGK	1.91±0.01	3.82±0.02	42.4±0.2	1.91±0.02	3.82±0.03	42.4±0.4
144-151	IKNTPLMA	1.88±0.02	1.88±0.02	20.9±0.2	1.88±0.01	1.88±0.01	20.9±0.1
158-166	DITFTDVTI	2.03±0.02	4.07±0.03	50.8±0.4	2.03±0.02	4.07±0.03	50.8±0.4
185-193	GNSVGVNII	2.44±0.01	4.87±0.02	69.6±0.3	2.44±0.01	4.87±0.02	69.6±0.3
216-223	GGTCIGGH	1.53±0.02	3.05±0.04	61.1±0.8	1.55±0.02	3.09±0.03	61.9±0.6
240-246	NVTIEHS	1.04±0.02	1.04±0.02	17.4±0.3	1.04±0.02	1.04±0.02	17.4±0.3
269-273	EITYS	1.01±0.01	1.01±0.01	12.6±0.1	1.01±0.01	1.01±0.01	12.6±0.1
298-304	GKPTNGV	1.37±0.02	1.37±0.02	15.3±0.2	1.40±0.01	1.40±0.01	15.6±0.1
334-341	CSDWTWDD	1.65±0.01	1.65±0.01	20.6±0.1	1.64±0.01	1.64±0.01	20.5±0.1
353-362	CKNFPSVASC	2.22±0.02	4.43±0.03	49.3±0.3	2.22±0.02	4.43±0.03	49.3±0.3

Residue #	Amino Acid Sequence	Residue #	Amino Acid Sequence
35-43	AAAAKAGKA	224-239	GLSIGSVGDRSNNVVK
64-68	TGLTS	247-250	TVSN
94-95	GE	258-268	KTISGATGSVS
124-131	KKPKFFYA	282-290	DYGVVIQQD
167-184	NNADGDTQGGHNTDAFDV	305-312	TIQDVKLE
185-193	GNSVGVNII	320-325	SGATEI
194-195	KP	342-351	VKVTGGKKSTA
204-208	LAVNS		

[1]Average shift in isotopic envelope = Average m/z of peptide in free EPG-II (wildtype) (50% D_2O) – Average m/z of peptide in water

[2]Total # of deuterons = Average shift in isotopic envelope * Charge on peptide

[3]% of deuterium incorporation = Total # of deuterons/Total # of Amino Acids in the peptide * 100 (Proline does not have an amide hydrogen and was not used in the calculations)

[4]Average shift in isotopic envelope = Average m/z of peptide in free EPG-II (wildtype)/substrate (50% D_2O) – Average m/z of peptide in water

Table 3.8: Regions on EPG-II (wildtype) showing average deuterium incorporation in free EPG-II (50% D_2O) as well as in presence of the substrate. Amino acids not observed in the experiment are shown below the table

Residue #	Amino Acid Squence	Average amount of deuterium incorporation in free EPG-II (mutant) (50% D_2O)			Average amount of deuterium incoporation in EPG-II (mutant) in presence of substrate (50% D_2O)		
		Average shift in isotopic envelope[1]	Total # of deuterons[2]	% incorporation[3]	Average shift in isotopic envelope[4]	Total # of deuterons	% incorporation
44-50	KCSTITL	1.51±0.02	1.51±0.02	21.5±0.3	1.52±0.01	1.52±0.01	21.7±0.1
74-82	FEGTTTFQY	2.47±0.02	4.94±0.04	54.9±0.4	2.48±0.01	4.95±0.02	55.0±0.3
99-104	VTGASG	1.06±0.02	1.06±0.02	17.6±0.3	1.06±0.02	1.06±0.02	17.6±0.3
117-123	GKGTSGK	1.33±0.01	2.67±0.01	38.1±0.2	1.34±0.01	2.68±0.02	38.3±0.3
158-166	DITFTDVTI	3.12±0.02	6.23±0.04	69.3±0.5	3.13±0.03	6.27±0.06	69.6±0.7
174-179	QGGHNT	1.14±0.02	1.14±0.02	18.9±0.3	1.15±0.01	1.15±0.01	19.2±0.2
216-222	GGTCIGG	1.42±0.02	2.83±0.03	40.5±0.4	1.42±0.02	2.83±0.03	40.5±0.4
244-248	EHSTV	1.01±0.01	1.01±0.01	20.3±0.1	1.02±0.02	1.02±0.02	20.4±0.3
268-273	SEITYS	1.72±0.01	1.72±0.01	28.7±0.2	1.73±0.01	1.73±0.01	28.9±0.1
298-304	GKPTNGV	1.68±0.02	1.68±0.02	27.9±0.3	1.68±0.02	1.68±0.02	28.1±0.3
315-323	TGSVDSGAT	2.99±0.01	5.97±0.01	66.4±0.1	2.98±0.02	5.96±0.03	66.2±0.4
334-341	CSDWTWDD	2.38±0.01	2.38±0.01	29.7±0.1	2.38±0.01	2.38±0.01	29.7±0.1
355-362	NFPSVASC	1.82±0.01	1.82±0.01	26.0±0.2	1.83±0.02	1.83±0.02	26.0±0.2

Residue #	Amino Acid Sequence	Residue #	Amino Acid Sequence
35-43	AAAKAGKA	210-215	ENINFT
83-89	EEWAGPLISMSGEHIT	223-236	HGLSIGSVGDRSNN
105-108	HLIN	249-253	SNSEN
124-128	KKPKF	261-267	SGATGSV
136-139	SSSI	289-290	QD
146-157	NTPLMAFSVQAN	305-314	TIQDVKLESV
167-173	NNADGDT	324-333	EIYLLCGSGS
180-188	DAFDVGNSV	342-354	VKVTGGKKSTACK

[1]Average shift in isotopic envelope = Average m/z of peptide in free EPG-II (mutant) (50% D_2O) – Average m/z of peptide in water

[2]Total # of deuterons = Average shift in isotopic envelope * Charge on peptide

[3]% of deuterium incorporation = Total # of deuterons/Total # of Amino Acids in the peptide * 100 (Proline does not have an amide hydrogen and was not used in the calculations)

[4]Average shift in isotopic envelope = Average m/z of peptide in free EPG-II (mutant)/substrate (50% D_2O) – Average m/z of peptide in water

Table 3.9: Regions on EPG-II (mutant) showing average deuterium incorporation in free EPG-II (50% D_2O) as well as in presence of the substrate. Amino acids not observed in the experiment are shown below the table

Residue #	Amino Acid Squence	% Deuterium incorporation in free EPG-I (wildtype)	% Deuterium incorporation in EPG-I (wildtype) in presence of substrate	% Deuterium incorporation difference
zero				
58-67	IEVPAGETLD	22.8±0.3	23.0±0.1	-0.2 ± 0.2
76-83	TITFEGTT	36.3±0.4	36.5±0.3	-0.2 ± 0.35
120-126	WDSKGTN	14.8±0.3	14.4±0.1	0.4 ± 0.2
138-143	HDVEDS	22.1±0.1	22.0±0.2	0.1 ± 0.15
194-201	TGVYISGA	22.6±0.2	22.6±0.2	0
215-223	GESISFTGG	47.9±0.1	47.7±0.1	0.2 ± 0.1
242-249	NTVKNVTI	56.8±0.5	56.0±0.5	0.8 ± 0.5
278-284	YSNIQLS	16.3±0.1	16.3±0.1	0
338-345	GSCSDWTW	49.3±0.4	49.3±0.1	0
359-368	CENVPSGASC	64.7±0.5	64.7±0.5	0
negative (exposure)				
33-39	STCTFTS	0.3±0.1	31.2±0.6	-30.8 ± 0.35
50-57	CSDVVLSS	1.3±0.3	45.0±0.9	-43.7 ± 0.6
102-108	LTVTMAD	0.3±0.1	26.9±0.3	-26.6 ± 0.2
144-152	TFKGINIKN	0.7±0.1	15.4±0.4	-14.7 ± 0.25
164-174	NVHLNDFTIDW	0.4±0.1	24.5±0.3	-24.1 ± 0.2
320-329	VTGTLEDDAT	0.4±0.1	14.8±0.2	-14.4 ± 0.15
positive (protection)				
92-98	GPLIRFG	24.7±0.3	1.0±0.2	23.7 ± 0.25
131-137	KPKFMYI	34.1±0.3	0.2±0.1	33.9 ± 0.2
157-162	AISVQA	18.0±0.3	0.3±0.1	17.7 ± 0.2
178-184	DDNGGHN	33.4±0.5	0.7±0.2	32.7 ± 0.35
207-214	DDCIAINS	55.3±0.5	0.5±0.3	54.6 ± 0.4
260-267	GVRIKTIY	52.1±0.5	0.7±0.3	51.4 ± 0.4
287-294	TDYGIVIE	39.6±0.3	0.3±0.1	39.3 ± 0.2
297-308	YENGSPTGTPST	46.4±0.4	0.5±0.1	45.9 ± 0.25

Table 3.10: Summary of peptides showing either protection against or exposure to deuterium incorporation in EPG-I (wildtype) in absence and presence of the substrate

Residue #	Amino Acid Squence	% Deuterium incorporation in free EPG-II (wildtype)	% Deuterium incorporation in EPG-II (wildtype) in presence of substrate	% Deuterium incorporation difference
zero				
50-57	LNNIEVPA	15.1±0.1	15.1±0.1	0
103-108	SGHLIN	20.4±0.1	20.7±0.5	-0.3 ± 0.3
117-123	GKGTSGK	42.4±0.2	42.4±0.4	0
144-151	IKNTPLMA	20.9±0.2	20.9±0.1	0
158-166	DITFTDVTI	50.8±0.4	50.8±0.4	0
185-193	GNSVGVNII	69.6±0.3	69.6±0.3	0
216-223	GGTCIGGH	61.1±0.8	61.9±0.6	-0.8 ± 0.7
240-246	NVTIEHS	17.4±0.3	17.4±0.3	0
269-273	EITYS	12.6±0.1	12.6±0.1	0
298-304	GKPTNGV	15.3±0.2	15.6±0.1	-0.3 ± 0.15
334-341	CSDWTWDD	20.6±0.1	20.5±0.1	0.1 ± 0.1
353-362	CKNFPSVASC	49.3±0.3	49.3±0.3	0
negative (exposure)				
28-34	DSCTFTT	0.2±0.2	43.3±0.3	-43.1 ± 0.25
44-49	KCSTIT	0.8±0.2	35.1±0.5	- 34.3 ± 0.35
69-79	GTKVIFEFTTT	1.0±0.4	81.5±0.5	-80.5 ± 0.45
96-102	HITVTGA	0.8±0.2	14.7±0.2	-13.9 ± 0.2
138-143	SITGLN	0.6±0.3	62.6±0.3	-62.0 ± 0.3
210-216	NIWFTGG	0.9±0.3	45.0±0.4	-44.1 ± 0.35
274-281	NIVMSGIS	0.7±0.4	28.3±0.5	-27.6 ± 0.45
313-319	SVTGSVD	0.3±0.2	32.9±0.2	-32.6 ± 0.2
positive (protection)				
58-63	GTTLDL	51.7±0.4	0.7±0.2	51 ± 0.3
85-93	WAGPLISMS	35.5±0.8	1.3±0.2	34.2 ± 0.5
109-116	CDGARWWD	55.3±0.4	0.9±0.4	54.4 ± 0.4
152-157	FSVQAN	20.2±0.3	0.9±0.2	19.3 ± 0.25
196-203	WVHNQEDC	93.9±0.4	0.8±0.4	93.1 ± 0.4
204-209	LAVNSE	51.7±0.4	0.7±0.2	51.0 ± 0.3
251-257	SENAVRI	45.0±0.4	0.9±0.3	44.1 ± 0.35
291-297	YEDGKPT	17.9±0.3	0.4±0.3	17.5 ± 0.3
325-332	IYLLCGSG	56.3±0.7	0.9±0.4	55.4 ± 0.55

Table 3.11: Summary of peptides showing either protection against or exposure to deuterium incorporation in EPG-II (wildtype) in absence and presence of the substrate

Residue #	Amino Acid Squence	% Deuterium incorporation in free EPG-II (mutant)	% Deuterium incorporation in EPG-II (mutant) in presence of substrate	% Deuterium incorporation difference
zero				
44-50	KCSTITL	21.5±0.3	21.7±0.1	-0.2 ± 0.2
74-82	FEGTTTFQY	54.9±0.4	55.0±0.3	-0.1 ± 0.35
99-104	VTGASG	17.6±0.3	17.6±0.3	0
117-123	GKGTSGK	38.1±0.2	38.3±0.3	-0.2 ± 0.25
158-166	DITFTDVTI	69.3±0.5	69.6±0.7	-0.3 ± 0.6
174-179	QGGHNT	18.9±0.3	19.2±0.2	-0.3 ± 0.25
216-222	GGTCIGG	40.5±0.4	40.5±0.4	0
244-248	EHSTV	20.3±0.1	20.4±0.3	-0.1 ± 0.2
268-273	SEITYS	28.7±0.2	28.9±0.1	-0.2 ± 0.15
298-304	GKPTNGV	27.9±0.3	28.1±0.3	-0.2 ± 0.3
315-323	TGSVDSGAT	66.4±0.1	66.2±0.4	0.2 ± 0.25
334-341	CSDWTWDD	29.7±0.1	29.7±0.1	0
355-362	NFPSVASC	26.0±0.2	26.0±0.2	0
negative (exposure)				
28-34	DSCTFTT	0.2±0.2	43.3±0.3	-43.1 ± 0.25
51-58	NNIEVPAG	1.5±0.2	60.1±0.9	-58.6 ± 0.55
65-73	GLTSGTKVI	0.5±0.1	86.8±0.3	-86.3 ± 0.2
140-145	TGLNIK	0.9±0.1	85.7±0.3	-84.8 ± 0.2
189-195	GVNIIKP	0.4±0.1	34.9±0.3	-34.5 ± 0.2
237-243	VVKNVTI	0.9±0.3	45.0±0.4	-44.1± 0.35
274-281	NIVMSGIS	0.7±0.4	25.7±0.3	-25.0 ± 0.35
positive (protection)				
59-64	TTIDLT	23.9±0.3	0.6±0.3	23.3 ± 0.3
109-116	CDGARWWD	51.6±0.5	0.5±0.3	51.5 ± 0.4
129-135	TYAHGLD	82.6±0.3	0.2±0.1	82.4 ± 0.2
151-155	AFSVQ	30.2±0.2	0.6±0.2	29.6 ± 0.2
196-203	WYHNQDDC	57.9±0.4	0.9±0.4	57.0 ± 0.4
204-209	LAVNSQ	36.2±0.3	0.2±0.1	36.0 ± 0.2
254-260	AVRIKTI	59.7±0.8	0.8±0.3	58.9 ± 0.55
282-288	DYGVVIQ	90.0±0.5	0.9±0.3	81.9 ± 0.4
291-297	YEDGKPL	77.1±0.3	0.7±0.3	76.4 ± 0.3
325-332	IYLLEGSG	65.3±0.4	1.0±0.3	64.3 ± 0.35

Table 3.12: Summary of peptides showing either protection against or exposure to deuterium incorporation in EPG-II (mutant) in absence and presence of the substrate

A

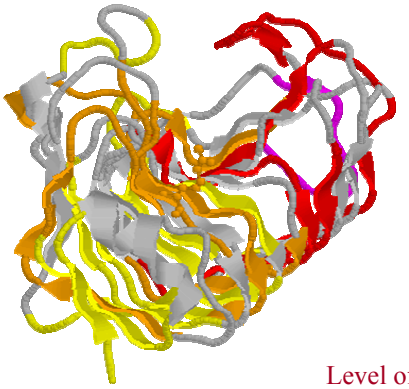

Level of deuterium incorporation in EPG-I (wildtype) in absence of the substrate (from Table 3.3, 3.4 and 3.7)

0-20% = yellow

21-40% = orange

41-60% = red

61-80% = magenta

81-100% = purple (none)

Amino Acids not observed = grey

B

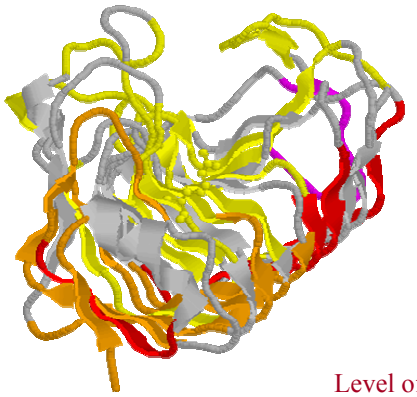

Level of deuterium incorporation in EPG-I (wildtype) in presence of the substrate (from Table 3.3, 3.4 and 3.7)

0-20% = yellow

21-40% = orange

41-60% = red

61-80% = magenta

81-100% = purple (none)

Amino Acids not observed = grey

C

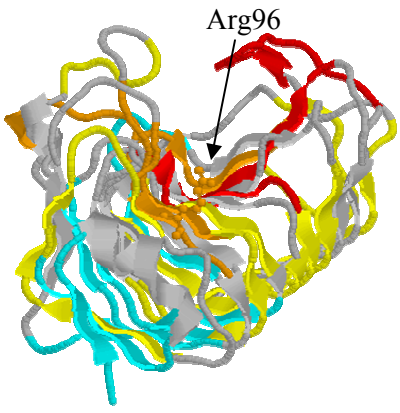

Level of protection against deuterium incorporation in EPG-I (wildtype) in presence of the substrate (from Table 3.3, 3.4 and 3.7)

<0% = cyan

0-20% = yellow

21-40% = orange

41-60% = red

61-80% = magenta (none)

81-100% = purple (none)

Amino Acids not observed = grey

Figure 3.6: Cartoon representation of the X-ray crystal structure of EPG-I (wildtype) from *Aspergillus niger*[34] showing levels of deuterium incorporation and protection in absence and presence of substrate

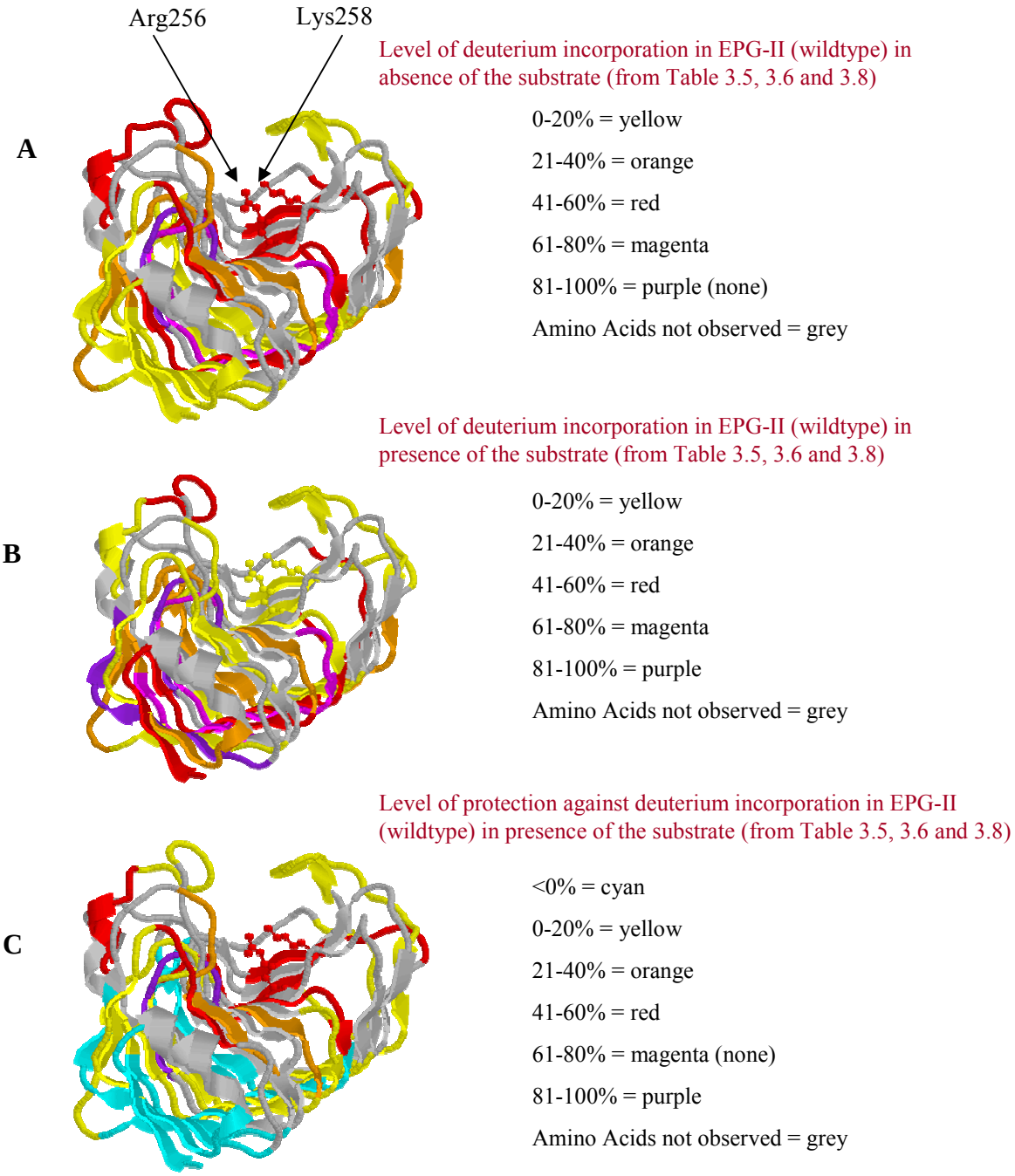

Figure 3.7: Cartoon representation of X-ray crystal structure of EPG-II (wildtype) from *Aspergillus niger*[31] showing levels of deuterium incorporation and protection in absence and presence of substrate

A

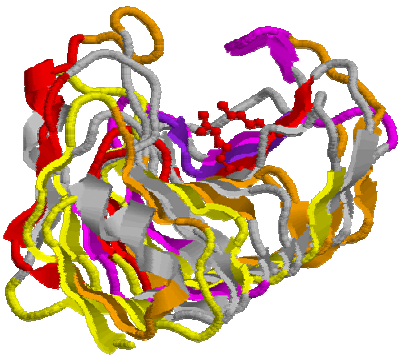

Level of deuterium incorporation in EPG-II (mutant) in absence of the substrate (from Table 3.1, 3.2 and 3.9)

0-20% = yellow

21-40% = orange

41-60% = red

61-80% = magenta

81-100% = purple

Amino Acids not observed = grey

B

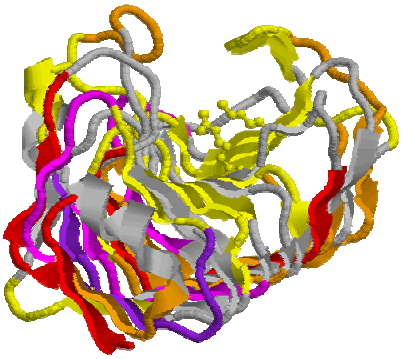

Level of deuterium incorporation in EPG-II (mutant) in presence of the substrate (from Table 3.1, 3.2 and 3.9)

0-20% = yellow

21-40% = orange

41-60% = red

61-80% = magenta

81-100% = purple

Amino Acids not observed = grey

C

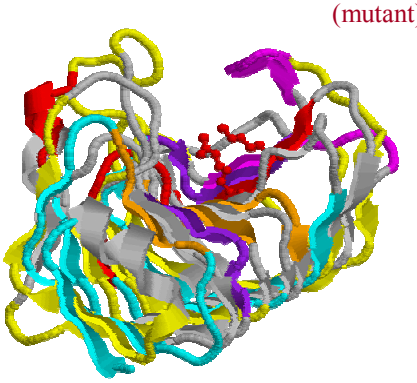

Level of protection against deuterium incorporation in EPG-II (mutant) in presence of the substrate (from Table 3.1, 3.2 and 3.9)

<0% = cyan

0-20% = yellow

21-40% = orange

41-60% = red

61-80% = magenta

81-100% = purple

Amino Acids not observed = grey

Figure 3.8: Cartoon representation of X-ray crystal structure of EPG-II (mutant) from *Aspergillus niger*[31] showing levels of deuterium incorporation and protection in absence and presence of substrate

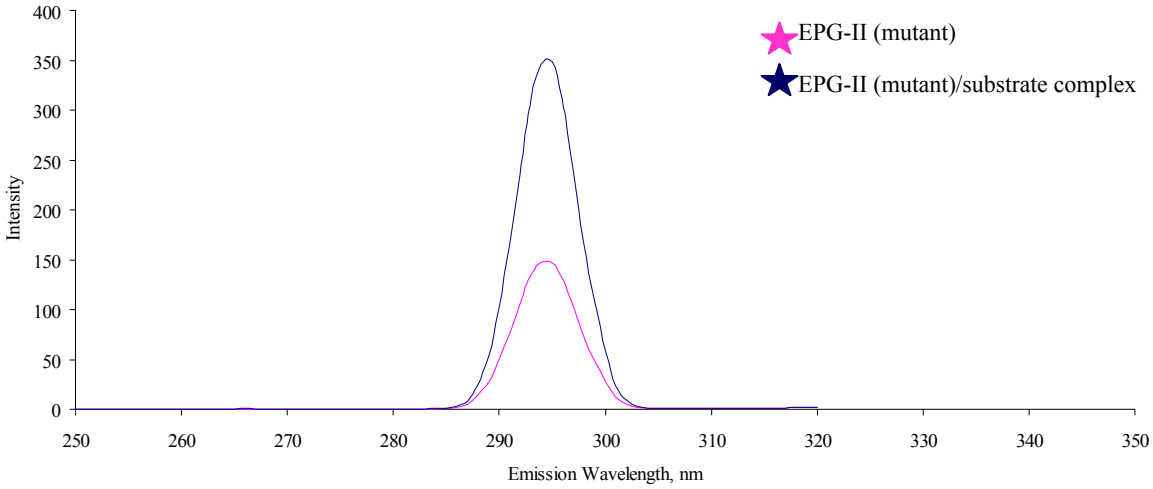

Figure 3.9: Fluorescence spectra of EPG-II (mutant) and EPG-II (mutant)/substrate complex.

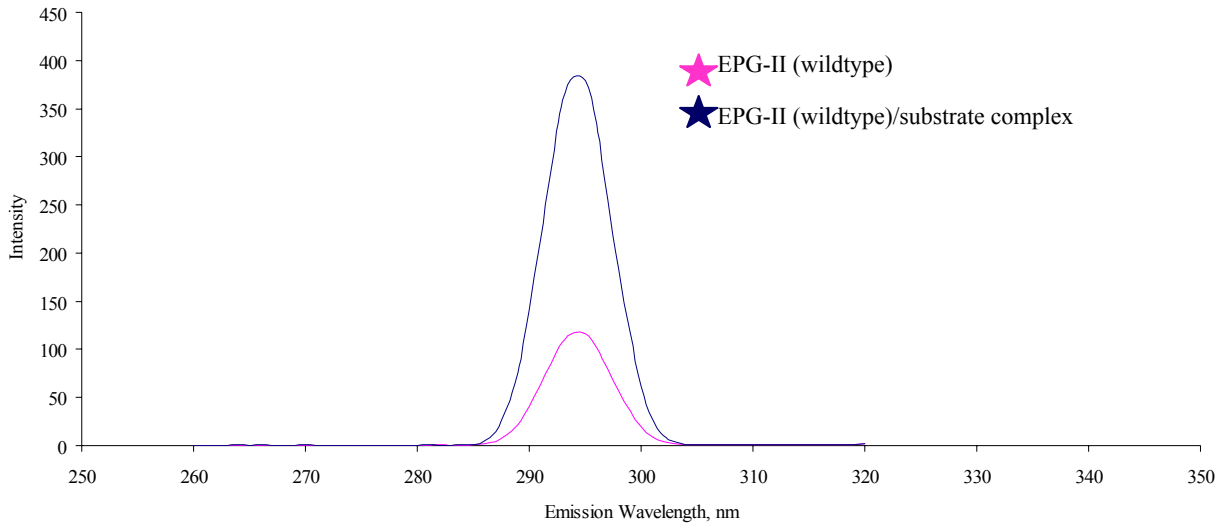

Figure 3.10: Fluorescence spectra of EPG-II (wildtype) and EPG-II (wildtype)/substrate complex.

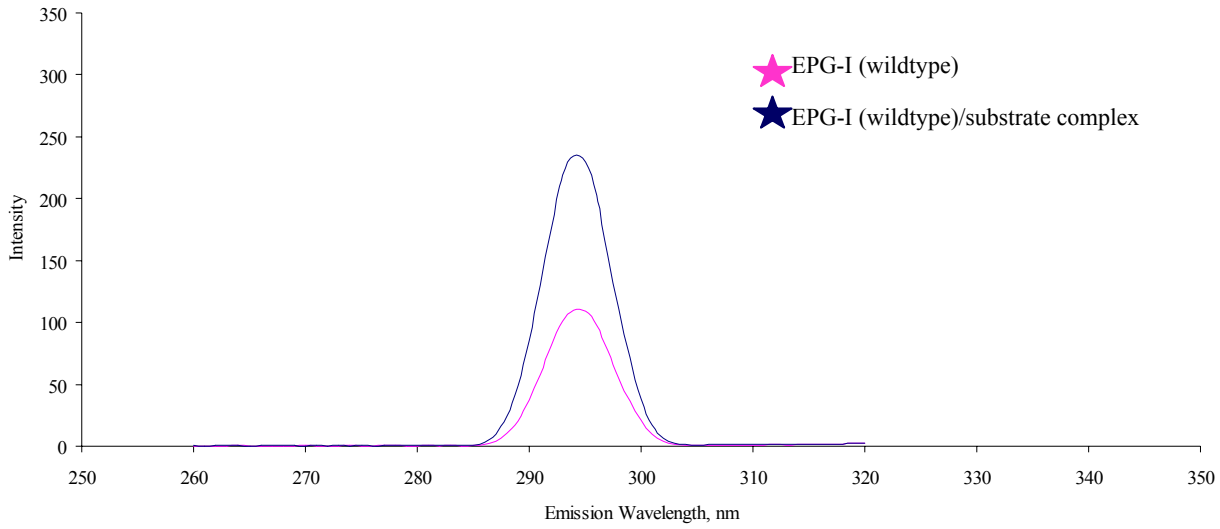

Figure 3.11: Fluorescence spectra of EPG-I (wildtype) and EPG-I (wildtype)/substrate complex.

Reference List

1. Lis, H.; Sharon, N. *Chem. Rev.* **1998,** 98, 637-674.
2. Varki, A. *Glycobiology* **1993,** 3, 97-130.
3. Bertozzi, C.R.; Kiessling, L. L. *Science* **2001,** 291, 2357-2364.
4. Emily, A.S.; William, D.T.; Kiessling, L.L.; Robert, M.C. *J. Am. Chem. Soc.* **2003,** 125, 6140-6148.
5. Sharon, N.; Lis, H. *Science* **1989,** 246, 227-246.
6. Hamuro, Y.; Coales, S.J.; Southern, M.R.; Nemeth-Cawley, J.E.; Stranz, D.D.; Griffin, P.R. *J. Biomolecular Tech.* **2003,** 14, 171-182.
7. Deng, Y.; Zhang, Z.; Smith, D.L. *J. Am. Soc. Mass Spectrom.* **1999,** 10, 675-684.
8. Weis, W.I.; Drickamer, K.; Hendrickson, W.A. *Nature* **1992,** 360, 127-134.
9. Merritt, E.A.; Sarferty, S.; Akker, F. van den, L` Holr C.; Martial, J.A.; Hol, W.G.J. *Protein Sci.* **1994,** 3(2), 166-175.
10. Ehring, H. *Anal. Biochem.* **1999,** 267(2), 252-259.
11. Zhang, Z.Q.; Smith, D.L. *Protein Sci.* **1993,** 2(4), 522-531.
12. Englander, S.W.; Sosnick, T.R.; Englander, J.J.; Mayne, L. *Curr. Opin. Struct. Biol.* **1996,** 6, 18-23.
13. Woods, V.L.Jr.; Hamuro, Y. *J. Cell Biochem.* **2001,** 37, 89-98.
14. Lanman, J.; Lam, T.T.; Barnes, S.; Sakalian, M.; Emmett, M.R.; Marshall, A.G.; Prevelige, P.E.Jr. *J. Mol. Biol.* **2003,** 325, 759-772.
15. Lam, T.T.; Lanman, J.K.; Emmett, M.R.; Hendrickson, C.L.; Prevelige, P.E.Jr. *J. Chromatogr. A* **2002,** 982, 85-95.
16. Turner, B.J.; Maurer, M. *Biochemistry* **2002,** 41, 7947-7954.

17. Mandell, J.G.; Baerga-ortiz, A.; Akashi, S.; Takio, K.; Komives, E.A. *J. Mol. Biol.* **2001,** 306, 575-589.

18. Mandell, J.G.; Falick, A.M.; Komives, E.A. *Anal. Chem.* **1998,** 70, 3987-3995.

19. Hamuro, Y.; Zawadzki, K.M.; Kim, J.S.; Stranz, D.; Taylor, S.S.; Woods, V.L.Jr. *J. Mol. Biol.* **2003,** 327, 1065-1076.

20. Zawadzki, K.M.; Hamuro, Y.; Kim, J.S.; Garrod, S.; Stranz, D.D.; Talyor, S.S.; Woods, V.L.Jr. *Protein Sci.* **2003,** 12, 1980-1990.

21. Anand, G.S.; Law, D.; Mandell, J.G.; Snead, A.N.; Tsigelny, I.; Talyor, S.S.; TenEyck, L.F.; Komives, E.A. *Proc. Natl. Acad. Sci. USA* **2003,** 100, 13264-13269.

22. Hamuro, Y.; Zawadzki, K.; Kim, J.M.; Taylor, S.S.; Woods, V.L.Jr. *Protein Sci.* **2002,** 11, 84-93.

23. Anand, G.S.; Hughes, C.A.; Jones, J.M.; Taylor, S.S.; Komives, E.A.; *J. Mol. Biol.* **2002,** 18, 377-386.

24. Mandell, J.G.; Falick, A.M.; Komives, E.A. *Proc. Natl. Acad. Sci. USA* **1998,** 95, 14705-14710.

25. Resing, K.A.; Hoofnagle, A.N.; Ahn, N.G. *J. Am. Soc. Mass Spectrom.* **1999,** 10, 685-702.

26. Neubert, T.A.; Walsh, K.A.; Hurley, J.B.; Johnson, R.S. *Protein Sci.* **1997,** 6, 843-850.

27. Engen, J.R.; Smith, D.L. *Anal. Chem.* **2001,** 73, 256A-265A.

28. Hoofnagle, A.N.; Resing, K.A.; Goldsmith, E.J.; Ahn, N.G. *Proc. Natl. Acad. Sci. USA* **2001,** 98, 956-961.

29. Engen, J.R.; Gmeiner, W.H.; Smithgall, T.E.; Smith, D.L. *Biochemistry* **1999,** 38, 8926-8935.

30. Anderson, M.D.; Shaffer, J.; Jennings, P.A.; Adams, J.A. *J. Biol. Chem.* **2001,** 276, 14204-14211.

31. Anand, G.S.; Hughes, C.A.; Jones, J.M.; Taylor, S.S.; Komives, E.A. *J. Mol. Biol.* **2002,** 323, 377-386.

32. Wang, Y.; Ganguly, A.K.; Gross, M.L. (eds): *Applied Electrospray Mass Spectrometry, Practical Spectroscopy Series* New York, Marcel Dekker, **2002,** 389-410.

33. Van Santen, Y.; Benen, J.A.E.; Schroer, K.H.; Kalk, K.H.; Armand, S.; Visser, J.; Dijkstra, B.W. *J. Biol. Chem.* **1999,** 274, 30474-30480.

34. Armand, S.; Wagemaker, M.J.M.; Sanchez-Torres, P.; Kester, H.C.M.; Van Santen, Y.; Dijkstra, B.W.; Visser, J.; Benen, J.A.E. *J. Biol. Chem.* **2000,** 275, 691-696.

35. King, D.; Lumpkin, M.; Bergmann, C.; Orlando, R. *Rapid Comm. Mass Spec.* **2002,** 16, 1569-1574.

36. Van Pouderoyen, G.; Snijder, H.J.; Benen, J.A.E.; Dijkstra, B.W. *FEBS Letters* **2003,** 554, 462-466.

37. Benen, J.A.E.; Kester, H.C.M.; Visser, J. *Eur. J. Biochem.* **1999,** 259, 577-585.

38. Smith, D.L.; Zhang, Z.Q.; Liu, Y.Q. *Pure Appl. Chem.* **1994,** 66, 89-94.

39. Wang, L.; Lane, L.C.; Smith, D.L. *Protein Sci.* **2001,** 10, 1234-1243.

40. Zhang, Z.; Smith, D.L. *Protein Sci.* **1996,** 5, 1282-1289.

41. Zhang, Z.; Post, C.B.; Smith, D.L. *Biochemistry* **1996,** 35, 779-791.

42. Smith, D.L.; Deng, Y.; Zhang, Z. *J. Mass Spectrom.* **1997,** 32, 135-146.

43. Bahrainwala, T.M.; Kumar, K.V.S.; Bergmann, C.; Orlando, R. *"To be submitted to Analytical Biochemistry"*.

CHAPTER 4

HYDROGEN/DEUTERIUM EXCHANGE STUDIES ON ENDOPOLYGALACTURONASES-POLYGALACTURONIC ACID-POLYGALACTURONASE INHIBITING PROTEINS BY NANOSPRAY IONIZATION MASS SPECTROMETRY[1]

[1]Bahrainwala T.M., Kumar K.V.S., Bergmann, C., Orlando, R. To be submitted to *Analytical Biochemistry*.

Abstract

Hydrogen/Deuterium exchange (H/D-Ex) mass spectrometry (MS) studies were carried out on endopolygalacturonase-I (EPG-I) and endopolygalacturonase-II (EPG-II) enzymes from *Aspergillus niger* in the presence and absence of the substrate, a mixture of GalA oligomers of dp 6-15. The study showed a decrease in deuterium incorporation in both the enzymes when it was bound to the substrate relative to that of the free EPGs, identifying the location of the substrate. The data obtained is in agreement with published site specific mutagenesis studies. A conformational change was observed for all the enzyme substrate complexes at regions remote from the substrate binding sites, leading to an increase in the amount of deuterium incorporation. The successful application of hydrogen/deuterium exchange coupled with mass spectrometry to study the protein-carbohydrate interaction led us to study the interactions of EPGs with polygalacturonase inhibiting proteins (PGIPs). Three different PGIPs were used, bean (var. Blue Lake), tomato (var. Celebrity) and pear (var. Bosch). Hydrogen/deuterium exchange-MS experiments were carried out on EPG-I/substrate and EPG-II/substrate in the presence of the three PGIPs. Fluorescence experiments provided additional information on the conformational changes that were observed for the EPG-I and EPG-II in the presence of substrate as well as in the presence of the inhibitors. The results thus obtained gave information on the location of the binding site of the inhibitors and suggested that the interaction of EPGs with the PGIPs were compatible with non-competitive inhibition.

Introduction

A major goal in plant pathology is to understand the molecular basis of pathogen recognition by plants. During pathogenesis, cell walls act as the first line of defense when pathogens attempt to colonize the plant tissue. Pectin is one of the principle components of the primary cell walls of dicotyledons and non-graminaceous monocotyledons. In order to penetrate the pectin layer a pathogen has a wide range of enzymes, including exo- and endo-polygalacturonase, pectate lyase, and pectin methyl esterase at its disposal[1,2]. Among the microbial phytopathogens are fungi, bacteria and viruses. Pectin degrading enzymes, including the endopolygalacturonases (EPGs), are among the first degradative enzymes to be secreted upon fungal infection[3,4]. EPGs degrade nonesterified regions of homogalacturonan, also known as polygalacturonic acid (PGA), found as a component of the pectin of plant cell walls. There is also strong correlative evidence supporting the involvement of EPGs in diseases characterized by soft-rotting or tissue maceration[5-7].

EPG fragmentation of homogalacturonan results in the transitory formation of elicitor-active oligogalacturonides (OGAs). These OGAs are then converted into smaller, biologically inactive fragments by EPG. Plants secrete proteins that specifically bind to EPGs and modify their enzyme action. These proteins, known as polygalacturonase inhibiting proteins (PGIPs), retard the activity of EPGs, thus counteracting fungal invasion by slowing the degradation of polygalacturonic acid in the cell wall and causing an increase in plant defense responses[8,9].

PGIPs are glycoproteins with varying sizes. PGIPs belong to the super family of leucine-rich repeat (LRR) proteins, and are found in the cell wall[10]. Most of them fall in the range of 35- to -54 kDa mostly due to post translational modifications, the molecular weight range of peptide backbone is about 33-36 kDa. PGIPs are specific inhibitors; they do not inhibit other cell-wall

degrading enzymes, and the percent inhibition of different fungal PGs differs. Many plants possess more than one PGIP with differential abilities to inhibit different PGs of pathogens[11-13]. Specificity of PG:PGIP interactions is based on the existence of multiple molecular forms of PGIP in a single host plant, for example in bean, five potential genes have been detected[14]. The PGIP family of proteins, present in the walls of dicots and non-graminaceous monocots, is in some cases capable of inhibiting greater than 99% of the activity of fungal EPGs[15-17]. They form high-affinity complexes with EPGs in a reversible, stoichiometric manner. The hydrolytic activity of PGA by an EPG/PGIP complex may be between one to two orders of magnitude slower than the free EPG[13]. This however, depends on the source of both the EPG and PGIP.

EPGs from a single strain of fungus may exist in a variety of isoforms. These isoforms may be expressed in multiple glycoforms and may differ in their modes of action as well as in their abilities to interact with and be inhibited by PGIPs[14,18]. Thus, the modes of action of PGA cleavage for a particular fungal EPG, coupled with its particular susceptibility to inhibition by PGIPs, are key factors that help determine the virulence of a potential fungal pathogen[13,19].

It has been shown that the degree of inhibition varies with different EPG/PGIP pairings. Additionally, two types of inhibition, competitive and non-competitive, have been reported. The data indicate that the location of interaction may differ, and in some cases may not be at the active site[20]. Further, recent evidence indicate that for at least some EPG/PGIP parings, the result may be an increase in PG activity, rather than inhibition[21].

Previously reported data showed that PGs could be divided into two subgroups based on their interactions with PGIPs from bean, tomato and pear. The PGs from the first group, including *A. niger* PG-I, and the *Cochliobolus sativus, Colletotrichum lindemuthianum,* and *Cryophonectria parasitica* PGs are inhibited by all the PGIPs tested. The PGs from the second

group, including *A. niger* PG-II, and *Fusarium moniliforme*, and *Postia placenta* are not or least inhibited by at least one of the PGIPs studied.[22]

The crystal structure of PGIP2 from *Phaselous vulgaris* was solved at 1.7 Å[23] and serves as the first crystal structure of a plant LRR protein and as a model for studying the structural organization and the modes of interaction of PGIPs and other plant LRR proteins. The structure also provides a molecular basis for understanding how PGIP inhibits PGs (figure 4.1). Previously[20] studied data have identified sites of nine amino acids in PGIPs and EPGs that could be candidates for mutation and therefore could alter the interactions of the two proteins. Further, site-directed mutagenesis experiments on PGIPs indicated there are regions which could be vital for binding to EPGs.[24]

The study of protein-carbohydrate interaction using hydrogen/deuterium exchange-mass spectrometry (H/D-Ex MS) presented in chapter 3 led us to study enzyme-inhibitor (protein-protein) interactions. The amide hydrogens in a peptide backbone are labile and exchange freely with protons in the solution if they are present on the exterior of the protein and accessible to the solvent. The rate at which amide hydrogens present on a protein backbone exchange either with hydrogen or deuterium in the solvent can be monitored by H/D-Ex MS experiments. When a protein is immersed in D_2O or a D_2O/H_2O mixture, amide hydrogens are replaced with deuterons, resulting in an increase in mass of 1 Da for each site of exchange, which is a mass increase which can be easily monitored by mass spectrometry.[25-27]

A procedure commonly used for carrying out H/D-Ex MS experiments is to incubate the protein in a deuterated environment for a defined period of time[28]. Typically D_2O is added directly to the protein sample and the sample is incubated in the deuterated environment. The sample is then added to an acidic solution (~ pH 2.5) containing denaturants that is maintained

near 0^0C. This particular step not only quenches the exchange reaction and slows down the back-exchange to hydrogen, but also facilitates digestion by acid proteases. The protein sample is then digested with an enzyme usually pepsin and the peptides obtained following the digestion are separated using HPLC. Pepsin is generally used in H/D-Ex experiments because its optimal activity is at low pH and it is under these low pH conditions in which the protein and peptide samples are maintained. The HPLC eluent also at low pH, is introduced directly into a mass spectrometer which records the spectrum. Since quenching and digestion are done in an ice bath, the half-life of the deuterium on the protein can be extended to 40-50 minutes[29]. Also the gradient used in these experiments is steep enough to elute the peptides quickly in order to minimize back-exchange, yet it is shallow enough to adequately separate the peptides. This all gives sufficient time to carry out the LC-MS analysis[30,31].

In protein-carbohydrate binding studies, the protein is studied in presence and absence of the substrate or ligand. The exterior amino acids that are present within the region of substrate binding are protected from deuterium incorporation when the substrate is present, thus identifying the location of substrate binding on the protein. This approach has been used to study protein-protein and protein-ligand interactions previously[32-34].

Analyses of the (EPG/PGA) protein-carbohydrate system led us to study protein (*Aspergillus niger*, EPGs)-protein inhibitor interactions (PGIPs: bean, tomato and pear). This paper describes these interactions and provides insight into the mechanism of inhibition. The method developed could be used in the future to study EPG-PGIP interactions from other fungi to ascertain what role they play in pathogenicity.

Experimental Methods

Materials:

Pepsin and D_2O were purchased from Sigma Aldrich (St. Louis, MO). Hydrochloric acid was purchased from J.T. Baker (Phillipsburgh, NJ). The D201E mutant form of EPG-II and the wild type EPG-I and EPG-II were generous gifts of the laboratory of Jaap Visser of Wageningen Agricultural University, The Netherlands, and were prepared as published[35]. The PGIPs [bean, (var. Blue Lake), tomato, (var. Celebrity), and pear (var. Bosch)] were purified as described by Cook et al[36]. The mixture of GalA oligomers of dp 6-15 was a kind gift of Stefan Eberhard of the CCRC. The liquid chromatography (LC) buffers were made with formic acid from J.T. Baker (Phillipsburg, NJ) and acetonitrile from Sigma Aldrich (St. Louis MO). The mobile phases for gradient elution were 0.1% formic acid (v/v) in MQ-H_2O (buffer A) and 0.1% formic acid (v/v) in Acetonitrile (buffer B).

Hydrogen/Deuterium Exchange-MS Experiments:

A total of six experiments were performed with EPG-I (wildtype), EPG-II (wildtype) and EPG-II (mutant D201E) with and without the substrate (mixture of GalA oligomers) and with the three different PGIPs, bean, tomato and pear. The six experiments performed with the EPG-I (wildtype) enzyme are summarized below:

1) EPG-I in H_2O

2) EPG-I in 50% D_2O

3) EPG-I bound with substrate in 50% D_2O

4) EPG-I bound with PGIP (bean) and then bound with substrate in 50% D_2O

5) EPG-I bound with PGIP (tomato) and then bound with substrate in 50% D_2O

6) EPG-I bound with PGIP (pear) and then bound with substrate in 50% D_2O

The EPG-I (wildtype) stock solution was 1.2 mg/ml and 10 µl aliquots were added in six Q-ToF vials (1-6). An equimolar amount of PGIP from bean, tomato and pear were added to vials 4-6 and 10 µl of distilled water was added to tubes 1-3 as a blank. All tubes were incubated at room temperature overnight to ensure interaction between EPG-I (wildtype)-PGIP complexes. Next, a 1000 molar excess of substrate at a concentration of 30mg/ml was added to vials 3-6 and all the six vials were incubated at room temperature overnight. Next, 50 µl of H_2O was added to vial 1 and 50 µl of D_2O was added to vials 2-6 to attain an approximately 50% D_2O concentration. The samples were then left to exchange overnight. At the end of incubation, the exchanged samples were quenched by cooling the samples in an ice bath and 10 µl of cold 10mM HCl was added to each vial to attain a pH of 2.5. Ten microliter of cold 1mg/ml pepsin was then added, and digestion was allowed to progress for 10 minutes. The peptides obtained on digestion were analyzed by LC-MS. For EPG-II (wildtype), the stock solution was 1.0 mg/ml and similar experimental conditions to those for EPG-I (wildtype) were used.

For EPG-II (D201E mutant) the stock solution was 1.0 mg/ml and 10 µl aliquots were added in six Q-ToF vials (1-6). An equimolar amount of PGIP from bean, tomato and pear were added to vials 4-6 and 5.0 µl of distilled water was added to tubes 1-3 as a blank. All tubes were incubated at room temperature overnight to ensure interaction between EPG-PGIP complexes. Next, a 100 fold excess of substrate (30mg/ml) was added to vials 3-6 and all the six vials were incubated overnight. Next, 20 µl of H_2O was added to vial 1 and 20 µl of D_2O was added to vials 2-6 to attain an approximately 50% D_2O concentration. The sample were then left to exchange overnight and at the end the samples were quenched by cooling in an ice-bath and 5.0 µl of cold 10mM HCl was added to each vial so as to attain a pH of 2.5. Ten microliters of cold 1.0 mg/ml pepsin was added, and digestion was carried out for 10 minutes.

In order to minimize any back-exchange of the deuterium, an ice bath was constructed so as to cool the 100 μl loops carrying the solvents. A reverse-phase HPLC column (300 μm I.D. x 5 cm, Vydac C18, 5 μm, 300 Å, Grace Vydac, USA) was used. The peptic digested samples were introduced into the Q-TOF-II (Micromass) mass spectrometer using a Waters CapLC which was modified such that it minimized the dead volume between the mixer and the nanocapillary column. A 15.0 min gradient program from 15.0% to 70.0% of B was used to elute the peptides with a flow rate of 4.0 μl/min. Solvent A was 0.1% formic acid in water and solvent B was 0.1% formic acid in acetonitrile. The Q-TOF-II was operated in MS only mode and spectra were acquired from 400 – 1800 m/z at a rate of 1 scan/second in the positive ion mode.

UV-fluorescence:

Using a Shimadzu spectrofluorophotometer RF-5301 PC, emission spectra were generated for EPG-I (wildtype), EPG-II (wildtype) and EPG-II (mutant). The experiments carried out for all the above enzymes are summarized as under:

For EPG-I (wildtype), the following spectra were obtained, free EPG-I (wildtype) (1), EPG-I (wildtype) in the presence of substrate (2), and EPG-I (wildtype) with three different PGIPs in the presence of the substrate (3-5). To accomplish this five 10 nM samples of EPG-I (wildtype) were prepared. An equal molar amount of PGIP (bean) (3), PGIP (tomato) (4) and PGIP (pear) (5) were added to the respective vials and allowed to incubate overnight. A 1000 fold molar excess of the substrate was added to sample vials 2-5. All samples were left at room temperature overnight. The samples were excited at 292 nm and the emission scanned from 250-350 nm.

For EPG-II (wildtype) similar experimental conditions as EPG-I (wildtype) were used to generate the fluorescence spectra. For EPG-II (mutant) experiment, the substrate was added in a 100 fold molar excess of the sample.

Results and Discussion

EPGs-substrate Interactions:

Pectinases are industrially important enzymes in the processing of agricultural products. They are used as aids for the extraction, clarification and maceration of fruits and vegetables by breaking down the pectin found in the middle lamella and primary cell walls of higher plants.[37,38] Due to its complex nature, the complete breakdown of pectin requires many different enzymes. Two general classes of enzymes cleave the glycosidic linkages on the backbone of these polysaccharides. The first is the hydrolases, including endopolygalacturonases and rhamnogalacturonases and the second is lyases, including pectin lyase, pectate lyase and rhamnogalacturonan lyase.[35]

Commercial enzyme preparations used in food processing are almost exclusively derived from *Aspergillus niger*, and are traditionally mixtures of polygalacturonases, pectate lyases and pectinesterases.[39] Homogenous polygalacturonase preparations are preferred for the separation of whole cells in the manufacture of baby foods, and as vitamins.[39] Novel fields of application can be envisaged for polygalacturonases in the production of oligogalacturonides as functional food components. Oligogalacturonides are functional food ingredients and many of these sugars possess properties that are beneficial to the health of consumers.[40] As the beneficial functional properties of oligogalacturonides become more widely understood, the use of purified polygalacturonase preparations will be necessary for their large-scale preparation in high yields. The use of hydrogen/deuterium exchange-MS experiments to study the binding of these enzymes

with the substrate seems a highly appropriate method to aid in our understanding of the differences in action of the various polygalacturonases.

Crystal structures are known for several classes of main chain depolymerizing pectinases.[41-47] The crystal structures of the EPG from the bacterium *Erwinia carotova* and of the EPG-I and EPG-II from the fungi *Aspergillus niger* have been determined.[48,49] EPG-I, like EPG-II, folds into a right-hand parallel β-helical structure. The prominent cleft along the barrel in EPG-I and EPG-II suggests a location for substrate binding. Site directed mutagenesis experiments have been performed on both the enzymes in an attempt to locate the key amino acids of the active site. These experiments have identified some of the amino acids located in the cleft of EPG-II as important for substrate binding and/or catalysis.[35] Similar experiments for the EPG-I have revealed that Arg96 is an important amino acid and plays a role in substrate binding.[48]

Hydrogen/deuterium exchange-MS experiments with mutant EPG-II from the fungus *Aspergillus niger* were performed in our laboratory using a Micromass conventional electrospray assembly.[50] In the present work we demonstrate the ability of hydrogen/deuterium exchange-mass spectrometry in conjunction with a nanoflow assembly to study the EPG-II mutant enzyme as well as the wildtype enzymes of EPG-I and EPG-II.

The enzymes, EPG-I and EPG-II from *Aspergillus niger* were chosen for the study because of the availability of the crystal structures and their well documented mechanism of actions. Both EPG-I as well as EPG-II enzymes are hydrolases, and as a result will not remain bound to the substrate for the duration of the experiment. For this reason, initial experiments with the substrate were carried out using a catalytically inactive EPG-II mutant. A number of mutants had been previously prepared and analyzed for activity and binding, and the D201E

mutant was selected. The mutant has a k_m approximately equal to that of the wildtype while it showed negligible hydrolytic activity.[35] Fluorescence experiments also revealed that the D201E mutant of EPG-II has binding properties similar to those of the wildtype EPG-II and will be discussed later in the paper. The nanospray configuration allowed us to carry out experiments with the EPG-II (wildtype) enzyme to monitor the changes, if any, in deuterium incorporation between the mutant D201E EPG-II and the wildtype enzyme when analyzed in the presence and absence of substrate. As no mutant is available for EPG-I, we simply expanded the scope of the experiment to use the wildtype enzyme. For the wildtype enzymes studied, the nanospray allowed us to use a large excess of substrate, so as to ensure that the substrate remained bound to the enzyme for the duration of the experiment.

The pH optimum for carrying out hydrogen/deuterium exchange experiments is 7.0, but the active pH range for both the enzymes, EPG-I and EPG-II lies between pH 4.0 and 5.0. Thus, the samples must therefore be allowed to exchange for more than the few minutes typically required of neutral pH protocols for hydrogen/deuterium exchange experiments. It was shown that the exchange rate decreases with a decrease in pH and a change in one pH unit equals a 10 fold change in exchange rate, with a minimum exchange rate at pH 2.5.[51,52]

The exchange rates for many of the amino acids within the EPG-I and EPG-II will be slowed down even further because they are present within the β-pleated sheets which made up a significant amount of the enzyme, including the entire cleft.[53,54]

The activity of the EPG-II with its natural substrate, polymeric homogalacturonan, has been published.[55] Deuterium exchange studies previously performed in our laboratory with the mutant EPG-II (D210E) were done with the octamer of homogalacturonan as the substrate. In the present work a mixture of GalA oligomers of dp 6-15 as the substrate was selected.

To study the binding of the various EPG-substrate pairs, three experiments each with EPG-I (wildtype), EPG-II (wildtype) and EPG-II (mutant D201E) were performed. For EPG-I (wildtype) the three experiments were: EPG-I in H_2O (control), EPG-I in 50% D_2O and EPG-I in the presence of the substrate in 50% D_2O. Similar procedures were followed for EPG-II (wildtype) and EPG-II (mutant), details are presented elsewhere[56].

The deuterium exchange was quenched by reducing the temperature and pH of the solution. The samples of EPG-I (wildtype), EPG-II (wildtype) and EPG-II (mutant) were digested with cold pepsin and the peptides obtained were separated and detected by LC-MS. The peptides obtained from each of the H_2O (control) trials were identified by matching their masses to those generated by a computer peptic digest of EPG-I (wildtype), EPG-II (wildtype) and EPG-II (mutant). For each enzyme studied, only those peptides that gave unambiguous matches were used in further analysis. Pepsin was used for digestion because its optimal activity is at low pH, condition required for H/D-Ex MS experiments. It was observed that pepsin consistently cleaved most of the hydrophobic residues as reported in the literature.[57,58]

The amount of deuterium incorporation into each peptide was then determined by comparing the spectra of deuterated peptides obtained in the presence and absence of substrate as shown in figures 4.2 and 4.3. In figure 4.2, 4.2A shows a triply charged peptide from EPG-II (wildtype) (H_2O) with m/z of 742.77. Figure 4.2B and 4.2C show a shift in the averaged isotopic envelope which can be used as an estimate of the mean deuterium incorporation for the peptide.[58] The averaged isotopic envelope increased by 1.18 and 1.34 indicating that the mean level of deuterium incorporation was approximately 3.54 and 4.02 deuterons respectively. Similarly, in figure 4.3, 4.3A shows a singly charged peptide from EPG-I (wildtype) (H_2O) with m/z of 900.57. Figure 4.3B has the same isotope pattern, indicating that no deuterium was incorporated

into the peptide when it was incubated in 50% D_2O. Figure 4.3C shows a change in the isotopic pattern in which the averaged isotopic envelop increased by 1.38 Da, indicating that the mean level of deuterium incorporation was approximately 1.38 deuterons.

Interestingly there were regions on EPG-II (wildtype) and EPG-II (mutant) enzymes, such as the binding cleft and the α-helix region near amino acids Asp110 – Trp 114, that underwent changes in deuterium incorporation. It was observed that the peptides present in the cleft region that incorporated deuterium in the absence of the substrate were now protected in its presence. This data was consistent with X-ray crystallography and site directed mutagenesis experiments that indicated that the substrate binds the enzymes linearly in the cleft region.[35]

The α helix around Asp110 incorporated deuterium in the absence of the substrate in both the mutant and wildtype EPG-II. Normally deuterium exchange is very slow in α helices because of the internal hydrogen bonding present. Further, in the presence of the substrate these enzymes were protected against deuterium exchange in the α helix region. The α-helix was located on the outside of the β barrel and should not be protected by the presence of substrate. Previous experiments on the EPG-II mutant performed in our laboratory had shown the same behavior for the α helix region.[50] The results were consistent with a conformational change taking place for the enzymes upon binding of the substrate in that region. In the presence of substrate these enzymes however incorporated deuterium into the β-pleated sheets on the underside of the barrel, suggesting a conformational change, most likely associated with the disruption of these sheets.

As reported previously[50], the mutant EPG-II undergoes a flexing of the β-sheets upon substrate binding, which was attributed to entropy considerations. NMR relaxation experiments

have also indicated that protein flexibility can increase in the presence of a ligand. Two observations were given by the authors of the NMR studies:

i) increase in flexibility was seen throughout the β-sheets upon binding to substrate,

ii) this could be associated with a corresponding decrease in flexibility of another region

Similar observations to those obtained by previously reported data were made for the EPG-II mutant in our study, indicating the reproducibility of the system when using either conventional or nanospray sources. The results obtained with the wildtype EPG-II had a similar pattern of protection and incorporation in the absence and presence of substrate respectively.

The wildtype EPG-I which has 60% sequence identity to that of the wildtype EPG-II has a k_m value approximately the same as the wildtype EPG-II as reported in the literature[55]. For wildtype EPG-I, the substrate binding cleft is much narrower than EPG-II, which contributed to retaining the substrate during binding. The peptides identified in the cleft region therefore do not incorporate deuterium in the presence of substrate. Site directed mutagenesis experiments have led to the proposal that the Arg96 which is positively charged binds the negatively charged substrate preventing its release and facilitates the movement of the retained substrate through the active site. Literature reports other enzymes showing similar behavior[48,59,60].

Incorporation of deuterium that was observed in the α-helices in the absence of substrate was missing when the substrate was bound to the enzyme, an observation very similar to the EPG-II enzymes studied. Reasons for these similarities in observations could be due to the fact the enzymes share 60% identical sequence, also have approximately the same k_m value and very similar 3D shape.

The EPG/substrate complexes were also analyzed by UV fluorescence. Fluorescence can be used to detect the general changes in protein structure because fluorescence can be affected by interactions with solvents and neighboring amino acid side chains. Tryptophan and tyrosine residues can both fluoresce, and if their microenvironment changes, a change in fluorescence intensity can be observed.[61] Tryptophans fluoresce when excited at 292 nm, hence the fluorescence experiment was done by exciting the sample at that wavelength. An increase in intensity was observed in the presence of the substrate as can be seen from figures 4.4, 4.5 and 4.6 for wildtype EPG-I, wildtype EPG-II, and mutant EPG-II respectively. This observation indicated that the tryptophan residues were undergoing a change in their environment. For EPG-II and EPG-I enzymes there were seven and five tryptophan residues present in their sequence respectively. For EPG-II, five of these were present on the underside far from the binding cleft and the remaining two were on one of the loops near the N-terminus. For EPG-I, two of these were present once again on the underside of the β-pleated sheets and three were present on one of the loops near the N-terminus. Whether or not it was the tryptophan that was causing a change in fluorescence signal in EPGs or not, it cannot be said with certainty at this point. However, the change in fluorescence intensity was consistent with the changes observed with hydrogen/deuterium exchange experiment. This change in intensity signal was also previously observed on mutant EPG-II.[50]

EPGs-PGIPs-substrate Interactions:

In this work we have investigated the EPGs and PGIP interactions using hydrogen/deuterium exchange-mass spectrometry. Different EPGs, i.e. wildtype EPG-I, wildtype EPG-II and mutant EPG-II were studied using three different PGIPs isolated from bean, tomato and pear. The PGIPs studied proved to be highly resistant to proteolysis by the enzyme used and

this may be related to the LRR structure of the protein.[62,63] This resistance of PGIPs proved to be very useful in our experiments, firstly because the peptide mass spectra of the EPGs studied were not further complicated by the appearance of the peptides from PGIPs and secondly, the intact PGIPs blocked regions of the EPGs studied from proteolytic digestion with pepsin, allowing the location of interaction to be probed by differential peptide mapping.

For all the EPGs that were studied, it was found that in the presence of PGIP a marked change in the pattern of deuterium exchange incorporation was observed and that the interactions of these PGIPs with EPGs were compatible with non-competitive inhibition. When the EPG-II mutant in 50% D_2O was studied it was observed that deuterium was not incorporated into the β-pleated sheets on the backside of the molecule. This however changed in the presence of the substrate, in which incorporation of deuterium was seen in the sheets on the underside of the barrel. This was as discussed above and in chapter 3, probably due to the disruption of the β-pleated sheets. When PGIP isolated either from bean, tomato or pear was added, the level of deuterium incorporation into these sheets was reduced. Protection of the residues in this region from exchange could be caused by the binding of these PGIPs to EPG-II (mutant). Another possibility could be that the binding may prevent the disruption of the sheets caused earlier in the presence of the substrate. Figure 4.7 shows a cartoon representation of *Aspergillus niger* EPG-II (mutant). The regions that showed protection from deuterium exchange in presence of PGIP-bean are colored red in the figure.

The studies also showed that for EPG-II the different PGIPs varied in their degree of deuterium incorporation, in which PGIP from bean showed the greatest protection followed by tomato and pear. This data was consistent with the inhibition studies which show the same trend.[21] Previously published data on the inhibition studies demonstrated that the EPGs do not

equally inhibit these PGIPs and the EPGs can be subdivided into two subgroups relative to their susceptibilities to inhibition by the PGIPs as determined by Cook et al.

The observation of the α-helix region Asp110 – Trp114 incorporating deuterium in the free EPG-II mutant and its subsequent protection in the presence of the substrate may indicate that the helix gets more structured when substrate was present or that the substrate protects it directly. In the presence of PGIPs also the α-helix region shows protection, possibly indicating the location of binding of the PGIPs in that region. From the data obtained it was seen that the peptides protected from hydrogen/deuterium exchange in the presence of the EPG/substrate complexes, were also protected in the presence of EPG/PGIPs/substrate interactions.

The studies for wildtype EPG-II with different PGIPs also showed a decrease in deuterium incorporation in the β-pleated sheets similar to the mutant EPG-II experiment. Results observed for the protection data in presence of the different PGIPs were similar, in which PGIP from bean showed the greatest protection followed by tomato and pear.

When wildtype EPG-I was studied, in the presence of the substrate similar results were obtained to those with mutant EPG-II and wildtype EPG-II. In the presence of different PGIPs, (bean, tomato and pear), the incorporation of deuterium was found to decrease in the β-pleated sheets, but the degree of protection did not vary considerably between the PGIPs. This was in accordance with the inhibition studies reported in literature, that show less variability in the inhibition of EPG-I by the various PGIPs.[22] Figure 4.8 shows a cartoon representation of wildtype EPG-I in the presence of bean PGIP. Protection from exchange in the presence of the inhibitor is shown in red in the figure.

The amount of deuterium incorporation into each peptide was determined by comparing the spectra of deuterated ones in the absence and presence of the substrate as well as in the

presence of the inhibitor as shown in figures 4.9 and 4.10. Calculations for incorporation or protection from the deuterium exchange were done as described for the EPG/substrate experiments. Figures 4.9 and 4.10 shows spectra from wildtype EPG-II and wildtype EPG-I experiments in the absence and presence of the substrate as well as in the presence of PGIP.

The fluorescence experiments provided additional information on the conformational changes observed within all the EPGs in the presence of different PGIPs-substrate system. Figures 4.4, 4.5 and 4.6 show the fluorescence of wildtype EPG-I, wildtype EPG-II and mutant EPG-II respectively. The experiment in each case was done in the absence and presence of the substrate as well as in the presence of three different PGIPs, namely from bean, tomato and pear. For the wildtype EPG-I fluorescence experiment the presence of all the three different PGIPs studied has a remarkable effect on the level of fluorescence. As can be seen from the figure 4.4, fluorescence in presence of PGIPs is lowered back to almost the same level as that of free EPG-I (wildtype). This shows that the PGIPs may be able to prevent some of the conformational changes that were taking place in the presence of the substrate. For mutant EPG-II and wildtype EPG-II, PGIPs from bean, tomato and pear showed different levels of fluorescence intensities as can be seen from the figures and 4.5 and 4.6. Pear PGIP showed less of a change in intensity compared to tomato and bean which lowered fluorescence back to the free EPG-II (mutant) and free EPG-II (wildtype) levels. This data was in agreement with the inhibition studies observed previously.[21] This decrease in intensity was observed in the case of all EPGs in the presence of PGIPs, and suggests its involvement in the change of tryptophan environment. This similarity between EPGs and different PGIPs can be seen in the figures 4.4, 4.5 and 4.6 respectively. The fluorescence experiments for all the EPGs studied also demonstrated that the all PGIPs were

compatible with noncompetitive inhibition, in which only a decrease in the rate of hydrolysis was observed.

Conclusion

In our investigation of EPG-PGIP interactions using hydrogen/deuterium exchange-mass spectrometry we determined that the presence of different PGIPs to EPGs showed a marked change in the pattern of deuterium incorporation and it also allowed us to assess the regions of interactions of EPGs with different PGIPs. It was seen that a decrease in deuterium incorporation was seen for all the EPGs where the PGIPs bound. The change was most noticeable for the β-pleated sheets on the underside of the barrel which incorporated deuterium in the presence of substrate. This incorporation indicated that there was disruption of β-sheets which was causing a conformational change in the EPGs. In presence of different PGIPs, mass spectral data were consistent with the inhibitors contacting the EPGs at a site remote from the substrate binding cleft, and subsequently restricting these conformational changes in the enzymes. The changes observed for the EPG-substrate systems which were minimized upon the inhibitor binding was also indicated from the fluorescence experiments performed.

Interestingly EPG-II enzymes showed different levels of protection from deuterium exchange in which the bean PGIP showed the greatest protection, followed by tomato and pear. This however, changed for EPG-I enzymes which showed similar levels of protection with all the three inhibitors studied. This was possible because the EPG-II is more specific than EPG-I, thus showing variation in their abilities to interact or be inhibited by PGIPs.

Also in case of the EPG-II enzymes, the α-helix region incorporated deuterium in free EPG-II experiments. The α-helix as well as the β-pleated sheets are slow to incorporate deuterium due to the presence of hydrogen bonding, hence the region incorporating deuterium

can be attributed to the fact that the α-helix may be loosely bound. This picture changes in presence of the substrate as well as the inhibitor, indicating that the helix region gets more structured and results in an increase level of hydrogen bonding with the region thus preventing exchange. These results together with previously reported data may suggest the location of PG:PGIP binding and also provides a means of understanding the variations in these interactions that are important for protein-protein interactions in pathogenicity.

Acknowledgement

The authors would like to thank the National Science Foundation (MCB-0115132) and the National Institutes of Health (1 P41 RR018502) for grants that supported this project. We would also like to express our gratitude to the laboratory of Jaap Visser at Wageningen Agricultural University, The Netherlands, for supplying us with the EPG samples required for carrying out the project work and also Stefan Eberhard of the CCRC for the polymeric substrate.

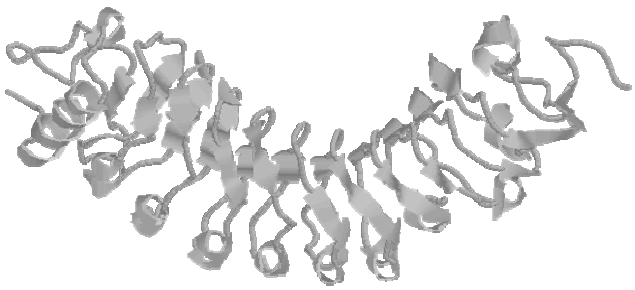

Figure 4.1: Cartoon representation of polygalacturonase inhibiting protein (PGIP2-bean).[23]

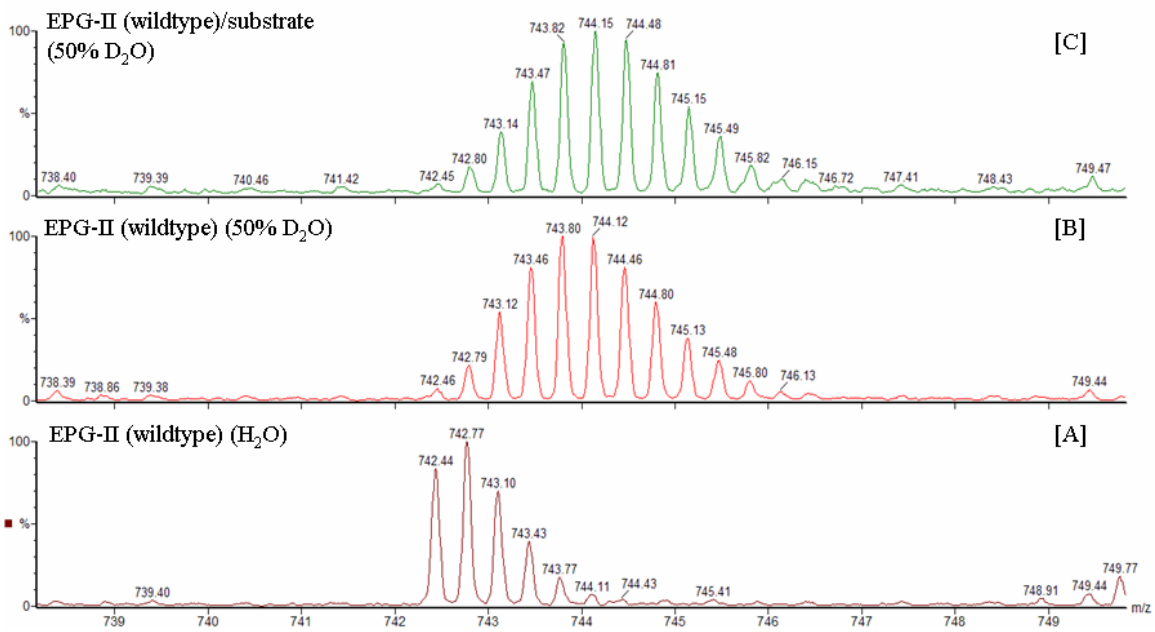

Figure: 4.2: Spectra of 742.77 m/z peptide

Figure 4.2A shows a triply charged peptide of EPG-II (wildtype) with m/z of 742.77. Figure 4.2B and 4.2C are EPG-II (wildtype) spectra in 50% D_2O in absence and presence of the substrate. Figure 4.2B and 4.2C shows a shift of the average isotopic envelop peak by 1.18 and 1.34 Da indicating that mean level of deuterium incorporation was 3.54 and 4.02 deuterons respectively.

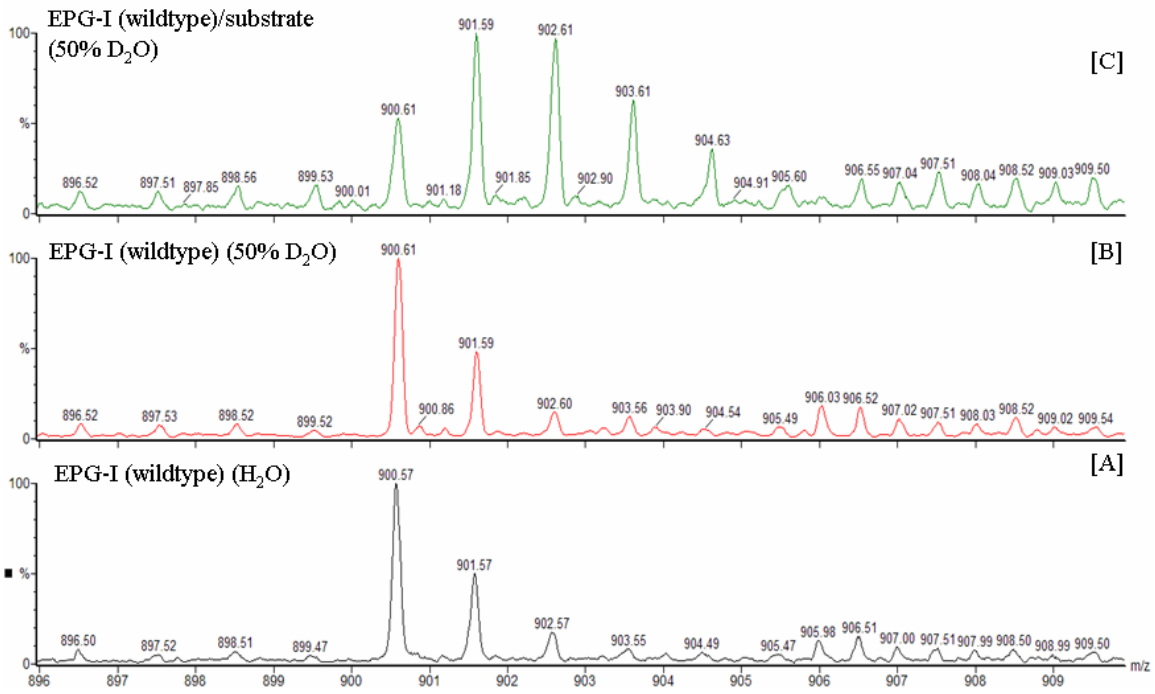

Figure: 4.3: Spectra of 900.57 m/z peptide

Figure 4.3A shows a singly charged peptide of EPG-I (wildtype) with m/z of 900.57. Figure 4.3B and 4.3C are EPG-I (wildtype) spectra in 50% in the absence and presence of substrate. Figure 4.3B has the same isotopic pattern, indicating no incorporation of deuterium into the peptide. Figure 4.3C shows a shift of the average isotopic envelop peak by 1.38 Da indicating that the mean level of deuterium incorporation was 1.38 deuterons.

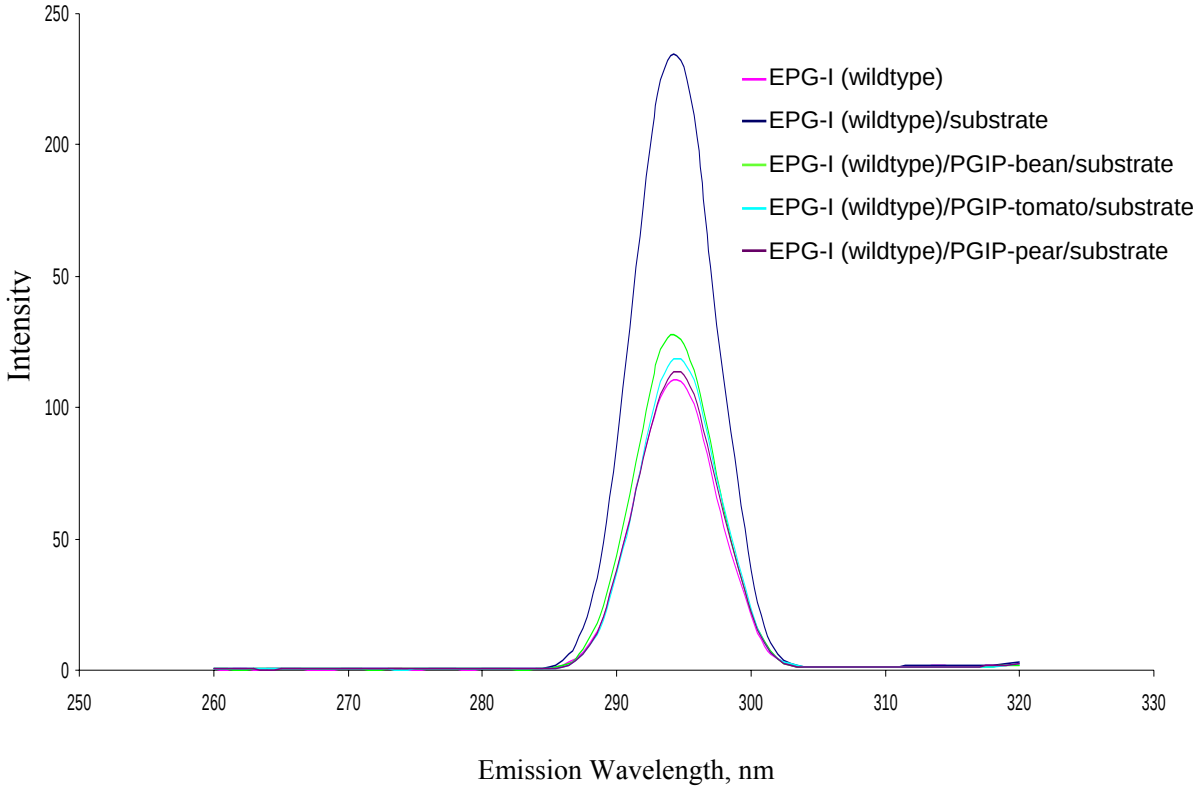

Figure 4.4: Fluorescence spectra of EPG-I (wildtype) with different PGIP binding studies

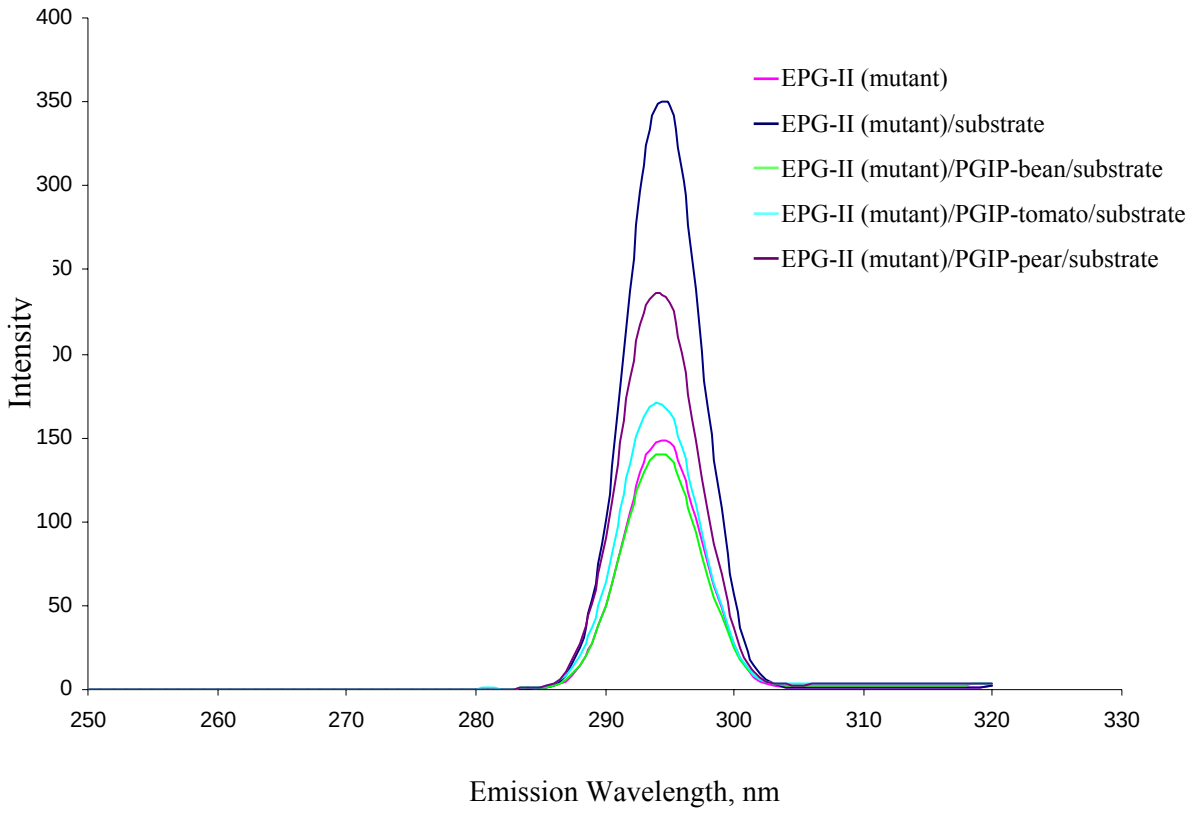

Figure 4.5: Fluorescence spectra of EPG-II (mutant) with different PGIP binding studies

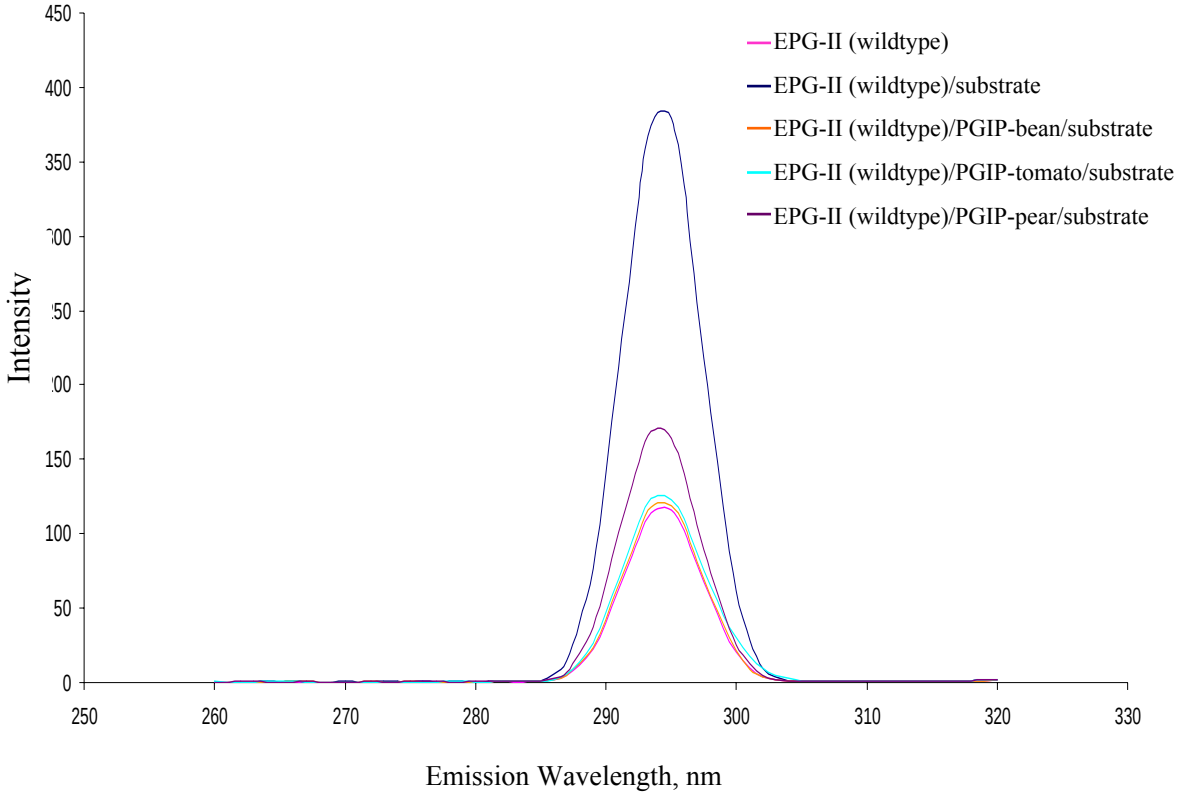

Figure: 4.6: Fluorescence spectra of EPG-II (wildtype) with different PGIP binding studies

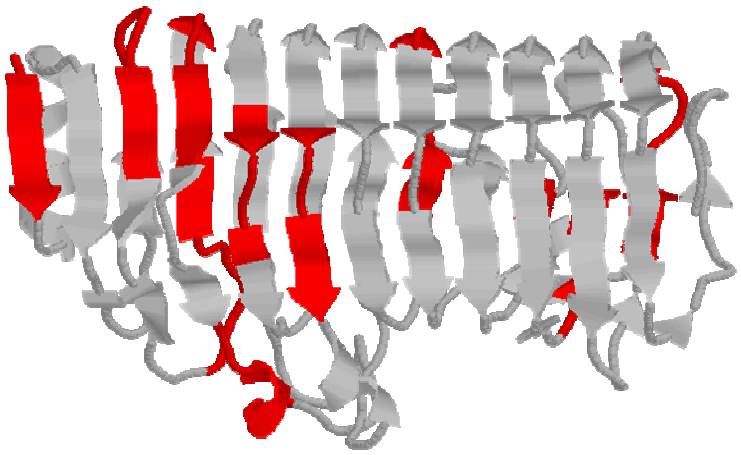

Figure: 4.7: Cartoon representation of the X-ray crystal structure of EPG-II from *Aspergillus niger*.[48] Protection from deuterium exchange by the presence of the inhibitor (PGIP-bean) is shown in red color

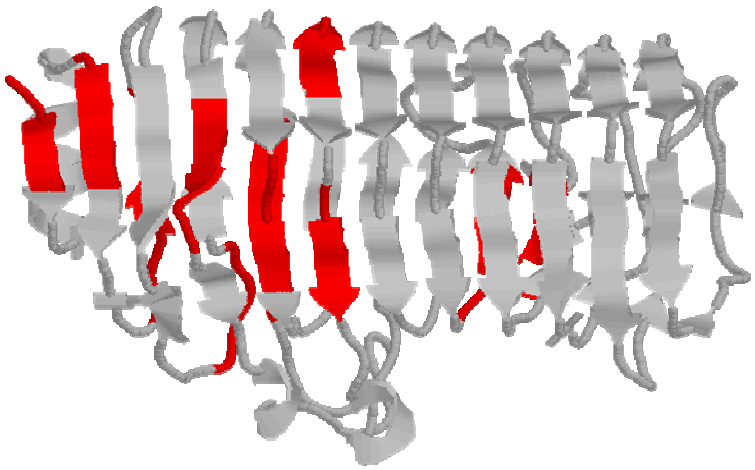

Figure: 4.8: Cartoon representation of the X-ray crystal structure of EPG-I from *Aspergillus niger*.[47] Protection from deuterium exchange by the presence of the inhibitor (PGIP-bean) is shown in red color

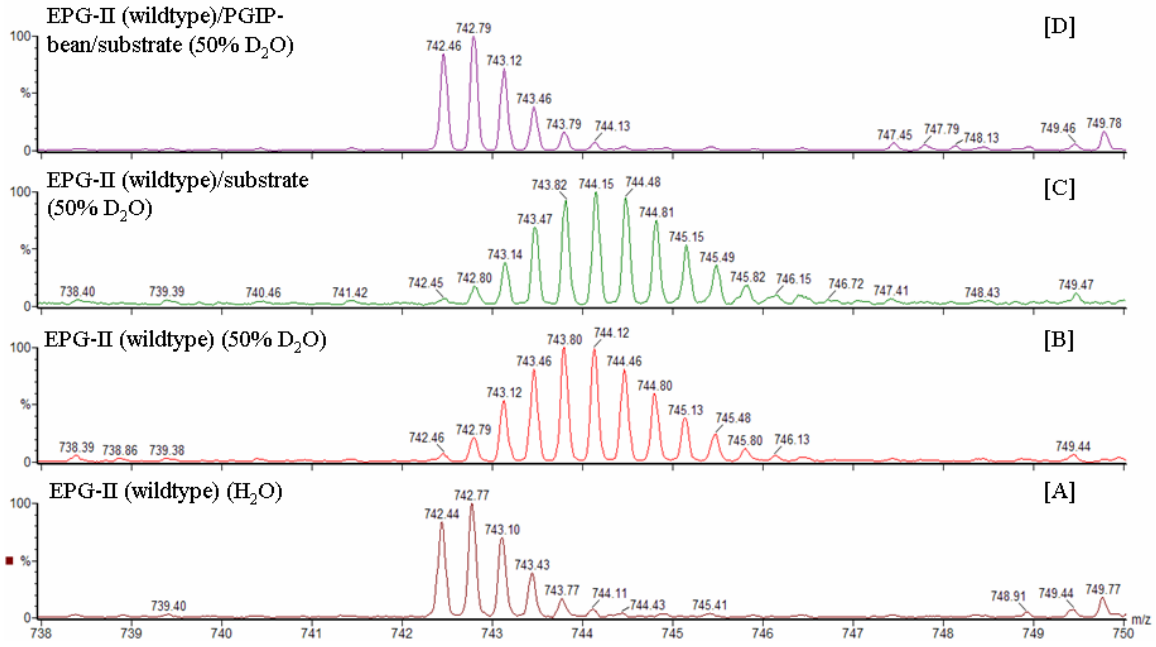

Figure: 4.9: Spectra of 742.77 m/z peptide

Figure 4.9A shows a triply charged peptide of EPG-II (wildtype) with m/z of 742.77. Figure 4.9B and 4.9C are EPG-II (wildtype) spectra in 50% D_2O in absence and presence of the substrate. Figure 4.9D is EPG-II (wildtype) spectra in 50% D_2O in the presence of the inhibitor PGIP-bean. Figure 4.9B and 4.9C shows a shift of the average isotopic envelop peak by 1.18 and 1.34 Da indicating that mean level of deuterium incorporation was 3.54 and 4.02 deuterons respectively. Figure 4.9D shows the same isotopic pattern as figure 4.9A indicating protection in presence of the inhibitor.

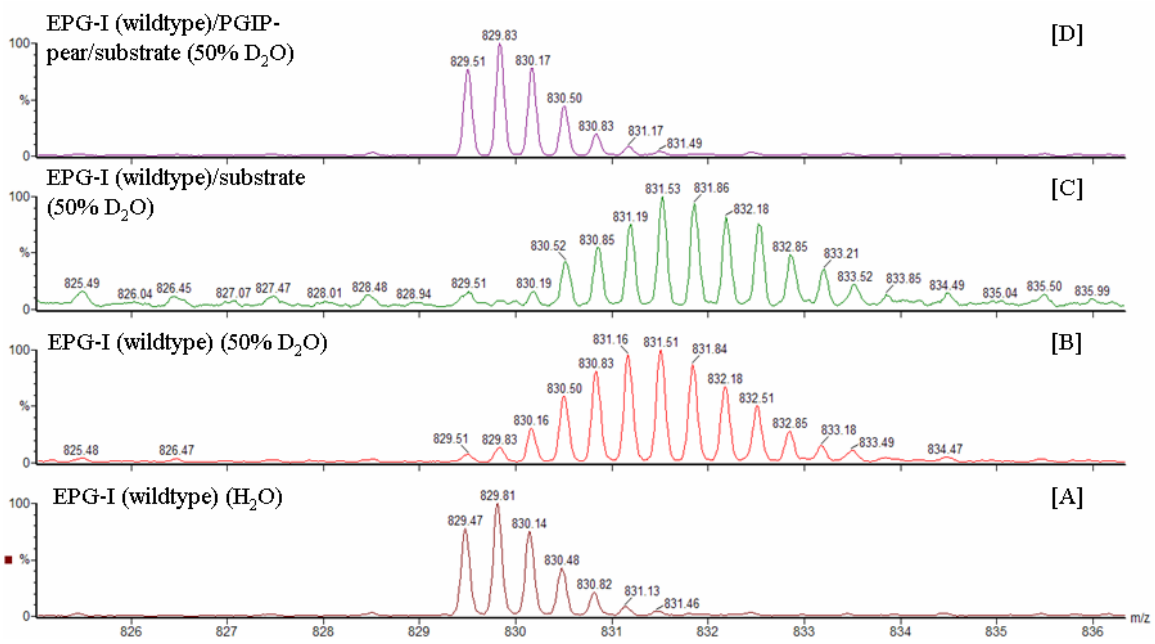

Figure: 4.10: Spectra of 829.81 m/z peptide

Figure 4.10A shows a triply charged peptide of EPG-I (wildtype) with m/z of 829.81. Figure 4.10B and 4.10C are EPG-I (wildtype) spectra in 50% D_2O in absence and presence of the substrate. Figure 4.10D is EPG-I (wildtype) spectra in 50% D_2O in the presence of the inhibitor PGIP-pear. Figure 4.10B and 4.10C show a shift of the average isotopic envelop peak by 1.49 and 1.85 indicating that mean level of deuterium incorporation was 4.47 and 5.55 deuterons. Figure 4.10D shows the same isotopic pattern as figure 4.9A indicating protection in presence of the inhibitor.

Reference List

1. de Vries, R.P.; Visser, J. *Microbiol. Mol. Biol. Rev.* **2001,** 65, 497-522.
2. Karr, A.L.Jr.; Albersheim, P. *Plant Pathol.* **1970,** 46, 69-80.
3. Hahn, M.G.; Bucheli, P.; Cervone, F.; Doares, S.H.; O'Neill, R.A.; Darvill, A.; Albersheim, P. *Plant-Microbe Interactions. Molecular and Genetics Perspectives* **1989,** 3, 131-181.
4. Cervone, F.; De Lorenzo, G.; Salvi, G.; Bergmann, C.; Hahn, M.G.; Ito, Y.; Darvill, A.; Albersheim, P. *Signal Molecules in Plants and Plant-Microbe Interactions* **1989,** H36, 85-89.
5. Bateman, D.F.; Basham, H.G. *Encyclopedia of Plant Physiology* (eds Heitefuss, R. and Williams, P.H.), Springer-Verlag, New York **1976,** 316-355.
6. Issiki, A.; Akimitsu, K.; Yamamoto, M.; Yamamoto, H. *Mol. Plant-Microb. Interact.* **2001,** 14, 749-757.
7. Huang, Q.; Allen, C. *Physiol. Mol. Plant Pathol.* **2000,** 57, 77-83.
8. Sheng-Cheng, W.; Bergmann, C.; Albersheim, P. *Plant Cell Walls* **2005,** http://www.ccrc.uga.edu/~mao/plapath/PPtext.htm
9. Cervone, F.; De Lorenzo, G.; Degra, L.; Salvi, G. *Plant Physiol.* **1987,** 85, 626-630.
10. Cervone, F.; De Lorenzo, G.; Aracri, B.; Bellincampi, D.; Caprari, C.; Devoto, A.; Leckie, F.; Mattei, B.; Nuss, L.; Salvi, G. *Biology of Plant-Microbe Interactions* (Stacey, G.; Mullin, B.; Gresshoff, P.M. Eds.) **1996,** 93-99.
11. Fielding, A.H. *J. Gen. Microbiol.* **1981,** 123, 377-381.
12. Abu-Goukh, A.A.; Greve, L.C.; Labavitch, J.M. *Physiol. Plant Pathol.* ***1983,*** 23, 111-122.

13. Cook, B.J.; Clay, R.P.; Bergmann, C.; Albersheim, P.; Darvill, A. *Mol. Plant-Microb. Interact.* **1999,** 12, 703-711.

14. Desiderio, A.; Aracri, B.; Leckie, F.; Mattei, B.; Salvi, G.; Tigelaar, H.; Van Roekel, J.S.C.; Baulcombe, D.C., Melchers, M.S.; De Lorenzo, G.; Cervone, F. *Mol. Plant-Microbe Interact.* **1997,** 10, 852-860.

15. Berger, D.K; Oelofse, D.; Arendse, M.S.; Du Plessis, E.; Dubery, I.A. *Physiol. Mol. Plant Pathol.* **2000,** 57, 5-14.

16. Gao, S.; Shain, L. *Physiol. Mol. Plant Pathol.* **1995,** 46, 199-213.

17. Cervone, F.; De Lorenzo, G.; Pressey, R.; Darvill, A.; Albersheim, P. *Phytochemistry* **1990,** 29(2), 447-449.

18. Cervone, F.; Hahn, M.G.; De Lorenzo, G.; Darvill, A.; Albersheim, P. *Plant Physiol.* **1989,** 90, 542-548.

19. Benen, J.A.E.; Kester, H.C.M.; Parenicov, L., Visser, J. *In Pectin and Pectinases* (Visser, J. Voragen, A.G.J., eds) **1996,** 221-230.

20. Stotz, H.U.; Bishop, J.G.; Bergmann, C.; Koch, M.; Albersheim, P.; Darvill, A.; Labavitch, J.M. *Physiol. Mol. Plant Pathol.* **2000,** 56, 117-130.

21. Kemp, G.; Stanton, L.; Bergmann, C.W.; Clay, R.P.; Albersheim, P.; Darvill, A. *Molecular Plant-Microbe Interactions* **2004,** 17, 888-894.

22. Brian,, J.C. *Studies of Polygalacturonases and polygalacturonase-inhibiting proteins* **1999.**

23. Di Matteo, A.; Federici, L.; Johnson, K.A.; Savino, C.; Tsernoglou, D.; Mattei, B.; Salvi, G.; De Lorenzo, G.; Cervone, F. **2002,** www.elettra.trieste.it/science/highlights/2002-2003/elettra-hl0203-pg016.pdf

24. Leckie, F.; Mattei, B.; Capodicasa, C.; Hemmings, A.; Nuss, L.; Aracri, B.; De Lorenzo, G.; Cervone, F. *EMBO J.* **1999,** 18, 2352-2363.

25. Katta, V.; Chait, B.T. *J. Am. Chem. Soc.* **1993,** 115, 6317-6321.

26. Zhang, Z.Q.; Smith, D.L. *Protein Sci.* **1993,** 2, 522-531.

27. Liu, Y.Q.; Smith, D.L. *J. Am. Soc. Mass Spectrom.* **1994,** 5, 19-28.

28. Hamuro, Y.; Coales, S.J.; Southern, M.R.; Nemeth-Cawley, J.F.; Stranz, D.D.; Griffin, P.R. *J. of Biomolecular Techniques* **2003,** 14, 171-182.

29. Ehring, H. *Anal. Biochem.* **1999,** 267, 252-259.

30. Smith, D.L.; Zhang, Z.Q. *Mass Spectrom. Rev.* **1994,** 13, 411-429.

31. Smith, J.B.; Liu, Y.Q.; Smith, D.L. *Exp. Eye Res.* **1996,** 63, 125-127.

32. Satako, A.; Takio, K. *Protein Sci.* **2000,** 9(12), 2497-2505.

33. Falick, A.M.; Komives, E.A. *Proc. Natl. Acad. Sci. U.S.A.* **1998,** 95, 14705-14710.

34. Farmer, T.B., Caprioli, R.M. *J. Mass Spectrom.* **1998,** 33, 697-704.

35. Armand, S.; Wagemaker, M.J.M.; Sanchez-Torres, P.; Kester, H.C.M.; van Santen, Y.; Eijkstra, B.W.; Visser, J.; Benen, J.A.E. *J. Biol. Chem.* **2000,** 275, 691-696.

36. Cook, B.J. *Studies of Polygalacturonases and Polygalacturonase-Inhibiting Proteins* **1999.**

37. Sreekantiah, K.R. *Indian Food Packer* **1975**, 29, 22-36.

38. Stutzenberger, F. *Encyclopedia of Microbiology,* Vol.3 (Lederberg, J.; ed.), **1992,** pp 327-337, Academic Press, New York

39. Lang, C.; Doernenburg, H. *Appl. Microbiol. Biotechnol*. **2000,** 53, 366-375.

40. Crittenden, R.G.; Playne, M.J. *Trends Food Sci. Technol*. **1996,** 7, 353-361.

41. Yoder, M.D.; Keen, N.T.; Jurnak, F. *Science* **1993,** 260, 1503-1507.

42. Lietzke, S.E.; Scavetta, R.D.; Yoder, M.D.; Jurnak, F. *Plant Physiol*. **1996,** 111, 73-92.

43. Pickersgill, R.; Jenkins, J.; Harris, G.; Nasser, W.; Robert-Baudoy, J. *Nat. Struct. Biol*. **1994**, 1, 717-723.

44. Mayans, O.; Scott, M.; Connerton, I.; Gravesen, T.; Benen, J.; Visser, J.; Pickersgill, R.; Jenkins, J. *Structure* **1997,** 5, 677-689.

45. Vitali, J.; Schick, B.; Kester, H.C.M.; Visser, J.; Jurnak, F. *Plant Physiol*. **1998,** 116, 69-80.

46. Petersen, J.N.; Kauppinen, S.; Carsen, S. *Structure* **1997,** 5, 533-544.

47. Pickersgill, R.; Smith, D.; Worboys, K.; Jenkins, J. *J. Biol. Chem*. **1998,** 273, 24660-24664.

48. van Pouderoyen, G.; Snijder, H.J.; Benen, J.A.E.; Dijkstra, B.W. *FEBS Letters* **2003,** 554, 462-466.

49. Van Santen, Y.; Benen, J.A.E.; Schroer, K.H.; Kalk, K.H.; Armand, S.; Visser, J.; Dijkstra, B.W. *J. Biol. Chem*. **1999,** 273, 24660-24664.

50. King, D.; Bergmann, C.; Orlando, R.; Benen, J.A.E.; Kester, H.C.M.; Visser, J. *Biochemistry* **2002,** 41, 10225-10233.

51. Bai, Y.; Milne, J.S.; Mayne, L.; Englander, S.W. *Proteins* **1993,** 17(1), 75-86.

52. Zhang, Z.; Smith, D.L. *Protein Sci.* **1993,** 2, 522-531.

53. Ehring, H. Anal. Biochem. 1999, 267, 252-259.

54. Milne, J.S.; Mayne, L.; Roder, H.; Wand, A.J.; Englander, S.W. *Protein Sci.* **1998,** 7, 739-745.

55. Benen, J.A.E.; Kester, H.C.M.; Visser, J. *Eur. J. Biochem.* **1999,** 259, 577-585.

56. Bahrainwala, T.M.; Kumar, K.V.; Bergmann, C.; Orlando, R. "*To be submitted to Rapid Communication in Mass Spectrometry*".

57. Falick, A.M.; Komives, E.A. *Proc. Natl. Acad. Sci. USA* **1998,** 95, 14705-14710.

58. Wang, L.; Lane, L.C.; Smith, D.L. *Protein Sci.* **2001,** 10, 1234-1243.

59. Parseigla, G.; Juy, M.; Reverbel-Leroy, C.; Tardy, C.; Belaich, J.P.; Driguez, H.; Haser, R. *EMBO J.* **1998,** 17, 5551-5562.

60. Parseigla, G.; Reverbel-Leroy, C.; Tardy, C.; Belaich, J.P.; Driguez, H.; Haser, R. *Biochemistry* **2000,** 39, 11238-11246.

61. Nichols, N.M.; Matthews, K.S. *Biochem. Biophys. Res. Commun.* **2001,** 288, 111-115.

62. Kajava, A.V. *J. Mol. Biol.* **1998,** 277, 519-527.

63. Leckie, F.; Mattei, B.; Capodicasa, C.; Hemmings, A.; Nuss, L.; Aracri, B.; DeLorenzo, G.; Cervone, F. *EMBO J*. **1999,** 18, 2352-2363.

CHAPTER 5

CONCLUSIONS

To invade plant tissues, phytopathogenic fungi produce several cell wall degrading enzymes, among them the endopolygalacturonases (EPG) catalyze the fragmentation and solubilization of homogalacturonan. Polygalacturonase inhibiting proteins (PGIPs), found in the cell wall of many plants, counteract fungal EPGs by forming specific complexes with them. The study of the interactions of PGIPs with EPGs plays an important part in the understanding of how plants are able to resist certain pathogens. The knowledge gained from these studies is of great importance to the agricultural communities, because it can lead to the production of pathogen resistant plants.

The research presented in this dissertation lays a ground work for studying the interactions of the different fungal enzymes, endopolygalacturonases and their carbohydrate substrate, polygalacturonic acid (PGA), using hydrogen/deuterium exchange-mass spectrometry (H/D Ex-MS). The EPGs from *Aspergillus niger*, studied were EPG-I (wildtype), EPG-II (wildtype) and the D201E mutant EPG-II. In addition to studying the enzyme-substrate complex, interactions of EPGs with different polygalacturonase inhibiting proteins were also carried out using H/D Ex-MS.

In the presence of substrate, protection was observed in the cleft region for the EPG-I and EPG-II enzymes. This was the same region that was indicated to be the active site for hydrolysis by site-directed mutagenesis experiments. Hydrogen/deuterium exchange in the presence of substrate not only provided the information on binding site, but it also provided information on the conformational changes that were associated with the binding system. The β-pleated sheets on the underside of the β-barrel showed disruption as incorporation of deuterium was seen during the enzyme-substrate binding experiment. The study demonstrated the successful use of

mass spectrometry with respect to the substrate which is typically difficult for NMR and X-ray crystallography methods.

The dissertation also focuses on the interaction of EPGs and different PGIPs. The PGIPs used in the study were from bean (var. Blue Lake), tomato (var. Celebrity) and pear (var. Bosch). For each of the PGIP interaction with the EPGs, the PGIPs showed that they contacted the EPGs at a site remote from the substrate binding cleft. This thus restricted conformational changes that were observed in the presence of the enzyme-substrate experiment. Additionally, it also indicates the location for all PGIP binding, suggesting that the interactions are compatible with non-competitive inhibition.